AD-A111 949 DAVID W TAYLOR NAVAL SHIP RESEARCH AND DEVELOPMENT CE--ETC F/G 13/10
A METHOD TO DETERMINE PRESSURE DISTRIBUTION ON A SHIP PROPELLER--ETC(U)
JAN 82 J SZANTYR

UNCLASSIFIED DTNSRDC/TRANS-354 NL

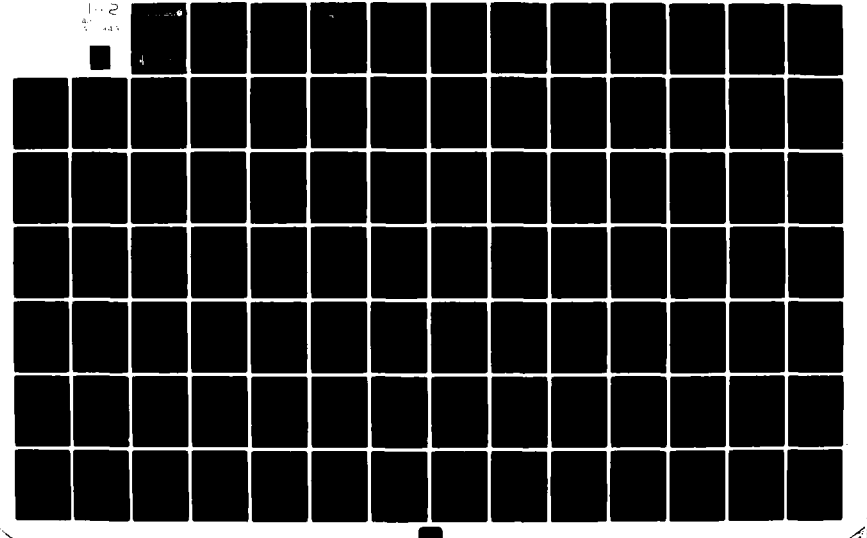

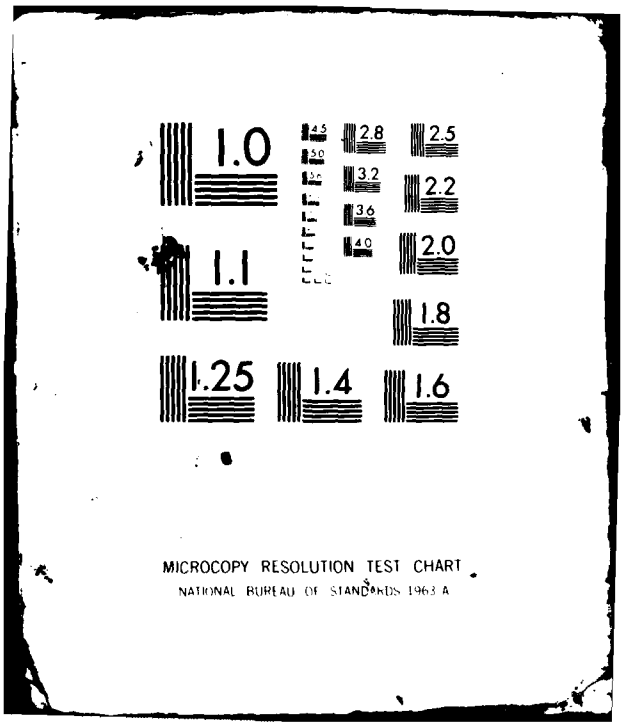
1.0
1.1
1.25
1.4
1.6
1.8
2.0
2.2
2.5
2.8
3.2
3.6
4.0
4.5
5.0
MICROCOPY RESOLUTION TEST CHART
NATIONAL BUREAU OF STANDARDS 1963 A

AD A111949

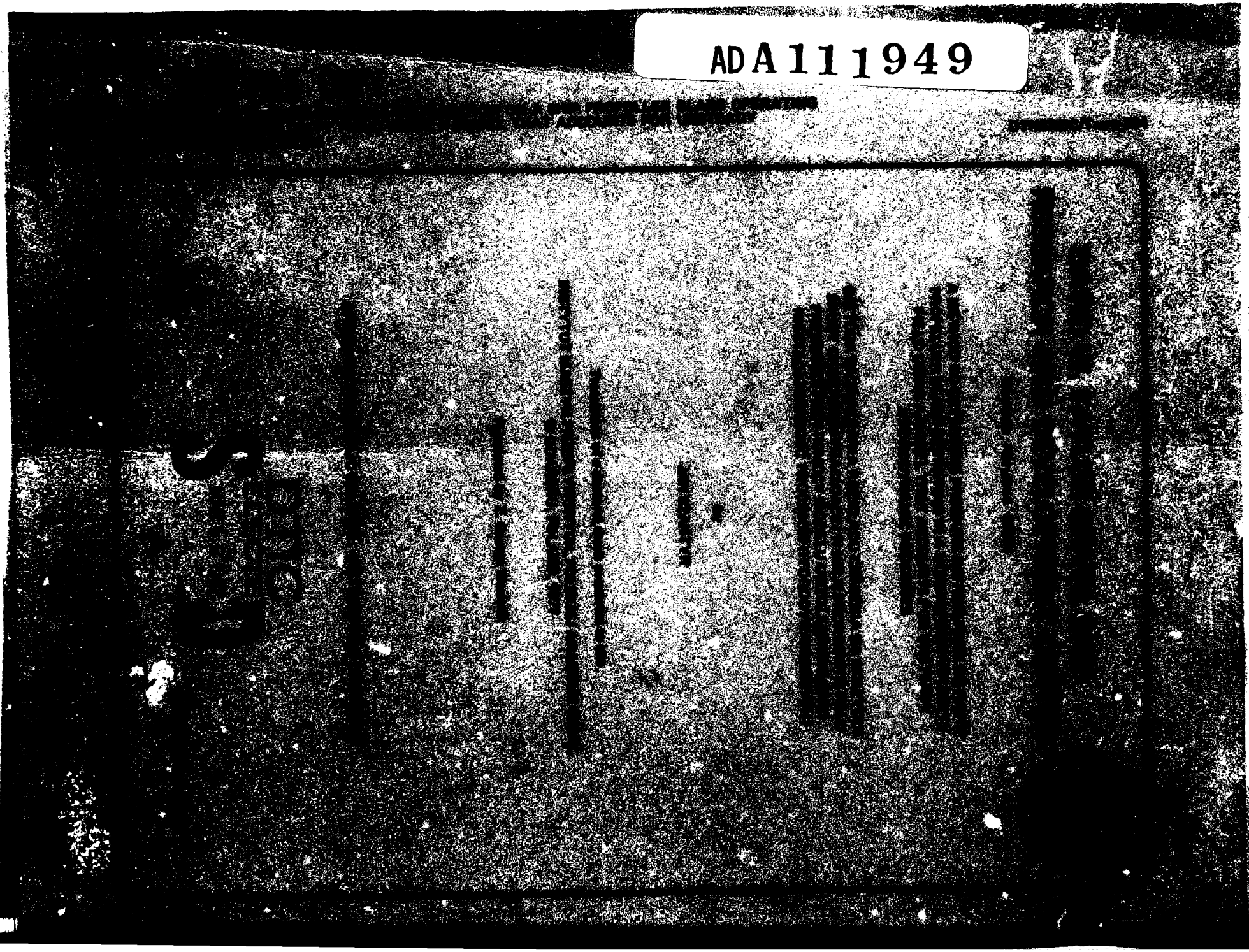

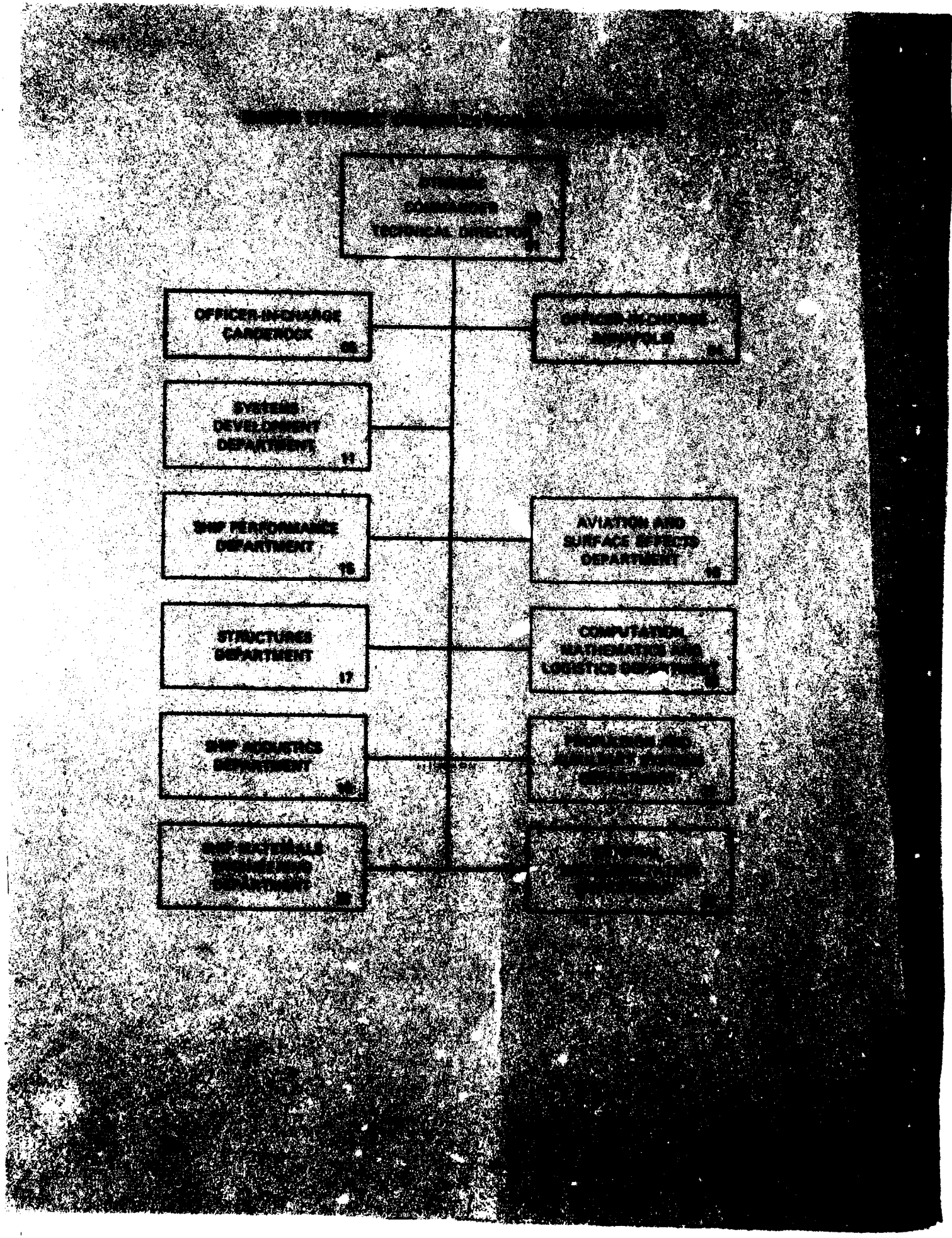
OFFICER-IN-CHARGE
CARDEROCK
SYSTEMS DEVELOPMENT DEPARTMENT
11
AVIATION AND SURFACE EFFECTS DEPARTMENT
STRUCTURES DEPARTMENT
17

UNCLASSIFIED

SECURITY CLASSIFICATION OF THIS PAGE *(When Data Entered)*

REPORT DOCUMENTATION PAGE		READ INSTRUCTIONS BEFORE COMPLETING FORM
1. REPORT NUMBER DTNSRDC/TRANS-354	2. GOVT ACCESSION NO.	3. RECIPIENT'S CATALOG NUMBER
4. TITLE *(and Subtitle)* A METHOD TO DETERMINE PRESSURE DISTRIBUTION ON A SHIP PROPELLER BLADE OPERATING IN A NONUNIFORM VELOCITY FIELD USING A MODEL THAT ACCOUNTS FOR UNSTEADY HYDRODYNAMIC PROCESSES. (METODA WYZNACZANIA ROZKŁADU CIŚNIENIA NA SKRZYDLE ŚRUBY OKRĘTOWEJ PRACUJĄCEJ W NIEJEDNORODYNM POLU PRĘDKOŚCI PRZY POMOCY MODELU UWZGLĘDNIAJĄCEGO NIESTACJONARNOŚĆ PROCESÓW HYDRODYNAMICZNYCH)		5. TYPE OF REPORT & PERIOD COVERED PhD Thesis, 1977 6. PERFORMING ORG. REPORT NUMBER
7. AUTHOR(s) Jan Szantyr		8. CONTRACT OR GRANT NUMBER(s)
9. PERFORMING ORGANIZATION NAME AND ADDRESS David W. Taylor Naval Ship Research and Development Center Bethesda, Maryland 20084		10. PROGRAM ELEMENT, PROJECT, TASK AREA & WORK UNIT NUMBERS Program Element 62543N Task Area 43-421 Work Unit 1506-102
11. CONTROLLING OFFICE NAME AND ADDRESS		12. REPORT DATE January 1982 13. NUMBER OF PAGES 124
14. MONITORING AGENCY NAME & ADDRESS *(if different from Controlling Office)*		15. SECURITY CLASS. *(of this report)* UNCLASSIFIED 15a. DECLASSIFICATION/DOWNGRADING SCHEDULE

16. DISTRIBUTION STATEMENT *(of this Report)*

APPROVED FOR PUBLIC RELEASE; DISTRIBUTION UNLIMITED

17. DISTRIBUTION STATEMENT *(of the abstract entered in Block 20, if different from Report)*

18. SUPPLEMENTARY NOTES

Translation by George Wachnik of a doctoral thesis submitted to the Polish Academy of Sciences, Institute of Fluid Flow Machinery, Ship Propeller Division, Gdansk, Poland, 1977.

19. KEY WORDS *(Continue on reverse side if necessary and identify by block number)*

Propeller design
Blade pressure distribution
Alternating loads
Marine propeller

20. ABSTRACT *(Continue on reverse side if necessary and identify by block number)*

DD FORM 1 JAN 73 1473 EDITION OF 1 NOV 65 IS OBSOLETE
S/N 0102-LF-014-6601

UNCLASSIFIED

SECURITY CLASSIFICATION OF THIS PAGE *(When Data En*

INSTYTUT MASZYN PRZEPŁYWOWYCH
POLSKIEJ AKADEMI NAUK
W GDAŃSKU

(INSTITUTE OF FLUID FLOW MACHINERY
SHIP PROPELLER DIVISION OF THE
POLISH ACADEMY OF SCIENCES
IN GDANSK, POLAND)

JAN SZANTYR

METODA WYZNACZANIA ROZKŁADU CIŚNIENIA NA SKRZYDLE ŚRUBY OKRĘTOWEJ PRACUJĄCEJ W NIEJEDNORODNYM POLU PRĘDKOŚCI PRZY POMOCY MODELU UWZGLĘDNIAJĄCEGO NIESTACJONARNOŚĆ PROCESÓW HYDRODYNAMICZNYCH

(A METHOD TO DETERMINE PRESSURE DISTRIBUTION ON A SHIP PROPELLER BLADE OPERATING IN A NONUNIFORM VELOCITY FIELD USING A MODEL THAT ACCOUNTS FOR UNSTEADY HYDRODYNAMIC PROCESSES)

PRACA DOKTORSKA
(DOCTORAL THESIS)

PROMOTER (ADVISOR): PROF. DR. INZ. HENRYK JARZYNA

GDAŃSK, POLAND, 1977

The technical review of the translation
by Drs. Jan Szantyr and Terry E. Brockett
are acknowledged and greatly appreciated.

Z.G.W.

DTIC
COPY
INSPECTED
2

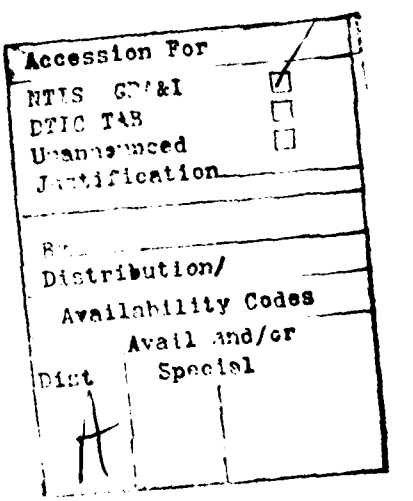

TABLE OF CONTENTS

I INTRODUCTION

In the latest shipbuilding developments there is a substantial increase in ship propeller loading. In particular, this applies to two types of ships: the first, fast container carriers and general cargo ships of 30 knots speed and shaft horsepower exceeding 50,000 per propeller, the second, large tankers and bulk carriers characterized by large propulsive power and low speeds. The latter ships, have in addition, very full hull forms, further aggravating the propeller operating conditions due to the increased nonuniformity of flow behind the ship. Thus, analysis of the cavitation inception on the propeller blade and determination of the induced alternating loads by the propeller on the ship hull are of particular importance in the design of the ship propeller. In most current propeller designs, these problems are at least as, if not more important than, the steady state propeller performance. There are significant problems in the use of experimental methods to design a propeller to perform in a strong nonuniform velocity field and to satisfy specified demands in the area of cavitation and the level of induced vibration. Such experimental efforts require complicated and expensive equipment, several propeller models (until one finds a configuration of desirable characteristics), establishment of a suitable velocity field in the propeller tunnel, testing, and data analysis. Model experiments of this type are so costly and time consuming that their repeated use for each propeller design is highly inadvisable. Therefore, it is essential to develop an analytical method to replace these experimental methods or to limit them to the final verification. The fundamental element of an analytical method to describe cavitation phenomena and unsteady loads induced in a ship propeller is an algorithm from which the pressure distribution on the surface of the propeller blade operating in a nonuniform ideal fluid flow can be determined.

A method is presented in this paper to determine the pressure distribution on a propeller blade of known geometry, performing in a known nonuniform velocity field. The method is based on a theoretical lifting surface model, taking into account, to a high degree, the phenomena of unsteady flow about the propeller. The accountability for flow unsteadiness is not limited to the phenomena on the propeller blade but also includes the structure of the flow behind the propeller. After completion of this computerized method, including subroutines that take into account viscosity and cavitation on the pressure distribution induced on the propeller blade, one has a proficient computer program that will permit:

a) evaluation of a complete design of a propeller performing in a nonuniform velocity

field in the area of cavitation and amplitude of vibrations transmitted through the propeller shaft.

b) improvements of a propeller, designed by any method, directed toward minimizing the vibrations transmitted through the propeller shaft and the reduction of the cavitation area of the blade or area susceptible to errosion. Improvements will be based on several propeller calculations with small, systematic geometrical changes from the initial design and the selection of the most suitable variant. This type of process should be considered a second phase in theoretical ship propeller design, indispensable in the case of propellers operating in a highly nonuniform velocity field.

c) development of design programs to determine the general principles of formulating the geometry of ship propellers intended to operate in a nonuniform velocity field. Because currently designed ships contain increasingly larger power plants and move at increasingly higher speeds, and because it is unlikely that we will be able to eliminate the nonuniformity of the velocity field upstream of the propeller flow, investigation of the principles that formulate the geometry of optimum propellers (with respect to cavitation and induced vibrations) operating in a nonuniform velocity field is imperative.

d) partial substitution of time- and money-consuming experimental methods.

In subsequent parts of this report, the theoretical basis of this analytical model, its numerical implementation, and preliminary validation are presented.

II EXAMPLES OF RELATED THEORETICAL METHODS

In the last two decades several different methods based on a theoretical lifting surface model were developed to design the geometry of a propeller blade for a given pressure distribution and to calculate the pressure distribution on a propeller blade from known propeller geometry. The many theoretical models used in those methods can be divided into two basic groups. One group simulates the propeller blade with a vortex surface of a continuous and varying distribution of circulation; the other group models the propeller blade by a layer of pressure dipoles. In the first case the distribution of induced velocities and the resulting pressures are obtained according to the law of Biot-Savart; in the second case the equation of the potential of a layer of pressure dipoles is used. Full equivalence between the two methods can be proven, at least in calculations of the steady type performance (i.e., propellers operating in a uniform or in an axially symmetric velocity field). All the theoretical methods differ significantly in numerous details concerning fidelity to physical phenomena affecting the performance of marine propellers and in their numerical solutions. Two examples of the most recent and, relatively, the most complex methods of calculating the hydrodynamic characteristics of marine propellers follow. Some of their elements have provided guidance in the course of the development of the method presented here.

The method based on the model of surface vortices was developed by a team headed by Professor J. Kerwin at the Massachusetts Institute of Technology. This method has been systematically improved during the past two decades [2, 9, 10] and it permits calculating the distribution of circulation on a propeller blade of any geometry (including propellers with skewed and raked blades), operating in an axially symmetric velocity field without cavitation. As seen previously, this method assumes a circumferentially uniform velocity field, implying that it does not include phenomena of an unsteady nature. Since a method based on a vortex model has not yet been published and applied to describe the unsteady processes, the following example was specifically chosen to illustrate the characteristic properties of the vortex model. In the method described in [2], the propeller blade is shown in a coordinate system as illustrated in Figure 1. This figure also indicates all the principal geometrical characteristics used to formulate the mathematical equations. The surface of the propeller blade is defined by: propeller pitch, maximum camber, maximum thickness, and the leading and trailing edges. All the characteristics are treated as functions of the propeller radius. To define the distribution of camber, as well as blade thickness

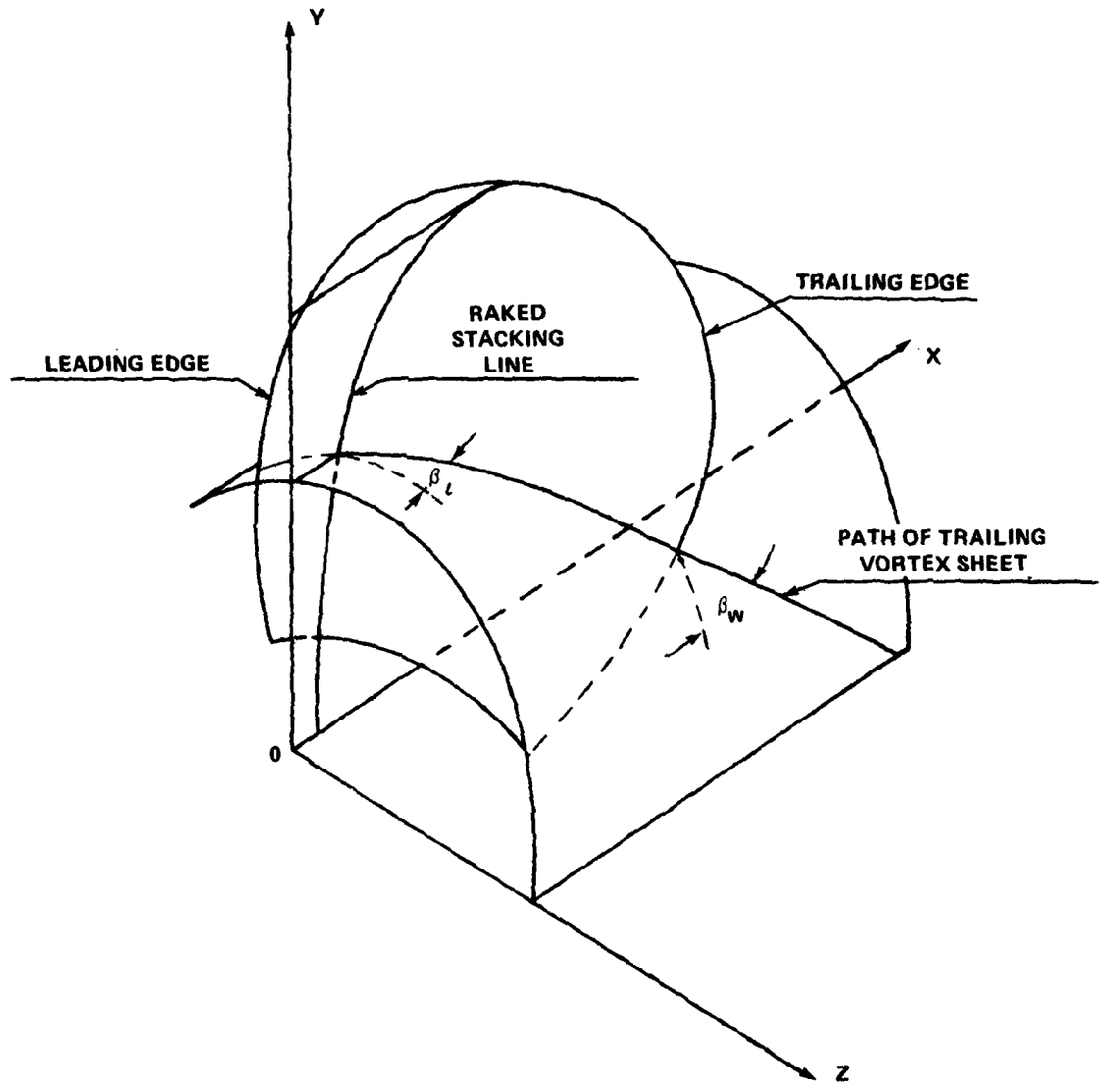

Figure 1 - Coordinate System Used in the American Method

along the chord, standard NACA methods are used (NACA a = 0.8 camber; NACA 66 distribution of the blade thickness). It is possible to implement other geometrical profiles.

The circulation of bound vorticity is defined as a sum of a six-term series.

$$\Gamma(\bar{r},s) = \sum_{m=1}^{3} \sin(m\cdot\bar{r}) \left[A_m \cdot f_1(s) + A_{m+3} \cdot f_2(s)\right] \tag{1}$$

where: $\bar{r}$ - is a radial coordinate of the propeller defined as:

$$\bar{r} = \arccos\left[\frac{1+\frac{r_h}{R}-\frac{2r}{R}}{1-\frac{r_h}{R}}\right]$$

r - radial distance from propeller axis

r_h - radius of the hub

R - maximum radius of propeller blade

s - nondimensional coordinate along the blade profile

$f_1(s)$ - distribution of circulation along the chord of an infinitely thin NACA a = 0.8 blade profile in two-dimensional flow

$f_2(s)$ - distribution of circulation along the chord of an infinitely thin flat plate operating at an angle of attack in two-dimensional flow

Functions $f_1(s)$ and $f_2(s)$ are normalized such that:

$$\int_0^1 f(s)\,ds = 10$$

The blade thickness is simulated by a distribution of sources of strength proportional to local change in profile thickness and velocity of inflow:

$$\delta(\bar{r},s) = V(\bar{r}) \cdot \frac{dt}{ds} \tag{2}$$

where: $\delta(\bar{r}, s)$ - source strength per unit of radial length

$V(\bar{r})$ - local inflow velocity as a function of radius

dt/ds - local change in the thickness of the blade along the chord length

The propeller blade is described by a surface defined by the mean lines of particular profiles located at appropriate angles of pitch (employing given values of the propeller rake and skew) and limited by the blade outline. On this surface the boundary

conditions must be satisfied as follows: at each point of the blade surface the full resultant flow velocity defined in a coordinate system of the blade must be tangent to that surface. The induced velocities at any point on the blade surface in each term of Equation (1), together with the associated trailing vortex, are calculated using the technique of a discrete network of vortex lines, presented in detail in [10]. The authors of this method assumed certain simplifications in defining the geometry of the surface formed by the trailing vortices behind the propeller blade. The hypothesis that the vortex sheet behind the propeller blade has a pitch angle equal to the hydrodynamic pitch angle of undisturbed flow $-\beta(\bar{r})$ has not been used. The Kutta condition, stating that this surface has a pitch equal to the geometrical pitch angle of the blade $-\varphi(\bar{r})$, has also been dismissed. It was assumed, indirectly, that:

$$\tan\beta_w(\bar{r}) = (1-d)\ \tan\varphi(\bar{r}) + d\cdot\tan\beta(\bar{r}) \tag{3}$$

where d is a constant ranging between 0 and 1. To arrive at a more exact solution it is helpful to go through an iterative process to establish a more accurate value of d. To save computational time, the authors have made systematic calculations to establish values of d that do not require further iterations for specific characteristics of real propellers. Their values are not included in the referenced publications.

Velocities induced by the set of sources modeling the blade thickness are established by a technique of discrete distribution of sources on the surface of the propeller blade introduced in [10]. Figure 2 illustrates the distribution of line vortices, sources, and control points used in this example. After all the induced velocities and undisturbed flow velocities have been accounted for, the boundary condition takes the form:

$$\sum_{m=1}^{6} A_m \left[u_a(m,n) - u_r(m,n)\left\{\frac{dx_s}{dr} + \theta\frac{d}{dr}r\tan\varphi\right\} - u_t(m,n)\cdot\tan\beta(n)\right] -$$
$$-\left[\tan\beta_l(n) - \tan\beta(r)\right]\omega r(n) + u_{as}(n) + u_{rs}(n)\left\{\frac{dx_s}{dr} + \theta\frac{d}{dr}r\tan\varphi\right\} + \tag{4}$$
$$+\ u_{ts}(n)\cdot\tan\beta_l(n) = 0$$

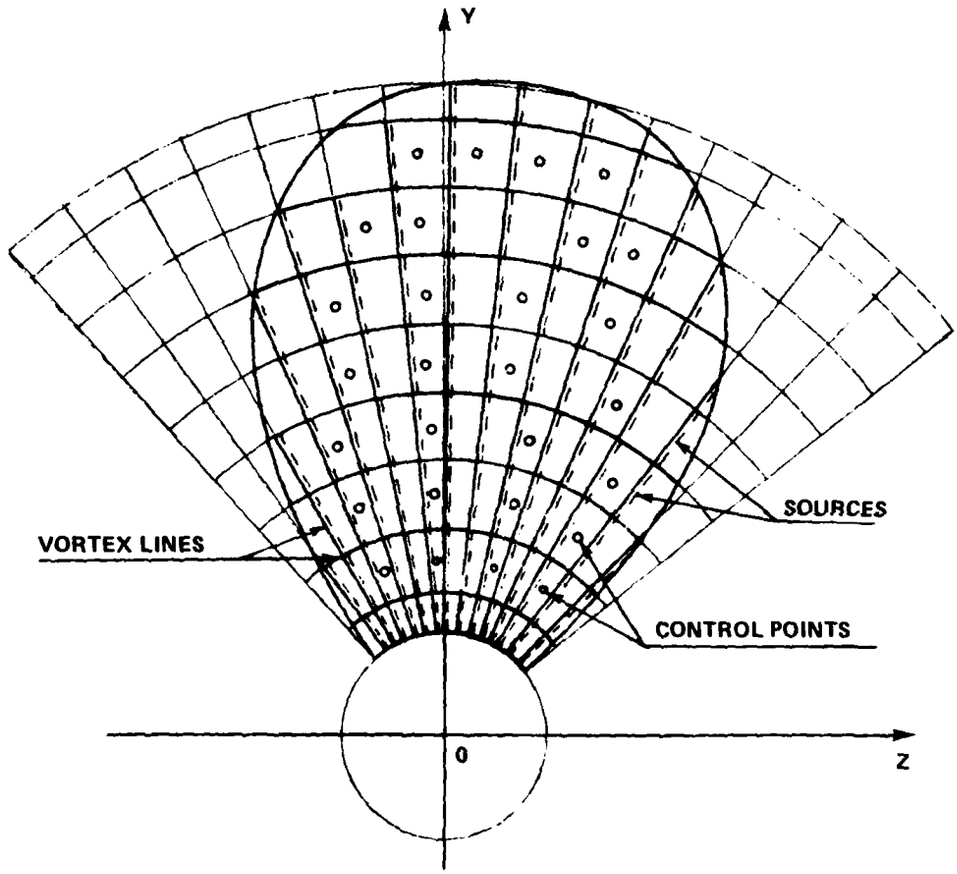

Figure 2 - Schematic of a Discrete Network of Singularities in the American Method

where: β_i - local pitch angle (accounting for the shape of camber)

u_a - axial
u_r - radial
u_t - tangential
} velocity induced by bound and trailing vorticis

u_{as} - axial
u_{rs} - radial
u_{ts} - tangential
} velocity induced by sources

φ - angle of pitch

β - inflow angle

Satisfying the boundary conditions at N points on the blade surface gives us a set of N linear equations with six unknown A_m values. This set of equations is solved by the least-square method. Normally 32 control points are used, four on each of the chosen eight radii. After these equations have been solved, the distribution of loads on the propeller blade can be established.

The method previously discussed is not used to establish the pressure distribution on the propeller blade; however, adapting it for that purpose would be very easy. This method could be used to calculate a full set of propeller characteristics, that is, the thrust, torque, and efficiency as a function of the advance coefficient. In this case the thrust and torque are calculated based on the Kutta-Joukowsky theorem corrected for viscous effects. Published results comparing analytical and experimental data indicate good agreement between calculated and measured hydrodynamic characteristics for propellers of varied geometries, from controllable pitch propellers to propellers with large skew (72°).

A method based on a model of a layer of dipoles was developed by the Wageningen Model Basin (Netherlands). Efforts based on the use of lifting-surface theory for marine propeller calculations were begun by Sparenberg [25] in 1959 and continued by Kuiper [12] and van Gent[4]. The development and improvements of two decades brought this analytical model, among others, to the point where it could be used to calculate marine propeller characteristics operating in a nonuniform velocity field, that is, to solve unsteady problems. The following assumptions were made in the development of the computational method.

a) The thickness of the propeller blade and the hub are not included. The only element of the propeller responsible for the hydrodynamic performance is the finite number of angularly, equally spaced lifting surfaces. The effect of blade thickness may be defined separately and introduced in the calculations in the form of additional flow disturbances.

b) The geometry of each lifting surface is defined by the projected outline of the propeller blade on a surface of constant pitch and without rake.

c) The bulk of the flow is homogeneous and parallel to the propeller axis. It is assumed that the deviation from this flow is small, allowing the use of a linear type of hydrodynamic formulation. This simplification permits the formulation of integral equations describing the distribution of pressure dipole strength on the lifting surface.

In Figure 3 the coordinate system used and the principal geometrical and kinematic quantities are illustrated. The set of equidistant lifting surfaces is defined as:

$$F_k = \theta + k \cdot \frac{2\pi}{Z} - a \cdot s + \omega t = 0 \qquad k = 0, 1, 2 \ldots (z-1) \tag{5}$$

where t = time

$a = \omega / V$

V = propeller effective advance velocity (but not the undisturbed flow)

ω = angular velocity of the propeller.

Deviations from the main homogenous flow are described by the vector $\bar{U}$, defined by components

$$U + u_0 + u_p \;,\; V_0 + v_p \;,\; w_0 + w_p$$

where the subscript o indicates disturbances present in the flow caused, for example, by the hull of the ship, and the subscript p indicates the induced velocities due to the propeller.

The inclusion of the blade camber form causes the lifting surface to be slightly offset from the propeller surface F_k^* and it is defined by:

$$F^* - \phi - a\,x + \omega \cdot t - f(x,r) = 0 \tag{6}$$

where: $f(x,r)$ - function defining the offset.

On the surface F* satisfies the boundary condition as follows:

The vector component of $\bar{U}$ defined in the coordinate system of the propeller and normal to the surface F* should be equal to zero on that surface. In mathematical terms this can be expressed as:

$$\frac{\partial F^*}{\partial t} + \bar{U} \cdot \operatorname{grad} F^* = 0 \tag{7}$$

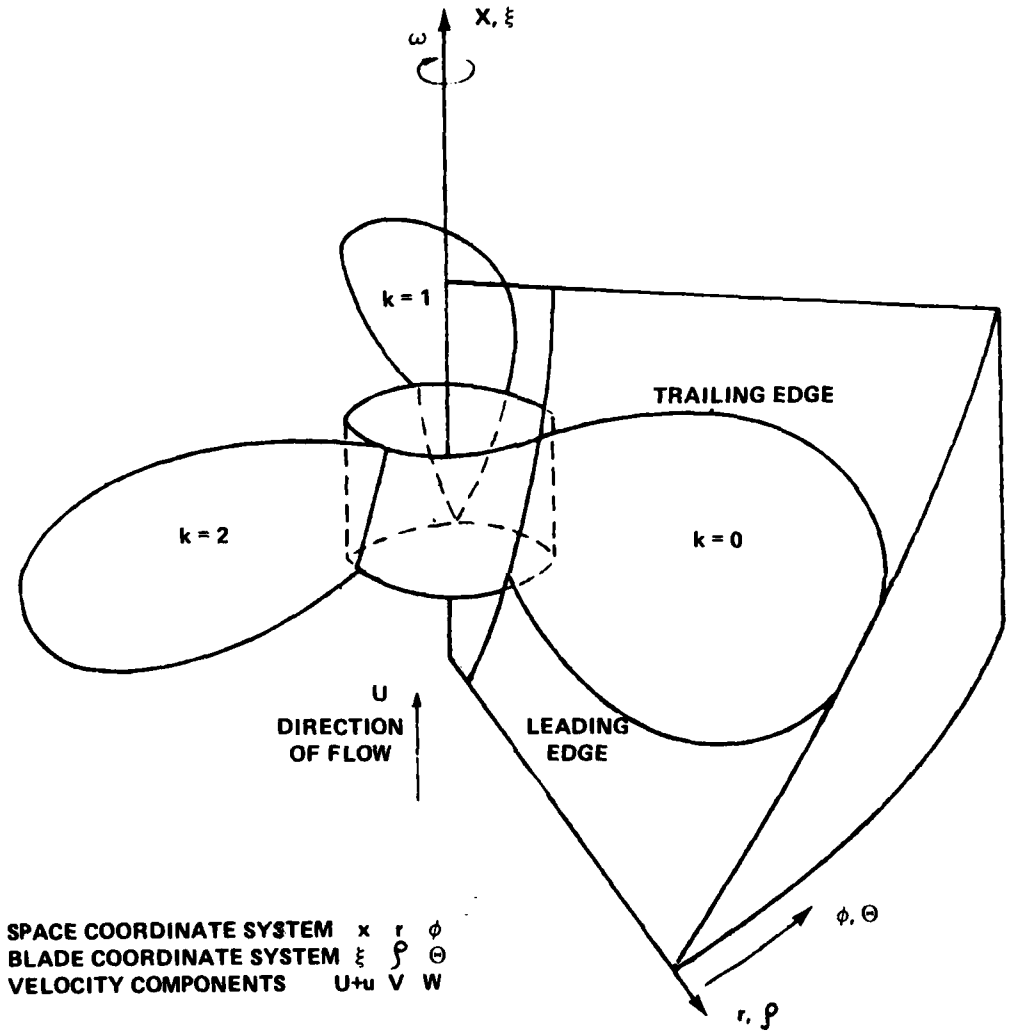

Figure 3 - Coordinate System in the Dutch Method

From the previous equation one can derive (assuming that disturbance velocities of the main flow are small) the following:

$$(a \cdot r\, u_0 - w_0) + r\, U\left(\frac{\partial f}{\partial x} + a - \frac{\omega}{U}\right) = -\left(a \cdot r\, u_p - w_p\right) \tag{8}$$

Velocities induced by the propeller were derived by linearization of equations of motion and have the form:

$$u_p(x, r, \phi, t) = -\frac{1}{\rho_w \cdot U} \int_{-\infty}^{x} \psi_x(x, r, \varphi, t)\, dx$$

$$w_p(x, r, \phi, t) = -\frac{1}{\rho_w \cdot U} \int_{-\infty}^{x} \psi_\phi(x, r, \phi, t)\, dx \tag{9}$$

$$v_p(x, r, \phi, t) = -\frac{1}{\rho_w \cdot U} \int_{-\infty}^{x} \psi_r(x, r, \phi, t)\, dx$$

where: ρ_w - water density

$\psi(x, r, \phi, t)$ - function describing the distribution of the pressure over the propeller blades

$\psi_x, \psi_\phi, \psi_r$ - derived functions depending on particular coordinates.

The velocity u_p is omitted because it is not present in the equation describing the boundary conditions (Equation (8)). Assuming that the field of pressures is caused by a single pressure dipole distributed at identically the same points of all the blades, the following expression results:

$$\psi(x, r, \phi, t) = \frac{\rho_w \cdot U^2}{4\pi} \sum_{k=0}^{z-1} \left[a \cdot \rho \cdot (x - \xi) - r \cdot \sin(\phi - \theta + k \cdot K)\right] \frac{p(\xi, \rho, t)}{R_k^3}\, d\xi\, d\rho$$

where: $R_k = \left[(x - \xi)^2 + r^2 + \rho^2 - 2 \cdot r \cdot \rho \cdot \cos(\phi - \theta + k \cdot K)\right]^{\frac{1}{2}}$ (10)

$$K = \frac{2\pi}{z}$$

Next we substitute the above function in Equation (9) and integrate s with respect to ξ and ρ within the boundaries of the blade. The resulting distribution of induced velocities may then be substituted into Equation (8), describing the boundary condition. Direct substitution causes difficulties in integration because R_k is equal to zero for some of the coordinate values on the surface F*. Because of this, another transformation of the boundary condition is necessary:

boundary condition is evaluated on the propeller surface defined by the following equation:

$$\phi - a \cdot x + \omega \cdot t = \varepsilon$$

that is separated by a small angle ε from the lifting surface F*. Then, we calculate the boundary of the right side of Equation (8) with ε approaching zero. The following equation results:

$$\frac{a \cdot r \cdot u_q - w_q}{U} + \left(\frac{\partial \varphi}{dx} + a - \frac{\omega}{U}\right) \cdot r =$$

$$= \lim_{\varepsilon \to 0} \left[\frac{1}{4\pi} \cdot \int_{r_i}^{r_0} d\rho \cdot \int_{x_t}^{x_t} d\xi \int_{-\infty}^{x-\xi} d\tau \sum_{k=0}^{z-1} p(\xi, \rho, t) \left\{ \frac{A}{R_k^3} + \frac{B}{R_k^5} \right\} \right] \qquad (11)$$

where:

$$\tau = x - \xi$$

$$A = a^2 \cdot r \cdot \rho + \cos(a \cdot \tau + \varepsilon + k \cdot K)$$

$$B = -3 \left\{ a \cdot r \cdot \tau - \rho \cdot \sin(a \cdot \tau + \varepsilon + k \cdot K) \right\} \cdot \left\{ a \cdot \rho \cdot \tau - r \cdot \sin(a \cdot \tau + \varepsilon + k \cdot K) \right\}$$

$$R_k = \left\{ r^2 + \tau^2 + \rho^2 - 2 \cdot r \cdot \rho \cdot \cos(a \cdot \tau + \varepsilon + k \cdot K) \right\}^{\frac{1}{2}}$$

This equation relates the geometry of the lifting surface, the kinematic disturbances of the fluid motion, and the distribution of the pressure p on the lifting surface. It is used to solve the problem of pressure distribution on a propeller blade of known geometry operating in a known velocity field. Because this equation is linear with respect to velocity and pressure, it can be used to study the behavior of the same propeller in different velocity fields utilizing the superposition theory.

The left side of Equation (11) describes the kinematic disturbances present in the flow (for example, the structure of the wake behind the ship hull). In actual calculations, it can be replaced with a function:

$$S(x,r,\phi,t) = \vartheta \cdot \cos(\mu\phi - \alpha) \cos(\nu\,\omega\,t - \beta) \tag{12}$$

where the amplitude ϑ, as well as the phase angles α and β can be functions of x and r. The integer μ defines the harmonic terms of a periodically varying wake, the integer ν defines the ratio of propeller vibration frequency to the rpm. Thus one function S one can describe three different cases:

a) a propeller operating in a uniform (steady) velocity flow ($\mu = \nu = o$)

b) a propeller operating in a nonuniform velocity flow ($\mu \neq o$, $\nu = o$)

c) a propeller with vibrating blades ($\nu \neq o$, $\mu = o$)

In the next analytical step we reduce the integral equations to a form of a set of linear equations. To avoid mathematical singularities, the kernels of the integral equations are split into singular, analytically integrable and nonsingular numerically integrable parts. The set of linear equations is solved with classical methods of numerical analysis. Certain assumptions about the character of the pressure distribution on the propeller blade are essential. That distribution is sought in the following form:

$$P(\Phi,\Theta) = \sum_{p=0}^{P} C_p(\Theta) \cdot H_p(\Phi) \tag{13}$$

where: Θ and Φ are coordinates defined as:

$$\cos\Theta = 1 - 2\cdot\left[\frac{\rho - r_i}{r_o - r_i}\right]$$

$$\cos\Phi = 1 - 2\cdot\left[\frac{s - x_t(\rho)}{b(\rho)}\right]$$

and where: $b(\rho)$ - chord length as a function of radius

$x_t(\rho)$ - coordinate of the trailing edge of the blade as a function of radius

r_i - propeller hub radius

r_o - propeller maximum radius

The function $H_p(\phi)$, describing the fundamental distribution of pressure along the chord, is assumed by the series:

$$H_p(\phi) = \frac{2}{\pi} \frac{\cos p\cdot\phi + \cos(p+1)\cdot\phi}{\sin\phi} \qquad p=0,1,2.... \tag{14}$$

Note that all the terms of this series have a singularity on the leading edge (ϕ = 0) and are equal to zero at the trailing edge ($\phi = \pi$). The coefficients $C_p(\Theta)$ describe the radial distribution of pressure, and it is their values we obtain by solving the integral, Equation (11), transformed into a set of linear equations.

The described method has not yet been used, for instance, to analyze cavitation problems or for the inverse calculation of the distribution of pressure on a propeller blade. The method was used to calculate propeller characteristics K_T, K_Q, $\eta_b = f(J)$ in a nonuniform velocity field. The calculations were directly comparable to the measured propeller tunnel results. The measured and calculated values were the fluctuations (that is, the oscillatory components) of certain propeller characteristics. Comparisons have shown that the method gives adequate agreement for propellers operating near their design point as well as propellers of relatively large expanded area ratio. For values of the advance coefficient less than the design point, agreement with experimental values deteriorates. Similarly, fluctuating side forces and blade bending moments calculated by this method indicated significantly less agreement than thrust and torque coefficients, even at the design point.

Both of the methods described above are not, unfortunately, completely comparable, because the first pertains only to known phenomena (a propeller operating in a uniform or axially symmetric flow). However, an analysis and comparison of certain characteristics of both methods can be made.

a) Definition of propeller geometry

Regarding the fidelity of the actual propeller geometry, the American Method has an easily recognized advantage over the Dutch method; it accommodates for the actual form of the blade outline with propeller skew, propeller rake, and the actual radial distribution of pitch as well as the actual shape of the blade profile. The Dutch model assumes that the propeller blade has a constant pitch along the radius and no rake. Neither method takes into account the presence of the propeller hub (at least if one considers satisfying the boundary condition).

Simplifications assumed in the Dutch method can be the cause of erroneous results when calculations are made for propellers of complicated geometry.

b) Preliminary assumptions about the character of the propeller blade load distribution

Both methods assume a certain defined character of the load distribution on a propeller blade. In both methods the distribution of load (circulation or pressure) along the radius of the propeller blade is calculated by solving the proper set of equations, and the form of this distribution results without any geometrical and kinematic restrictions. The load distribution along the section chord in the American method is defined in the form of a sum of two fundamental distributions dependent on the angle of attack and the curvature in the meanline, while the Dutch method requires this distribution in the form of a trigonometric series. The Dutch method allows a less restricted shape of the resultant load distribution along the chord, which is preferred in the analysis of unsteady flow. This method also does not require information on the type of sectional profile for the propeller for which the calculations are made. The American solution seems sufficient to define all characteristics of propellers operating in a uniform velocity field.

c) Boundary conditions

In both methods boundary conditions are satisfied based on the same assumptions, stating that the resultant velocity vector of the flow, experienced in the coordinate system for the propeller blade, must be tangent to the blade surface. The essential difference is the form of the control surface, where the condition is tested, which in the American model is the actual surface of the blade (with the exception of its thickness). The Dutch employ the projection of the actual surface of the propeller blade. In addition, the American method takes into account the radial component of the induced velocities on the propeller blade, which are omitted in the Dutch method. The formulation of the boundary condition indicates certain advantages of the American method. It should be added that both analytical models omit the effect of the contraction of the stream behind the propeller.

d) Accuracy of the analytical method

Accuracy of the method means there is good agreement between the analytical prediction and pertinent experimental validations. Figure 4 shows a comparison between analytical and experimental data in the American method. The results were

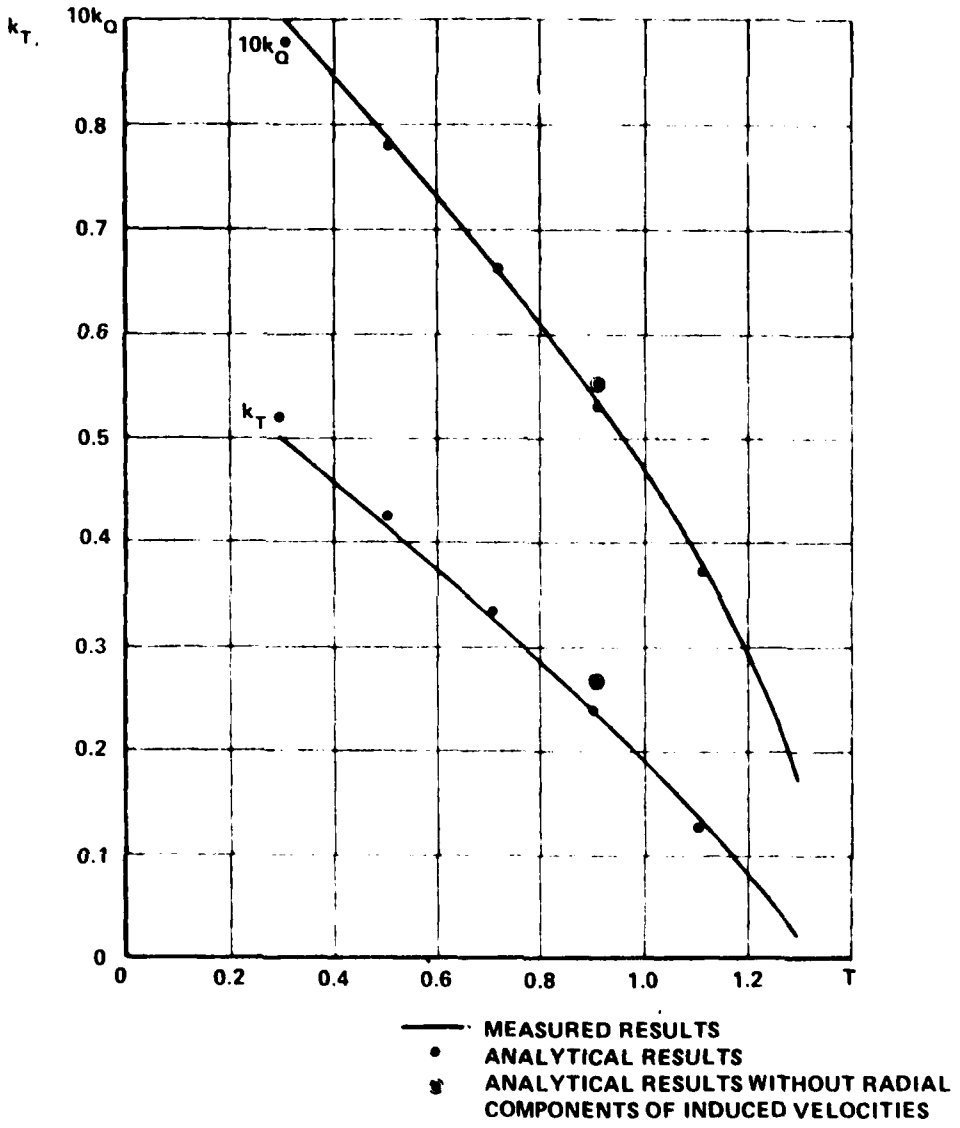

Figure 4 - Comparison of Cumming's Method with Experimental Results

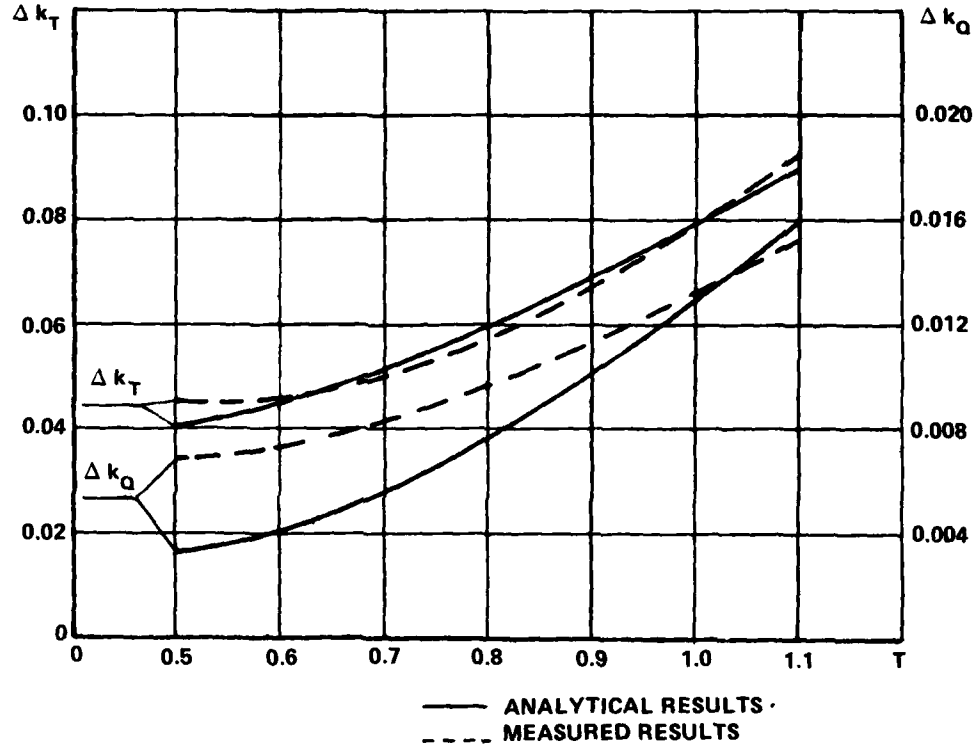

Figure 5 - Comparison of the Dutch Method with Experimental Results

obtained for a five-bladed propeller with a very large blade skew (72°) and a large rake. Figure 5 illustrates a similar comparison for the Dutch method. In this comparison the purpose of the calculations and experiments was not so much the steady-state magnitudes of thrust and torque as the fluctuation on a three-bladed propeller operating in a uniform velocity field together with a three-cycle variation in the circumference. Both figures are from the original publications by the authors of each method.

Evaluating the results, the American method compares very well with experimental data for the full range of advance coefficients, while the Dutch method compares well only close to the design point of the propeller. We could then conclude that the American method is a better one, this, however, should be offset by the fact that the Dutch method had a more difficult problem to solve.

III PRELIMINARY ASSUMPTIONS OF THE PRESENT THEORETICAL METHOD

Before we begin to construct a method to calculate the distribution of pressure on a propeller blade operating in a nonuniform velocity field, the following assumptions are made:

a) The geometry of the propeller for which the calculations are made is fully and accurately defined. The following characteristics are known: propeller diameter, hub diameter, number of blades, radial distribution of the chord lengths, angle of pitch, maximum thickness and camber of blade, and skew and rake. One also has available the section profile of the blade, that is the distribution of thickness and camber along the chord. No restriction is placed on the propeller geometry.

b) The actual velocity field of the fluid in the plane of the propeller is known. The velocity field is defined by three orthogonal velocity vectors for a series of chosen points in the propeller disk. The axial variation of velocity is neglected, primarily because it is small within the space occupied by the propeller and because it is not very likely that such information could be available. It is assumed that the given velocity field does not require any modification for scale effects or the change in flow about the ship due to propeller operation.

c) The propeller under evaluation operates in an ideal fluid, that is, inviscid, incompressible, and isothermal, performing in a homogeneous field of mass forces of unit strength. The flow is potential in the overall field, with the exception of the vortex sheets. The undisturbed velocity of the flow in the axial direction is known. This velocity can also be identified with the velocity of the ship. The propeller rpm is known.

d) In this analytical method use is made of lifting-surface theory, in which the propeller is represented by a discrete network of singularities, composed of vortex lines simulating the load distribution on the propeller blade and sources simulating the thickness of the blade.

e) Because this analytical method will form the basis for a computer calculation its structure should ensure the most efficient computational process. Therefore, certain simplifications are made with the assurance that they do not impair the results but do improve the effectiveness of numerical processes.

IV THE STRUCTURE OF THE PROPELLER BLADE VORTEX MODEL

Two right-handed coordinate systems describing the propeller are introduced in Figure 6. The first, a rectangular coordinate system OXYZ, with the OX axis pointing in the direction of flow and the OY axis along the axis of one of the propeller blades. The second is a polar coordinate system OXRH. The simultaneous introduction of two coordinate systems is dictated by the fact that some of the vector operations performed later are simpler in one system and some are simpler in the other. In some instances a local orthogonal coordinate system OXRT is used, with the origin located on the blade surface at some selected point.

On each blade a discrete set of points W is defined, establishing the structure of the network of singularities. Points W are defined by the following coordinates in the orthogonal coordinate system:

$$\begin{aligned} WX(k,\iota) &= A_2 \cdot \sin P(k) - M(k) \cdot m(\iota) \cdot \cos P(k) + E(k) \\ WY(k,\iota) &= R(k) \cdot \cos A_3 \qquad\qquad k = 1, 2, 3 \ldots n_1 \\ WZ(k,\iota) &= R(k) \cdot \sin A_3 \qquad\qquad \iota = 1, 2, 3 \ldots n_2 \end{aligned} \tag{15}$$

where:

$$\begin{aligned} A_2 &= S(k) - \frac{1}{2}F(k) + x(\iota) \cdot F(k) \\ A_1 &= A_2 \cdot \cos P(k) + M(k) \cdot m(\iota) \cdot \sin P(k) \\ A_3 &= A_1 / R(k) \end{aligned}$$

The terms in the above equations are defined as follows:

- P(k) - radial distribution of propeller blade pitch angle
- M(k) - radial distribution of the maximum camber
- E(k) - values of rake at given radii
- S(k) - values of blade skew
- F(k) - chord length at given radii
- R(k) - radii of selected blade profiles
- $x(\iota)$ - coordinates defining location of points along the chord of a blade profile
- $m(\iota)$ - meanline offsets at points $x(\iota)$

As can be seen from the above, the location of n_1, n_2 points is defined on the surface formed by the meanline composing the propeller blade. Using this set of points, one specifies, in turn, the orthogonal coordinates of two sets of vectors $\overline{B}$ and $\overline{T}$, defining appropriate segments of the vortex lines associated with the blade

PRECEDING PAGE BLANK-NOT FI

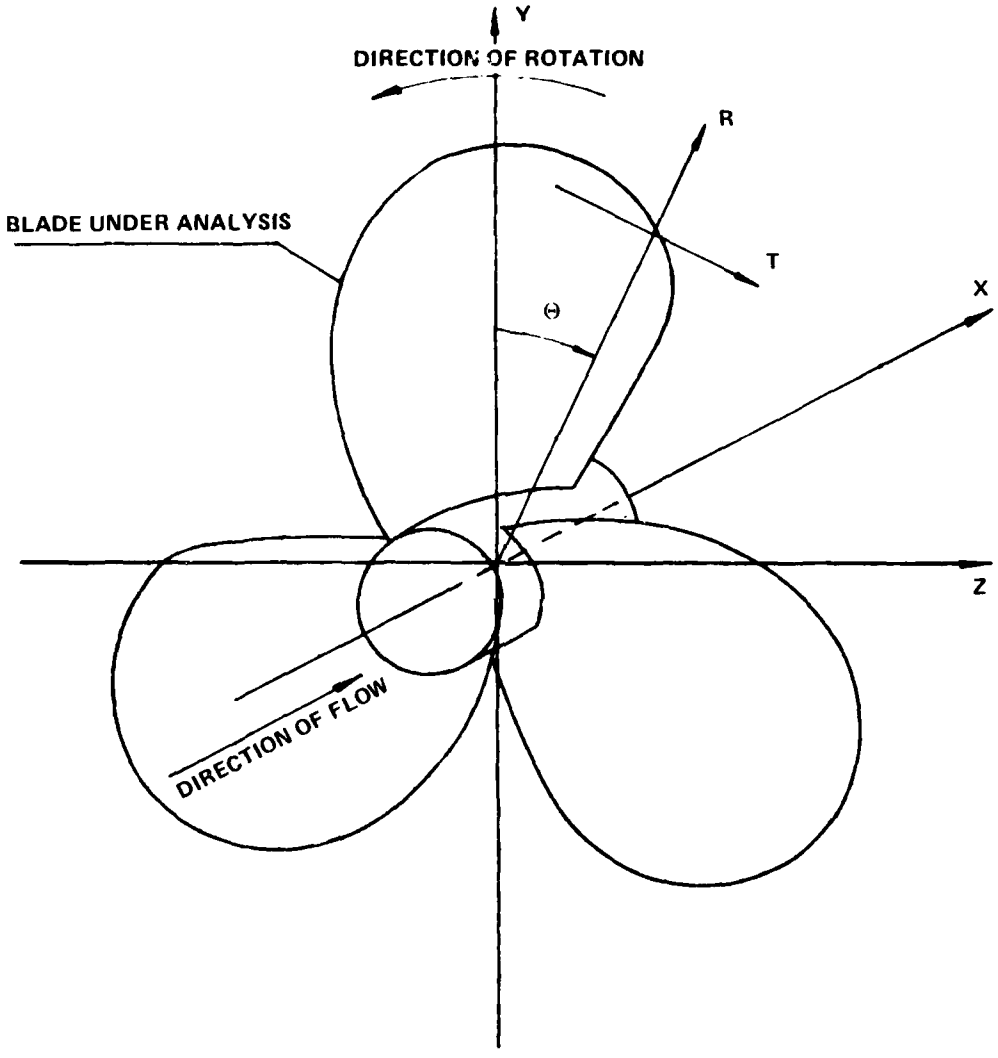

Figure 6 - Coordinate System Used in the Method Presented

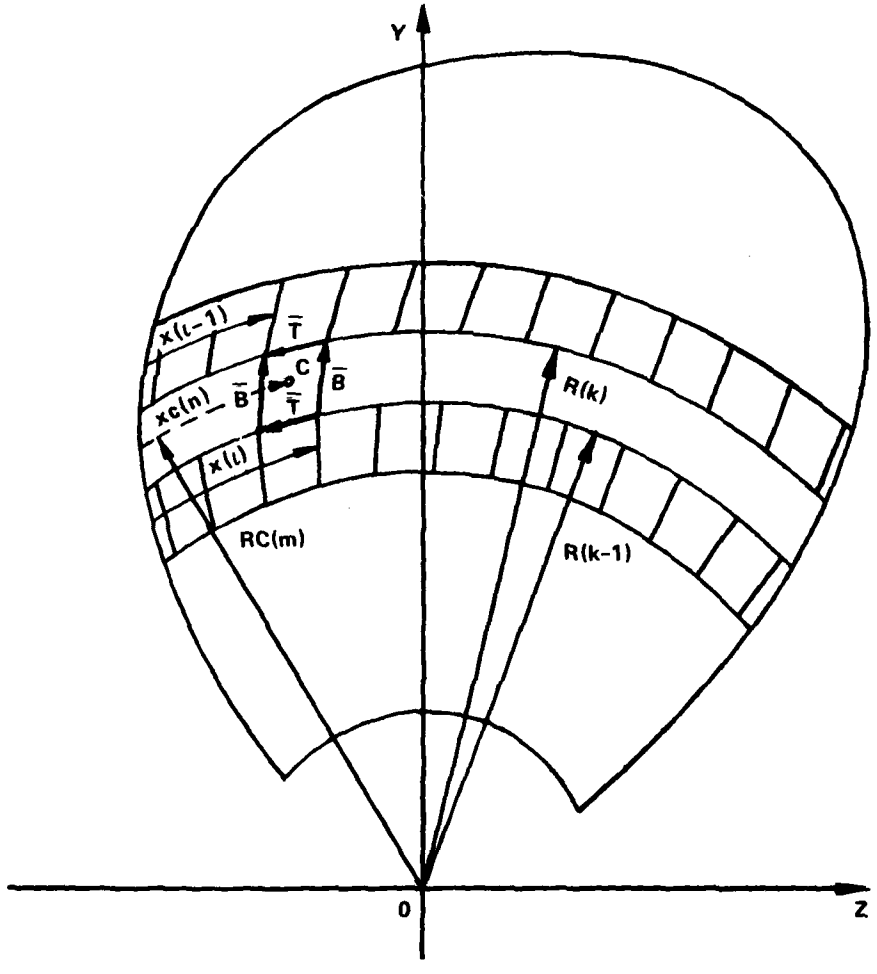

Figure 7 - Schematic of a Discrete Network of Vortices on a Propeller Blade

and the trailing vortex lines. Coordinates of these vectors are defined by the following equations:

$$\left.\begin{aligned} BX(k,l) &= WX(k+1,l) - WX(k,l) \\ BY(k,l) &= WY(k+1,l) - WY(k,l) \\ BZ(k,l) &= WZ(k+1,l) - WZ(k,l) \end{aligned}\right\} \quad \begin{aligned} k &= 1,2 \ldots n_1 - 1 \\ l &= 1,2 \ldots n_2 \end{aligned}$$

$$\left.\begin{aligned} TX(k,l) &= WX(k,l) - WX(k,l+1) \\ TY(k,l) &= WY(k,l) - WY(k,l+1) \\ TZ(k,l) &= WZ(k,l) - WZ(k,l+1) \end{aligned}\right\} \quad \begin{aligned} k &= 1,2 \ldots n_1 \\ l &= 1,2 \ldots n_2 - 1 \end{aligned} \qquad (16)$$

Also defined are the coordinates of the midpoints of all the vectors in both sets using simple relationships:

$$\left.\begin{aligned} BSX(k,l) &= \tfrac{1}{2}\left[WX(k+1,l) + WX(k,l)\right] \\ BSY(k,l) &= \tfrac{1}{2}\left[WY(k+1,l) + WY(k,l)\right] \\ BSZ(k,l) &= \tfrac{1}{2}\left[WZ(k+1,l) + WZ(k,l)\right] \end{aligned}\right\} \quad \begin{aligned} k &= 1,2 \ldots n_1 - 1 \\ l &= 1,2 \ldots n_2 \end{aligned}$$

$$\left.\begin{aligned} TSX(k,l) &= \tfrac{1}{2}\left[WX(k,l) + WX(k,l+1)\right] \\ TSY(k,l) &= \tfrac{1}{2}\left[WY(k,l) + WY(k,l+1)\right] \\ TSZ(k,l) &= \tfrac{1}{2}\left[WZ(k,l) + WZ(k,l+1)\right] \end{aligned}\right\} \quad \begin{aligned} k &= 1,2 \ldots n_1 \\ l &= 1,2 \ldots n_2 - 1 \end{aligned} \qquad (17)$$

All of the above calculations are made for the first propeller blade, later called the analyzed blade. Equivalent geometrical characteristics for the remaining blades may be obtained by a simple transformation of the location of the coordinate system OXYZ where the OY axis will coincide with a given blade. However, only on the surface of the analyzed blade is the set of points C defined, which will be used to satisfy the boundary condition. Points C are chosen in such a way that they are always located in the middle of the rectangles formed by vectors $\overline{B}$ and $\overline{T}$. Because it is not necessary for each rectangle to have a control point C, the radii RC(m) (m=1, 2,...n_3) and the coordinate along the chord xc(n) (n=1,2,...n_4) defines the location of those points. One may define coordinates of the control points as follows:

$$
\begin{aligned}
CX(m,n) &= \tfrac{1}{2}\left[TSX(k,l-1) + TSX(k-1,l-1)\right] \\
CY(m,n) &= \tfrac{1}{2}\left[TSY(k,l-1) + TSY(k-1,l-1)\right] \qquad m = 1,2\ldots n_3 \\
CZ(m,n) &= \tfrac{1}{2}\left[TSZ(k,l-1) + TSZ(k-1,l-1)\right] \qquad n = 1,2\ldots n_4 \\
C\Theta(m,n) &= \operatorname{arctg}\left[\frac{CZ(m,n)}{CY(m,n)}\right]
\end{aligned}
\tag{18}
$$

In the previous equations k has a value such that $R(k) > RC(m) \wedge R(k-1) < RC(m)$*, and l has a value such that $x(l) > xc(n) \wedge x(l-1) < xc(n)$.

In addition, at all points C, unit vectors normal to the surface described with a set of points W are calculated. The coordinates of these vectors are calculated by taking the vector product of two vectors tangential to this surface. To accomplish this we use the adjacent vectors forming the sides of the rectangle that contains the control point and is composed of two vectors $\overline{B}$ and two vectors $\overline{T}$. They are defined in the following form:

$$
\begin{aligned}
NX(m,n) &= \frac{AY \cdot BZ - AZ \cdot BY}{ABL} \qquad m = 1,2\ldots n_3 \\
NY(m,n) &= \frac{AZ \cdot BX - AX \cdot BZ}{ABL} \qquad n = 1,2\ldots n_4 \\
NZ(m,n) &= \frac{AX \cdot BY - AY \cdot BZ}{ABL}
\end{aligned}
\tag{19}
$$

where, appropriately:

$AX = TSX(k,l-1) - TSX(k-1,l-1)$ and similarly for the remaining coordinates

$BX = BSX(k-1,l) - BSX(k-1,l-1)$ and similarly for the remaining coordinates

$$ABL = \left[(AY \cdot BZ - AZ \cdot BY)^2 + (AZ\ BX - AX\ BZ)^2 + (AX\ BY - AY \cdot BZ)^2\right]^{\frac{1}{2}}$$

*Translators note: Symbol $\wedge$ - intersection, both, and.

$A \wedge B$ - intersection of A and B, both A and B.

where k and ι are selected such that: $R(k) > RC(m) \wedge R(k-1) < RC(m)$, $x(\iota) > xc(n) \wedge x(\iota-1) < xc(n)$.

As one may observe from the above equations, the choice of the values of R(k), $x(\iota)$, RC(m), and xc(n) define the geometry of a discrete network of vortex lines and control points on the propeller blade. To get the correct calculated results, these quantities should not be arbitrarily chosen. The following rules should be observed:

a) Control points should be separated from the propeller blade edges with at least three vortex lines in order to eliminate the so-called edge effect. This effect contributes to a totally incorrect value of the induced velocities at locations too close to the edge of a discrete vortex network.

b) The vortex network should be more closely spaced in areas in which one may expect rapid changes in the bound circulation distribution.

The justification and correctness of these rules are confirmed by the author's calculations and many publications outside Poland. This problem is discussed in Section XVI. In the practical case of a distribution of a collection of elements C, $\overline{B}$, and $\overline{T}$ on an analyzed propeller blade, to satisfy rules "a" and "b" requires a fairly closely spaced network of vortex elements. Because of this, a less densely spaced network of vortices was used on the remaining blades where there are fewer control points. The coordinates of the elements in that network are defined in a manner similar to those previously defined with the exception that they have different values of R(k) and $x(\iota)$. Thus, one can save time computing the induced velocities.

In addition to the vortex lines, a field of sinks is distributed on all the propeller blades to simulate finite blade thickness. These sinks are straight lines segments of continuous and uniform distribution of strength. The segments coincide with the segments of vortex lines characterizing the blade bound circulation; they have the same geometrical characteristics as vectors $\overline{B}$ but are not vectors themselves.

V THE STRUCTURE OF THE FREE VORTEX SHEET MODEL IN THE PROPELLER WAKE

The geometry of singularities extending behind the ship propeller is now the most controversial element of the propulsor vortex model. There are many different concepts for formulating this region, from a line vortex forming correct helical surfaces to concentrate vortices shed from the propeller blade tips and the propeller hub. Between the two extremes there are concepts to approximate the surface vortex with a series of "vortex disks" (the so-called staircase approximation) or to partially account for the correct deformation of propeller surface vortices (for example, by considering the contraction of the stream behind the propeller). It is obvious that the theory that assumes the existence of regular helical surfaces behind the propeller formed by shedding vortices, taken from the field of aerodynamic lifting-wing theory, does not account for the actual physical phenomena associated with the ship propulsor. Because of this, in the most recent investigations, the hypothesis assuming deformation of the free vortex sheets relatively close to the training edge of the propulsor and then making use of the converging forms of vortices gains credibility. Unfortunately, this model, although simulating the actual physics, has not been sufficiently developed to employ in the method presented here. It was possible to structure the computer program only, such that any future planned application of newly developed theoretical model of the propeller wake would require minimal changes. It was decided to use a model of the propeller wake with some traditional elements of lifting-surface theory and some new ones that consider the operation of a propeller in a circumferentially nonuniform velocity field. The existence of vortex sheets extending to infinity behind each propeller blade is assumed. In general, these surfaces are not regular helical surfaces. It is also assumed that the stream behind the propeller does not contract, which means that the vortex line trailing from the propeller blade at a radius R(k) remains on the surface of a cylinder of that radius. The whole trailing stream behind the propeller is divided into two parts: the unsteady region extending from $\Theta = 0°$ to $\Theta = 2\pi N$ that is, having N turns of the propeller surface, and the steady-state region where $\Theta > 2\pi N$. The steady-state region in a practical case is limited to six full turns of the propeller surface, because the induced velocities on the propeller blade beyond that are negligibly small. The unsteady region is an area in which the influence of an onset nonuniform velocity field on the geometry and intensity of circulation of the vortex lines forming a free surface is apparent. The steady-state region is formed as though the propeller operated in a circumferentially averaged velocity field. Limiting the unsteady region to N turns of

the helical propeller generated surface (in practice, frequently one turn) is justified by the substantial reduction of the induced velocities resulting from the increased distance of the line vortex elements from the control point. For example, the vortex segment located at $\Theta = 2\pi$ induces in the region of the propeller blade, for normal values of pitch angle of the helical vortex, only 2% to 5% of the induced velocity for a similar segment located near the control point.

Figure 8 illustrates schematically an expanded vortex surface extending behind one of the propeller blades. As shown in the figure, the unsteady region of the stream behind the propeller is further divided into sectors. The number of sectors may vary, depending upon the number of angular positions of the propeller analyzed in one revolution. The intensity of the circulation of the vortex lines in respective sectors and the angle of pitch depend upon the phenomena taking place on the propeller blade. Thus, for a propeller operating in a circumferentially nonuniform velocity field, parameters describing the free vortex surface will be different for each segment. To simulate this pnenomenon in the vortex model of the ship propeller, it is helpful to divide the unsteady region of the stream behind the propeller into separate sectors. It is assumed that in a given sector each vortex line has constant circulation intensity and constant angle of pitch independent of coordinate Θ. However, these parameters may be different in the neighboring sectors even for the vortex lines lying on the same radius R(k). At a given angular position of the propeller Θ, the strength of the vortex lines in the first sector and their angle of pitch depend directly on the distribution of circulation and induced velocities on the propeller blade at that location. After the propeller turns an angle of $d\Theta$ equal to an angular displacement of a sector, parameters that have been described sector 1 are "transferred" to sector 2, while characteristics of sector 1 are made dependent upon the new conditions on the propeller blade, equivalent to location $\Theta_2 = \Theta_1 + d\Theta$. After analysis of a full revolution of the propeller, one obtains a complete description of one revolution of the unsteady free vortex sheet behind the propeller blades. The geometry and intensity of the vortex lines in the steady region, however, are based on calculations for a circumferentially averaged velocity field. The theoretical model of the stream behind the propeller is characterized by a combination of interdependencies between free vortex sheets and the propeller blades. Parameters describing the unsteady region contain, in essence, the "history" of the propeller operating in a nonuniform velocity field, influencing the induced velocities on the propeller blade, in turn determining the actual distribution of circulation found on the blades

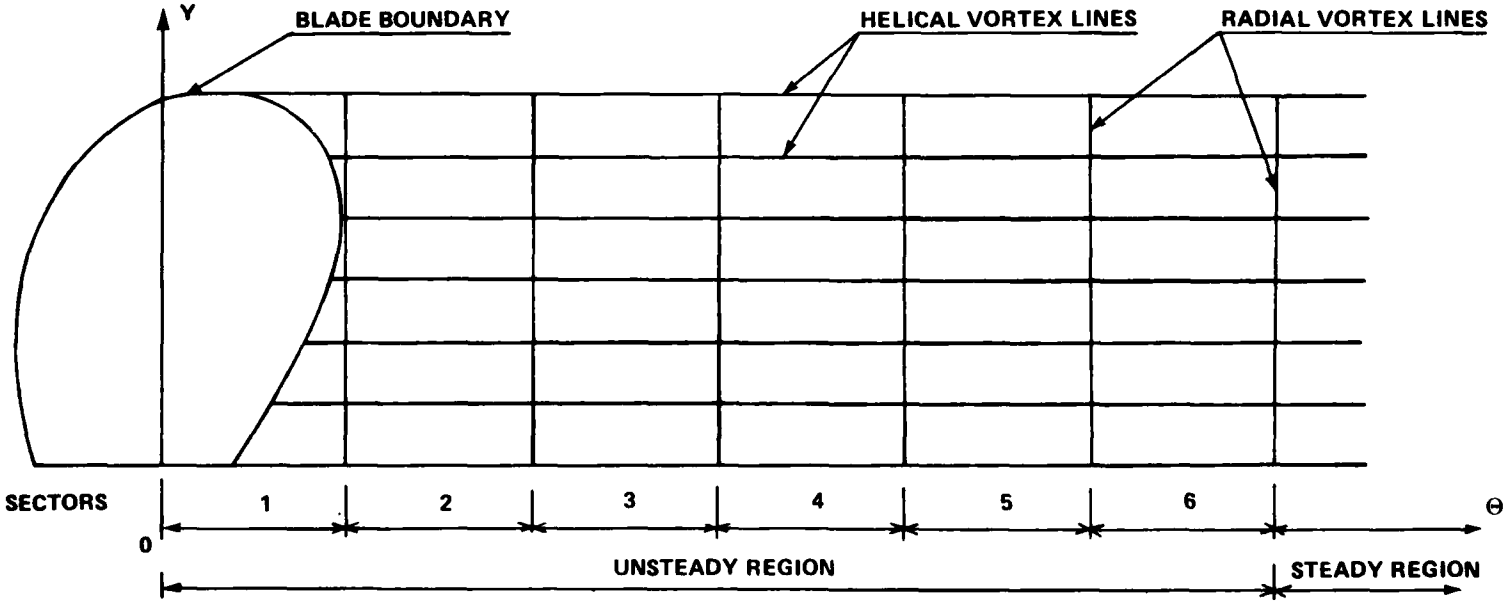

Figure 8 - Schematic of an Expended Free Vortex Sheet

as well as the strength and angles of pitch of the line vortex in the first sector. Allowing varying circulation strength of the same vortex line necessitates the use of radially oriented line vortices on the free surfaces in the neighboring sectors. This follows from the Helmholtz theory of circulation. In this way, each sector of the unsteady region is composed of a radial vortex defining the leading edge of the sector, several regular helices at the radii R(k) and pitch angles β (k), and a radial vortex defining the trailing edge of the sector. The only exception here is the first sector, which begins at the trailing edge of the propeller blade. A detailed schematic of a single sector is given in Figure 9. In the figure the radial vortex at the leading edge of the sector is rectilinear, which is the case only where the propeller blade does not have rake or skew. When it does, the vortex has rake and skew formed by the propeller blade. From this vortex, subsequent segments of the helical vortices follow. If these segments have different values of pitch, then, after rotating an angle $d\Theta$, establishing the size of a sector, each one will attain a different distance along the x axis. From a mathematical average of these distances, one may establish a distance dx, which defines the location of the next radial vortex, establishing the end of one sector and the beginning of the next sector. The helical vortices so constructed are not continuous and at points between two sectors there are several interruptions, which become smaller as $d\Theta$ is decreased. These discontinuities do not present difficulties in the calculations of velocities induced by the free vortex sheets. The basic advantage of such a construction of a propeller wake flow model is the elimination of a characteristic deformation of a free vortex sheet that would be unavoidable if one tried to build them from infinite, continuous helices of different values of pitch.

The most frequently used method to determine the angle of pitch of the lines forming the free vortex sheets is the process of iteration, where the controlling parameter ascertaining that proper values of these angles are attained may be, for example, the propeller thrust loading coefficient. Such a process is very time consuming, and one frequently encounters serious difficulties in reaching adequate convergence, particularly for propellers operating significantly far from the design point. On the other hand, my own analytical explorations as well as the results of foreign authors confirm that, from the point of view of calculating the induced velocities, it is far more important to know the correct strength of the vortex lines rather than their angle of pitch. In other words, even a few percent error in the estimation of the pitch angle of the vortex line causes relatively negligible error

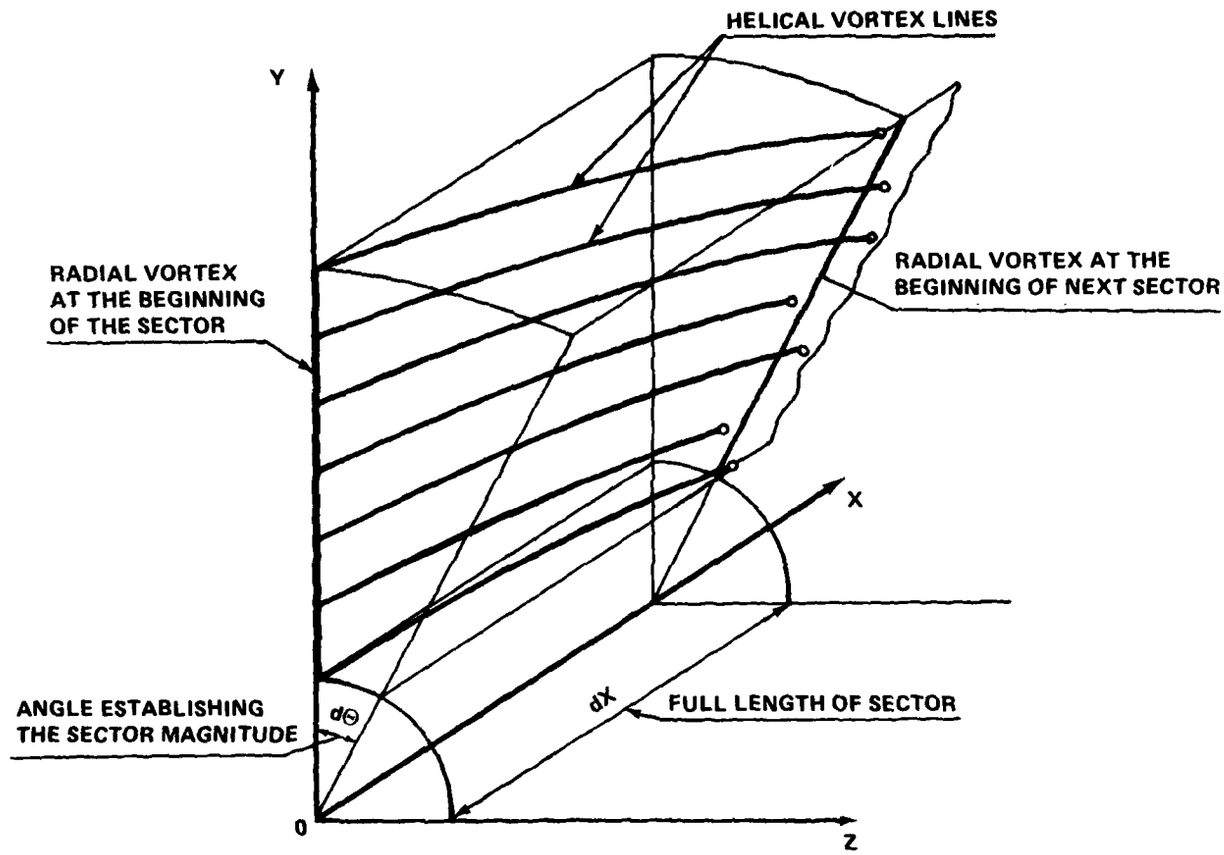

Figure 9 - Schematic of a Single Sector of the Unsteady Region of Axonometric Projection

in the calculation of the velocities induced by the distribution of singularities modeling the whole propeller. Thus it was decided to use a simpler method of determining the pitch angle of the vortex line in the stream behind the propeller, defined as:

$$\beta(k) = d \cdot P(k) + (1-d) \cdot \delta(k) \qquad k = 1,2 \ldots n_1 \tag{20}$$

where: $\beta(k)$ - angle of pitch of the vortex line directly behind the propeller blade at a radius R(k)

$P(k)$ - angle of pitch of the propeller blade at R(k)

$\delta(k)$ - angle of inflow, determined for the propeller axis from known local inflow velocities for a given blade position

d - correlation coefficient, determined on the basis of analysis of propeller performance calculated by the vortex theory

The use of this formulation permits us to separate the problem of specifying the geometry of both regions of the propeller wake from the calculations of circulation strength of the different vortex lines in those regions. The geometry of the flow behind the propeller can be defined only on the basis of the propeller configuration and the character of the outside velocity field. The definition of the vortex strength in particular sectors of the unsteady region will require the use of fairly complex steps, described in detail in the subsequent sections of this report.

VI FUNCTION DESCRIBING THE DISTRIBUTION OF CIRCULATION OF BOUND VORTICES

The unknown distribution of circulation of the bound vortices on the propeller blade is sought in the form of a continuous function defined on the blade surface. There are different formulations describing the distribution of circulation in different applications of lifting-surface models. Trigonometric series have been used in this method, primarily because of the simplicity of performing different mathematical operations on it and also because it has inherent flexibility and adaptability to the changes in flow about the propeller blade. Two new coordinates, related to x(l) and R(k) are introduced on the blade in the following way:

$$\begin{aligned} \vartheta(l) &= \arccos\left[1 - 2\cdot x(l)\right] \qquad l = 1,2 \ldots n_2 \\ \varphi(k) &= \arccos\left[\frac{\frac{1}{2}(1+R_p) - R(k)}{\frac{1}{2}(1-R_p)}\right] \qquad k = 1,2 \ldots n_1 \end{aligned} \tag{21}$$

where: R_p - radius of the propeller hub

It should be indicated, that of the new coordinates, the propeller blade occupies a form of a square region because both coordinates vary in the range of $(0, \pi)$. This substantially simplifies all the operations connected with the trigonometric functions. It is assumed that the distribution of circulation bound to the blade in the direction of the coordinate, ϑ, that is, along the selected blade profile chord, can be expressed with a function:

$$G(\vartheta) = A_1 \cdot \operatorname{ctg}\frac{\vartheta}{2} + \sum_{i=2}^{n_6} A_i \cdot \sin(i-1)\cdot\vartheta \tag{22}$$

The first expression of the series has a singularity (approaching infinity) at the leading edge of the profile ($\vartheta = 0$) and is equal to zero at the trailing edge. All other expressions of the series are equal to zero on both the leading and the trailing edge of the profile. The form of this function is not arbitrary but is derived from a theoretical solution of the two dimensional flow around an infinitesimally thin profile solved by Glauert.

In principle, this function is the sum of an infinite series, however, because all practical calculations are made for a specific number of terms, n_6 is indicated as a limit. To establish the change in the distribution of circulation along the radius, all coefficients of the series (22) are made dependent upon φ:

$$A_i = \sum_{j=1}^{n_5} a(i,j) \cdot \sin j\varphi \tag{23}$$

Substituting (23) into (22), one obtains the final form of the function describing the distribution of bound circulation in the propeller blade:

$$G(\vartheta,\varphi) = \sum_{j=1}^{n_5} \left[a(1,j) \cdot \sin j\varphi \cdot \operatorname{ctg} \frac{\vartheta}{2} + \sum_{i=2}^{n_6} a(i,j) \sin j\varphi \cdot \sin(i-1)\vartheta \right] \tag{24}$$

This function fulfills all the requirements imposed on the distribution of bound circulation, that is, it is equal to zero at the trailing edge, the tip of the blade, and the hub of the propeller. The presence of the singularity on the leading edge of the blade is necessary for correct simulation of blade loading under large, nonideal angles of attack. On the other hand, this singularity precludes the correct establishment of the magnitude of circulation and pressure in close proximity to the leading edge. However, another advantage of function (24) is in the ability to perform simple analytical integration to any desirable limits. The use of the distribution functions permits the simple determination of the strength of the free vortex line contributing to a discrete network of singularities, this applies equally well to vortex lines in the region of the propeller blade and in the stream behind the propeller. The strength of each vortex line has a form of a polynomial with unknown $n_5 \cdot n_6$ factors a(i,j). The determination of these factors is synonymous with the definition of the distribution of blade loading and permits the calculation of the distribution of pressure on the propeller blade. The number of terms in function (24) should be chosen based on a compromise between the size of the computer used to make such calculations and the desire of how faithfully we wish to model the actual loading on the propeller blade.

VII THE BOUNDARY CONDITION AND ITS IMPLICATIONS

The boundary condition used in the method described in this report is the same as it is in other analytical lifting surface models. It states: at every point on the propeller blade surface, the vector component of the velocity flow normal to that surface should be equal to zero. This theorem appears totally self-evident, since there cannot be a flow of fluid across a solid boundary such as the propeller blade. However, the application of this theorem in the case of a propeller operating in a strongly nonuniform velocity field may have a serious deviation from reality. In such a case one may expect local momentary separations and turbulence on the propeller blade and, as a result of these, the actual flow about the propeller may not follow the propeller surface but some surface that includes such separations. Unfortunately, theoretical models of marine propellers do not allow inclusion at present of these phenomena in the boundary condition, and it was decided to retain the traditional definition. Mathematically we define the boundary condition as:

$$VE + \sum_{i=1}^{Z} VW(i) + \sum_{i=1}^{Z}\sum_{j=1}^{N} VZ(i,j) + VC + \sum_{i=1}^{Z} VQ(i) = 0 \qquad (25)$$

where: VE - normal vector component of the inflow velocity

VW - normal vector component of the induced velocity due to singularities defining the propeller blade

VZ - normal vector component of the induced velocity due to a specific sector of the propeller wake unsteady region

VC - normal vector component of the induced velocity due to a steady state region of the propeller wake

VQ - normal vector component of the induced velocity due to a source distribution simulating the finite thickness of the propeller blade

Z - number of propeller blades

N - number of sectors of the unsteady region of the propeller wake

In Equation (25) some of the components are given and some are unknown or more precisely, dependent on unknown factors a(i,j) in the equation defining the distribution of circulation. In the method defining the distribution of pressure on the propeller blade, this equation will be used in two different forms. The first pertains to the calculations of the average of the inflow (onset) velocity field.

$$\sum_{i=1}^{Z} VW(i) + \sum_{i=1}^{Z}\sum_{j=1}^{N} VZ(i,j) + VC = -VE - \sum_{i=1}^{Z} VQ(i) \qquad (26)$$

The left side of Equation (26) contains the terms with the unknown factors a(i,j) and the right side contains factors that are known and defined on the basis of cognizance of the outside flow field or the known intensity of sources simulating finite thickness of the propeller blade. The basic aim of the calculations for the circumferentially averaged inflow (onset) velocity field is to establish the strength of vortex lines in the steady state region of the propeller wake. In subsequent calculations performed for particular positions of the propeller in a nonhomogeneous velocity field, the boundary condition assumes the form:

$$VW(1) + VZ(1,1) = -VE - \sum_{i=1}^{Z} VQ(i) - \sum_{i=2}^{Z} VW(i) - \sum_{j=2}^{N} VZ(1,j) - \sum_{i=2}^{Z}\sum_{j=2}^{N} VZ(i,j) \qquad (27)$$

As implied in Equation (27), only in this case are the induced velocities on the first propeller blade analyzed and the first sector located just behind that blade in the unsteady region of the propeller blade dependent upon the unknown a(i,j). The remaining velocities are known and are derived from the uniform inflow (onset) velocity field or induced by the singularity network of known intensities.

The boundary condition expressed by Equations (25), (26), and (27) should be fulfilled everywhere on the propeller blade. In practice, however, it is checked in a number of chosen control points C. For each of these points we can write equations of the form of Equation (25), obtaining, finally, a matrix $n_3 \cdot n_4$ of equations with factors a(i,j) unknown. The calculation of the normal components of the particular velocity vectors is simplified by the earlier introduction of unit vectors normal to the blade surface at points C.

VIII ONSET VELOCITY FIELD

The characteristics of the onset velocity field that may, for example, be a result of ship wake (backwash or wake current) should be given in the standard form shown in Figure 10. In the propeller disk area, a set of points is defined located on n circles with radii R(k) and, at the same time, on radially oriented straight line segments. The angular spacing between the radial segments in the propeller disk is constant. In each of the selected points the three normal components of the velocity are given: the axial component VEX, the radial component VER, and the tangential component VET in the form of nondimensional quantities normalized on the basis of ship speed. The vector components are positive; VER is directed toward the tip of the propeller blade and VET opposite to the direction of the propeller rotation. The given values are then substituted in the Fourier series in accordance with the method of Reference [22]. The terms of the series are calculated separately for each circumference of radius R(k) and each velocity component. The number of terms defined by this process is equal to the number of given points on each circumference; that is, the maximum amount of information is used. Applying the Fourier series is a very simple way of establishing the three components of the external velocity for a point on any of the coordinates within the propeller disk. For points situated on any one circumference R(k), all that is necessary is to sum up the proper set of terms in the Fourier series for angles defining the location of those points. For example, for the points located on different radii RC(m) it is necessary, after the summations have been made for the adjacent radii R(k) and the appropriate angles, to interpolate the data along the radius. This interpolation is done with second-order curvature over the three closest points given. Thus, we can determine the local magnitudes of the external velocity vector components for each control point on the analyzed propeller blade at some angular propeller position. The magnitude of the angular coordinate for which the summation of the Fourier series is made is equal to:

$$\phi = C\Theta(m,n) + i\,\frac{2\pi}{N} \tag{28}$$

where: $C\Theta(m,n)$ - angular coordinate of the control point

N - total number of analyzed angular propeller positions

i - number of propeller position under analysis

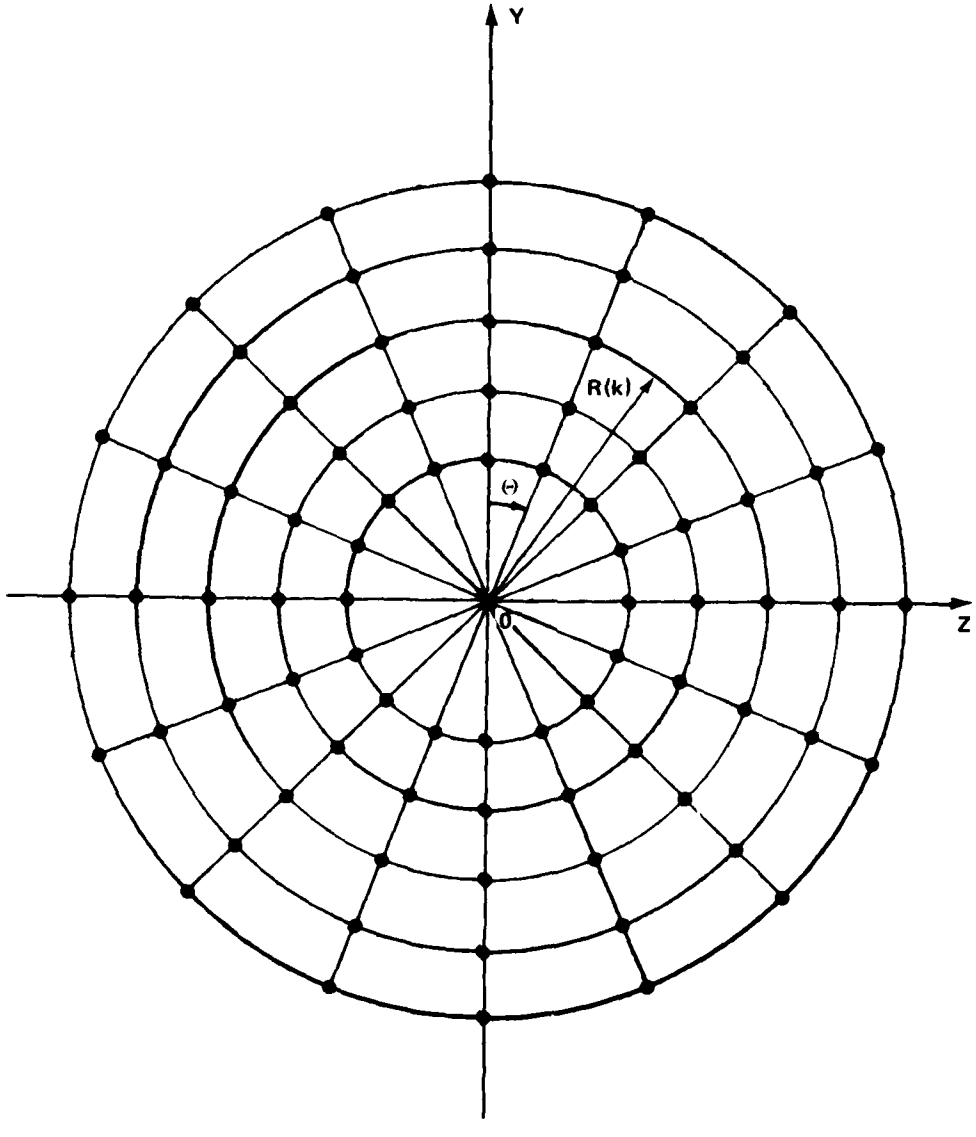

Figure 10 - Distribution of Points where the Onset Velocity Vectors are Defined

The approaching (inflow) velocity vector components to this control point may be expressed as follows:

$$\begin{aligned} VEX &= \sigma_X \cdot VS \\ VEY &= \sigma_R \cdot VS \cdot \cos C\Theta(m,n) - \left[\sigma_T \cdot VS + 2\pi \cdot RC(m) \cdot R_{ps}\right] \cdot \sin C\Theta(m,n) \\ VEZ &= \sigma_R \cdot VS \cdot \sin C\Theta(m,n) + \left[\sigma_T \cdot VS + 2\pi \cdot RC(m) \cdot R_{ps}\right] \cdot \cos C\Theta(m,n) \end{aligned} \tag{29}$$

where: R_{ps} - propeller revolutions per second

VS - ship speed

σ_X, σ_R, σ_T - the sums of appropriate Fourier series terms after interpolations have been made per the following equations:

$$\sigma_X = \sigma_1 \frac{[RC(m)-R(k)]\cdot[RC(m)-R(k+1)]}{[R(k-1)-R(k)]\cdot[R(k-1)-R(k+1)]} + \sigma_2 \frac{[RC(m)-R(k-1)]\cdot[RC(m-R(k+1)]}{[R(k)-R(k-1)]\cdot[R(k)-R(k+1)]} +$$

$$+\sigma_3 \frac{[RC(m)-R(k-1)]\cdot[RC(m)-R(k)]}{[R(k+1)-R(k-1)]\cdot[R(k+1)-R(k)]}$$

$$\sigma_1 = \sum_{i=1}^{M} FCX(k-1,i)\cdot\cos i\phi + \sum_{i=1}^{M} FSX(k-1,i)\cdot\sin i\phi$$

$$\sigma_2 = \sum_{i=1}^{M} FCX(k,i)\cdot\cos i\phi + \sum_{i=1}^{M} FSX(k,i)\cdot\sin i\phi$$

$$\sigma_3 = \sum_{i=1}^{M} FCX(k+1,i)\cdot\cos i\phi + \sum_{i=1}^{M} FSX(k,i)\cdot\sin i\phi$$

and similarly for the remaining components. The indices are selected so that $R(k+1) < RC(m) \wedge R(k) < RC(m)$. Calculations of the projection of the vector normal to the surface of the propeller blade does not present difficulties:

$$VE = VEX \cdot NX(m,n) + VEY \cdot NY(m,n) + VEZ \cdot NZ(m,n) \tag{30}$$

Equations (29) and (30) are also used in the course of calculations for the circumferentially averaged velocity field; however, quantities σ_x, σ_R, and σ_T represent, in this case, average values obtained by summing appropriate terms of the Fourier series for all the selected points on the circumference of R(k) and dividing the sums by the number of points M.

IX VELOCITIES INDUCED BY SINGULARITIES MODELING THE PROPELLER BLADES

In the region of the propeller blades one finds two kinds of singularities inducing velocities in the surrounding area, these are: line vortex segments and sources (sources need not be prejudged, that is, they can be either sources or sinks). To determine velocities induced by the vortex lines, we use the law of Biot-Savart in the form:

$$\bar{V} = \frac{\gamma}{4\pi} \cdot \frac{\bar{B} \times \bar{L}}{L^3} \tag{31}$$

where: $\bar{V}$ - induced velocity vector

γ - strength of induced vortex line

$\bar{B}$ - vector of the vortex line segment

$\bar{L}$ - position vector from the vortex line to the control point

The method of applying Equation (31) for calculating the induced velocities on the propeller blade is shown in Figure 11. Two types of vortex lines are apparent here: vortices bound to the blade $\bar{B}$ and trailing vortices $\bar{T}$. For each type of vortex line, different methods of calculating the strengths are used. The strength of any bound vortex line segment can be calculated in the following way:

$$\gamma_B = \frac{(R_T - R_p) \cdot F(m)}{[R(m+1) - R(m)]} \int_{\varphi_1}^{\varphi_2} \int_{\vartheta_1}^{\vartheta_2} G(\vartheta, \varphi)\, d\vartheta\, d\varphi \tag{32}$$

where: R_T - propeller tip radius

$G(\vartheta, \varphi)$ - function defining distribution of circulation by Equation (24)

The term in front of the double integral in Equation (32) is a result of integration in coordinates $\vartheta\varphi$. Equation (32) can be interpreted in the following way: To each bound vortex line segment there is some assigned elementary area bound by coordinates φ_1, φ_2 and ϑ_1, ϑ_2. The circulation distributed over this area continuously by the function $G(\vartheta, \varphi)$ is replaced with a concentrated vortex $\bar{B}$ of intensity γ_B. Integration of the function $G(\vartheta, \varphi)$ is relatively straightforward and as a result we obtain a polynomial with unknown values of a(i,j):

$$\int_{\varphi_1}^{\varphi_2} \int_{\vartheta_1}^{\vartheta_2} G(\vartheta, \varphi)\, d\vartheta\, d\varphi = \sum_{i=1}^{n_5} \sum_{j=1}^{n_6} J(i,j) \cdot a(i,j) \tag{33}$$

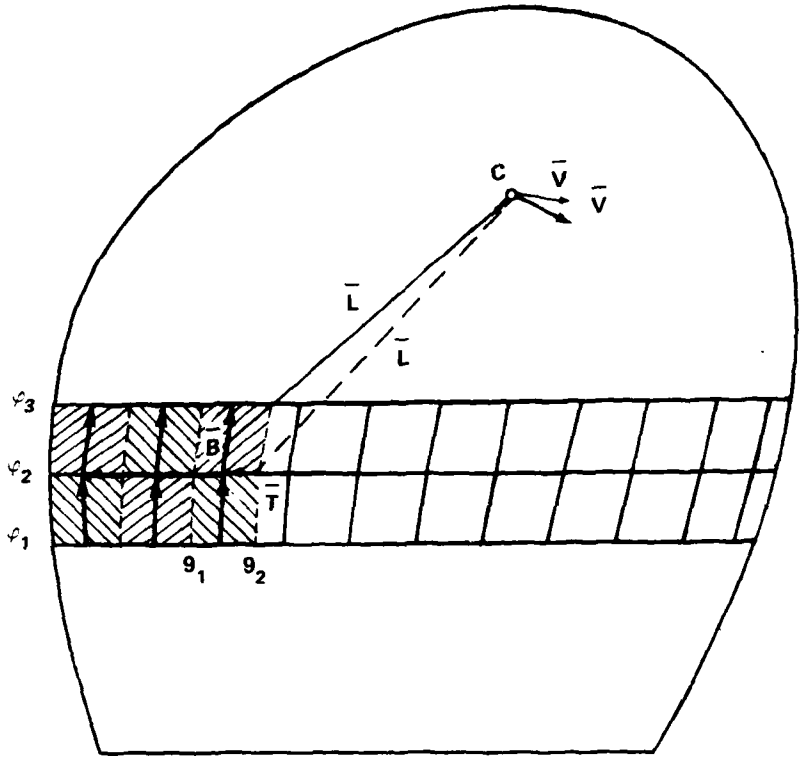

Figure 11 - Definition of Velocities Induced by Singularities Modeling the Propeller Blades

where: J (i,j) - integrals of the appropriate trigonometric functions.
Equation (31) may be expressed in terms of coordinates of appropriate vectors in the following way:

$$VX = \left[BY(m,n)\cdot LZ - BZ(m,n)\cdot LY\right]\cdot\frac{(R_T-R_p)\cdot F(m)}{\left[R(m+1)-R(m)\right]}\cdot\frac{\sum_{i=1}^{n_5}\sum_{j=1}^{n_6}J(i,j)\cdot a(i,j)}{4\pi\cdot\left[LX^2+LY^2+LZ^2\right]^{3/2}}$$

$$VY = \left[BZ(m,n)\cdot LX - BX(m,n)\cdot LZ\right]\frac{(R_T-R_p)\cdot F(m)}{\left[R(m+1)-R(m)\right]}\cdot\frac{\sum_{i=1}^{n_5}\sum_{j=1}^{n_6}J(i,j)\cdot a(i,j)}{4\pi\left[LX^2+LY^2+LZ^2\right]^{3/2}} \qquad (34)$$

$$VZ = \left[BX(m,n)\cdot LY - BY(m,n)\cdot LX\right]\frac{(R_T-R_p)\cdot F(m)}{\left[R(m+1)-R(m)\right]}\frac{\sum_{i=1}^{n_5}\sum_{j=1}^{n_6}J(i,j)\cdot a(i,j)}{4\pi\cdot\left[LX^2+LY^2+LZ^2\right]^{3/2}}$$

where: LX = CX (k,1) - BSX (m,n)

and so forth for the remaining coordinates.

Equations (34) define vector components of the velocity induced by the bound vortex $\bar{B}(m,n)$ at the control point C(k,1). It is possible to obtain a simple projection of this velocity normal to the surface of the blade at the point C(k,1) according to the equation:

$$VN = VX\cdot NX(k,l) + VY - NY(k,l) + VZ - NZ(k,l) \qquad (35)$$

and projections of this vector along the radial and tangential directions:

$$VR = VZ\cdot\sin C\Theta(k,l) + VY\cdot\cos C\Theta(k,l)$$
$$VT = VZ\cdot\cos C\Theta(k,l) - VY\cdot\sin C\Theta(k,l) \qquad (36)$$

Determination of components of velocities induced by the trailing vortices is accomplished with similar equations. The only difference is that another method is used for calculating the intensity of the trailing vortex segment $\bar{T}$:

$$\gamma_T = \frac{(R_T-R_p)\cdot F(m)}{\left[R(m+1)-R(m)\right]}\left[\int_{\varphi_2}^{\varphi_3}\int_{0}^{\vartheta_2}G(\varphi,\vartheta)\,d\vartheta\,d\varphi - \int_{\varphi_1}^{\varphi_2}\int_{0}^{\vartheta_2}G(\varphi,\vartheta)\,d\vartheta\,d\varphi\right] \qquad (37)$$

The previous equation can be interpreted as follows: The strength of the vortex segment $\overline{T}$ is equal to the difference of the circulation intensities of two adjacent bound segments located between the coordinates ϕ_3, ϕ_2 and ϕ_2, ϕ_1 in the region from the leading edge $\vartheta = 0$ to a coordinate defining the segment position $T \cdot \vartheta = \vartheta_2$. Such a formulation ensures that the vortex network satisfies the Hemholz circulation theorem.

Note that the above method of applying the law of Biot-Savart gives accurate results only when the control point is located sufficiently far from the elemental line of the line vortex. Analytical examination proved that the following relation is necessary:

$$L \geq 10 \cdot B \tag{38}$$

In practice for the case in which Equation (38) is not satisfied, the vector $\overline{B}$ is divided into a sufficient number of segments of equal circulation intensity γ_B. For each segment the component of induced velocity is established separately according to Equation (34). A method for calculating a control point lying in proximity to the vortex line is shown in Figure 12. Similar principles are applied to establish velocities induced by the vortex lines $\overline{T}$.

The equations discussed so far apply to the case in which the control points and the singularities are located on the same propeller blade, that is, on the analyzed blade. To calculate velocities induced by singularities located on the remaining blades, we use transformation equations based on a rectangular coordinate system rotated at an angle equal to the difference between the analyzed blade and the blade on which the singularities are located. These equations have the form:

$$\begin{aligned} Y_n &= Y_S \cos\frac{2\pi}{Z}(i-1) - Z_S \cdot \sin\frac{2\pi}{Z}(i-1) \\ Z_n &= Y_S \cdot \sin\frac{2\pi}{Z}(i-1) + Z_S \cdot \cos\frac{2\pi}{Z}(i-1) \end{aligned} \tag{39}$$

where: Y_n, Z_n = coordinates in the new coordinate system (coordinate x remains unchanged)

Y_s, Z_s - coordinates in the original coordinate system

i - number of the blade on which the singularities are located

Quantities BY, BZ, TY, TZ, BSY, BSZ, TSY, and TSZ are subject to transformation according to Equation (39). After these quantities are transformed, they can be inserted directly into Equation (24).

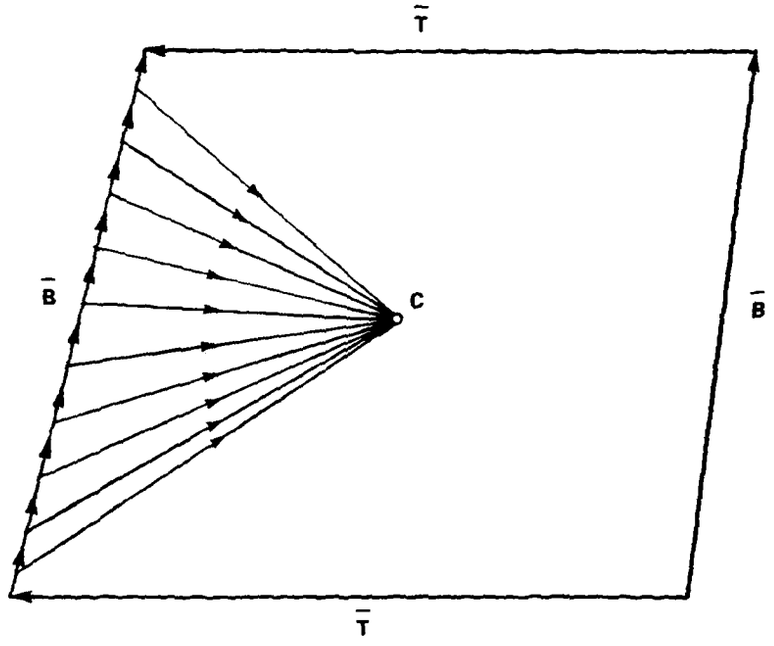

Figure 12 - A Method of Calculating Induced Velocities when the Singularities and the Control Point are Near Each Other

A table of induction coefficients is calculated in accordance with the above equations separately for each of the propeller blades and separately for each component VX, VR, VT, and VN of the induced velocity. For the whole propeller then, we have 4 · Z separate tables of induction coefficients. A table of induction coefficients is a matrix of $n_3 \cdot n_4$ lines and $n_5 \cdot n_6$ columns; that is, the number of lines is equal to the number of control points distributed on the analyzed blade, and the number of columns is equal to the number of terms in the function defining the distribution of circulation. If we designate the table of induction coefficients by I(p,q), and if the indices defining the element in the table are interrelated with the indices defining the control point C(k,1) as well as an unknown coefficient of circulation distribution a(m,n), then they are related by the following relationships:

$$\begin{aligned} p &= (k-1)\cdot n_4 + l \quad \text{when } C(k,l) \qquad k = 1,2 \ldots n_3 \;;\; l = 1,2 \ldots n_4 \\ q &= (m-1)\cdot n_6 + n \quad \text{when } a(m,n) \qquad m = 1,2 \ldots n_5 \;,\; n = 1,2 \ldots n_6 \end{aligned} \tag{40}$$

Each element in the table I(p,q) was derived through a summation of factors a(m,n) obtained by Equation (34) performed for all segments of the vortex lines distributed on a given propeller blade at a specified control point C(k,1) and a defined component of induced velocity. As an example, we give a complete definition for one term I(p,q) in the table of induction coefficients for the axial component of induced velocity:

$$\begin{aligned} I(p,q) = \sum_{m=1}^{n_2-1} \sum_{n=1}^{n_2-1} & \frac{\left\{BY(m,n)\cdot\left[CZ(k,l) - BSZ(m,n)\right] - BZ(m,n)\left[CY(k,l) - BSY(m,n)\right]\right\}}{4\pi\left[R(m+1) - R(m)\right]} \\ & \frac{(R_T - R_p)\cdot F(m) J_B(i,j)}{\left\{\left[CX(k,l) - BSX(m,n)\right]^2 + \left[CY(k,l) - BSY(m,n)\right]^2 + \left[CZ(k,l) - BSZ(m,n)\right]^2\right\}^{3/2}} + \\ + \sum_{m=1}^{n_1} \sum_{n=1}^{n_2-1} & \frac{\left\{TY(m,n)\cdot\left[CZ(k,l) - TSZ(m,n)\right] - TZ(m,n)\cdot\left[CY(k,l) - TSY(m,n)\right]\right\}}{4\pi\left[R(m+1) - R(m)\right]} \\ & \frac{(R_T - R_p)\cdot F(m)\cdot J_T(i,j)}{\left\{\left[CX(k,l) - TSX(m,n)\right]^2 + \left[CY(k,l) - TSY(m,n)\right]^2 + \left[CZ(k,l) - TSZ(m,n)\right]^2\right\}^{3/2}} \end{aligned} \tag{41}$$

where: $J_B(i,j)$ - integral of a trigonometric function multiplied by a(i,j) used to calculate velocity induced by a bound vortex

$J_T(i,j)$ - integral of a trigonometric function multiplied by a(i,j) used in the calculation of velocities induced by the trailing vortex

Obviously: $p = (k-1) \cdot n_4 + \iota$; $q = (i-1) \cdot n_6 + j$

Consequently, if the values a(i,j) are known (thus determining the distribution of bound vorticity on any propeller blade), a simple determination of an assumed component of an induced velocity at an assumed control point on the analyzed blade is possible. All that is necessary is to multiply a(i,j) by I(p,q) taken from an appropriate line of the table of induction coefficients and to sum the calculated products.

The second kind of singularity present on a propeller blade is the source simulating the finite thickness of the blade. The process of establishing the strength of each source and the related induced velocities is done separately from the calculations of circulation distribution. Therefore, in Equations (26) and (27) describing the boundary condition, velocities induced by the sources are always presented as given. From the equation for the potential of the point source located in a three-dimensional space, we introduce a function for the induced velocity

$$VQ = \frac{1}{4\pi} \frac{Q}{L^2} \tag{42}$$

where: Q - source strength

L - vector length connecting the source with the control point

VQ - source induced velocity in the direction consistent with L

To use Equation (42) one must know the strength of all the sources that form a discrete source network as described in Section IV. Figure 13 illustrates the method. Each source line Q(m,n) represents a certain portion of the propeller blade volume included by radii R(m+1) and R(m) and chordwise coordinates x(n+1) and x(n). As a consequence of the assumption of the boundary condition that there be no flow across the propeller blade surface (in this case we mean the low and high pressure surfaces of the blade), the sources Q(m,n) should have an intensity sufficient to compensate for the fluid inflow to the assigned volume. Mathematically, one can express this as follows:

$$Q(m,n) = \frac{dV_{ol}}{dx} \cdot V + \frac{dV}{dx} \cdot V_{nl} \tag{43}$$

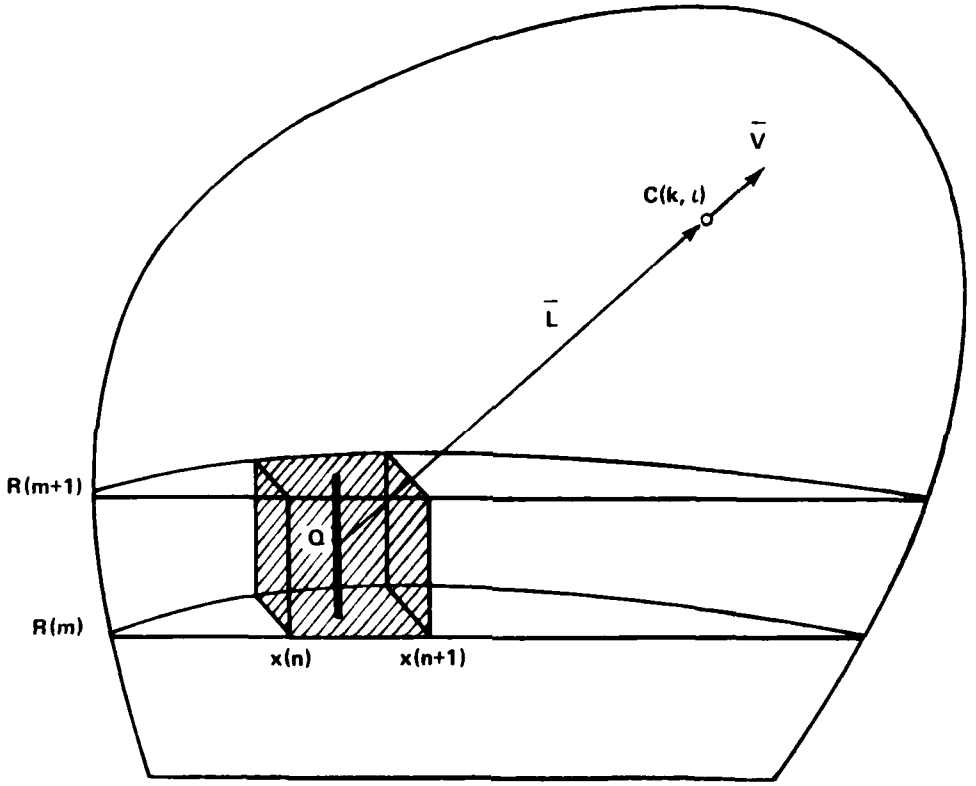

Figure 13 - Method for Establishing Velocities Induced by Sources Simulating the Finite Blade Thickness

where: V - velocity of the fluid inflow to the elemental volume assigned to the source

V_{ol} - volume of the blade element

The first term of Equation (43) represents the source output equivalent to the increase in volume of a given element of the blade between x(n) and x(n+1), and the second term -xpresses the source output as a result of the velocity change in fluid motion in that segment. Because the calculations of the second term, particularly for a propeller operating in a nonuniform velocity field, turned out to be very difficult and did not affect the final results significantly. it was decided to assume a fixed velocity of inflow at each propeller blade radius. Furthermore, it was decided to use, in the calculations of the strength of a particular source, a circumferentially averaged velocity of a nonuniform velocity field:

$$V = \sqrt{VEX^2 + [2\pi R(k) \cdot R_{ps} - VET]^2} \tag{44}$$

where: VEX, VET indicate averaged values at radius R(k)

With such simplifying assumptions it is possible to establish velocities induced by the sources at all control points before the distribution of circulation is established, and it is possible to include these velocities as given in the boundary condition. Velocity components induced by the source Q(m,n,) at a control point C(k,1) can be defined by the following equations:

$$VQX = \frac{Q(m,n)}{4\pi} \cdot \frac{LX}{(LX^2 + LY^2 + LZ^2)^{3/2}}$$

$$VQY = \frac{Q(m,n)}{4\pi} \cdot \frac{LY}{(LX^2 + LY^2 + LZ^2)^{3/2}} \tag{45}$$

$$VQZ = \frac{Q(m,n)}{4\pi} \cdot \frac{LZ}{(LX^2 + LY^2 + LZ^2)^{3/2}}$$

where: LX = CX(k,1) - BSX(m,n) and similarly for the other components.

It should also be clarified why sources in the form of straight line segments of continuous and uniform intensity are considered, since Equation (42), valid for a point source, was used to establish induced velocities. Similar to the case of vortex lines,

this equation is used only when the length of the vector $\overline{L}$ is at least ten times greater than the length of vector $\overline{B}$ (equal to the length of segment Q). In the remaining cases we divide segment Q into an appropriate number of parts and integrate numerically, as was done with the vortex lines. When Equation (45) is used for the remaining propeller blades, the transformation equations should be used to calculate components of the vector $\overline{L}$.

X VELOCITIES INDUCED BY FREE VORTEX SHEETS

To calculate the velocities induced by free vortex sheets located in the propeller wake, we use the Biot-Savart law. On the basis of that law, equations are derived for a particular velocity component induced, respectively, by a segment of a helical vortex and a segment of a radial line vortex. The geometrical basis for these relationships is shown in Figure 14. Velocity components induced by the segment of helical vortex $\overline{T}$ at the control point C on the analyzed blade are expressed by the equation:

$$VX = \frac{\gamma_T}{4\pi} \cdot \frac{R^2 - R \cdot RC \cos\alpha}{\left[X_p^2 + RC^2 + R^2 - 2 \cdot R \cdot RC \cdot \cos\alpha\right]^{3/2}}$$

$$VR = \frac{\gamma_T}{4\pi} \cdot \frac{R \cdot x_p \cdot \cos\alpha - R \cdot tg\beta \cdot \sin\alpha}{\left[X_p^2 + RC^2 + R^2 - 2 \cdot R \cdot RC \cdot \cos\alpha\right]^{3/2}}$$

$$VT = \frac{\gamma_T}{4\pi} \cdot \frac{R \cdot x_p \cdot \sin\alpha - R \cdot tg\beta + R \cdot tg\beta \cdot \cos\alpha}{\left[X_p^2 + RC^2 + R^2 - 2 \cdot R \cdot RC \cdot \cos\alpha\right]^{3/2}} \qquad (46)$$

$$VY = VR \cdot \cos C\Theta - VT \cdot \sin C\Theta$$

$$VZ = VR \cdot \sin C\Theta + VT \cos C\Theta$$

$$VN = VX \cdot NX + VY \cdot NY + UZ \cdot NZ$$

where: $\alpha = \frac{2\pi i}{Z} + \Theta_{st} + j \, d\Theta$

- i - blade number behind which the free vortex sheet is placed
- j - consecutive number designating an elementary segment of the helical vortex within a given sector
- Θ_{st} - initial angular coordinate of the sector
- $d\Theta$ - angle describing the size of the elementary helical vortex segment
- $X_p = X_{st} + j \cdot d\Theta \cdot tg\beta$
- X_{st} - distance from the radial vortex at the leading edge of a sector to the control point (along the x axis)

The intensity of the vortex line γ_T is defined by Equation (37) by integration with respect to ϑ in the interval from 0 to π_1 and it has the form of a polynomial with unknown factors a(i,j). To calculate the velocities induced by the helical vortex

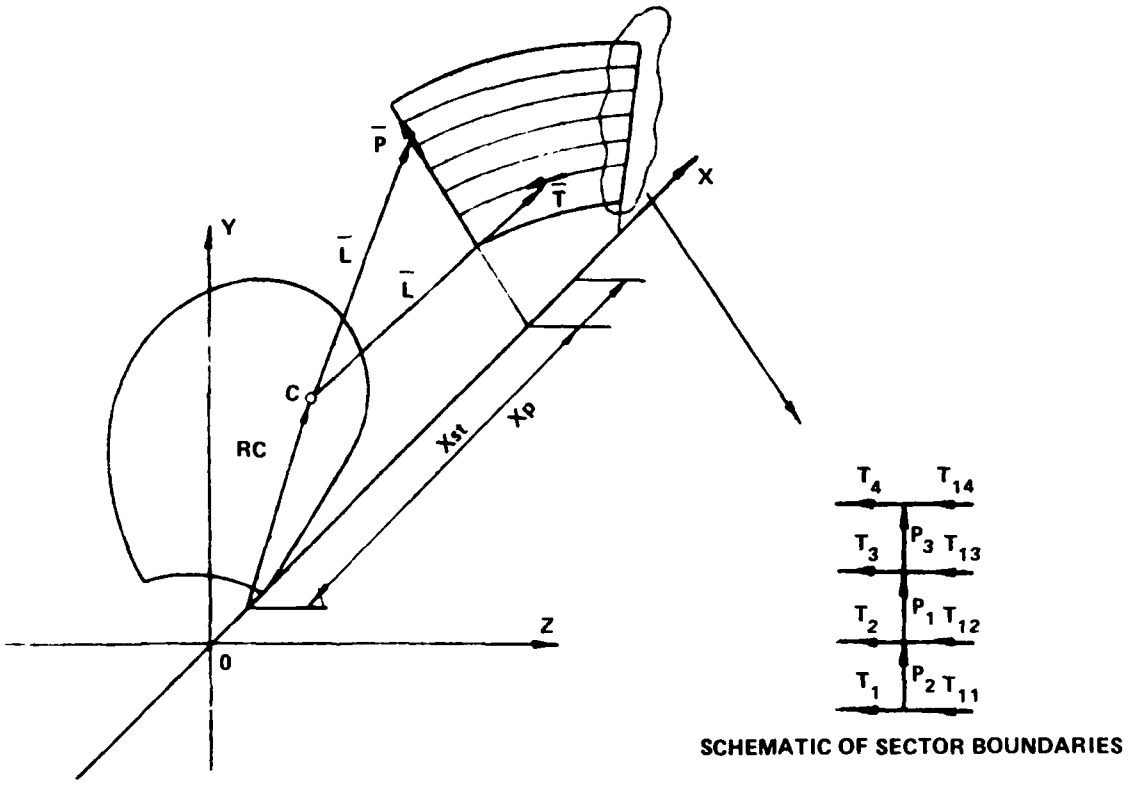

Figure 14 - Designation of the Velocities Induced by the Singularities Forming the Free Vortex Sheet

segment contained within one sector, numerical integrations by Simpson's rule are performed by dividing the helix into an appropriate number of elementary segments dH. A large number of elementary segments is chosen for the sectors near the propeller blade and a smaller number for sectors located farther away from the propeller blade, so that an optimum compromise is reached between accuracy of integration and length of calculations.

Equations have also been derived for the vector components induced at the control point C by the segment of the radial vortex line $\bar{P}$:

$$VX = \frac{\gamma_P}{4\pi} \frac{R \cdot \sin\alpha}{\left[X_p^2 + RC^2 + R^2 - 2 \cdot R \cdot RC \cdot \cos\alpha\right]^{3/2}}$$

$$VR = \frac{\gamma_P}{4\pi} \frac{X_p \cdot \sin\alpha}{\left[X_p^2 + RC^2 + R^2 - 2 \cdot R \cdot RC \cdot \cos\alpha\right]^{3/2}} \qquad (47)$$

$$VT = \frac{\gamma_P}{4\pi} \frac{X_p \cdot \cos\alpha}{\left[X_p^2 + RC^2 + R^2 - 2\,R \cdot RC \cdot \cos\alpha\right]^{3/2}}$$

VY, VZ, VN - *as in Equations* (46)

α_p - } indicates the same quantities as in Equation (46) but calculated for

X_p - } the vortex line segment

As mentioned before, because the presence of radial vortex lines stems from the Helmholtz theorem describing circulation conservation, the strength of these vortex lines will be different from zero only when segments of the same helical vortices in adjacent sectors have different circulation strengths. In such a case the strength of each radial segment is dependent on the adjacent segments of the helix (compare with Figure 14):

$$\gamma_{P1} = \gamma_{T11} - \gamma_{T1}$$

$$\gamma_{P2} = \gamma_{P1} + \gamma_{T12} - \gamma_{T2} \qquad \text{and so forth}$$

Similarly, as in the case of the propeller blades when Equations (46) and (47) are used, one calculates tables of induction coefficients I(p,q). These tables are calculated separately for each sector of the unsteady region of the propeller wake, for the steady region, and for the axial, radial, tangential, and normal components of the induced velocities. To describe fully the velocity in the wake of the

propeller defined by N sectors behind propeller with Z number of blades, it is necessary to calculate 4Z(N+1) tables. The dimensions of the tables, the method of calculation, and the interpretation of the induction coefficients calculated for the stream in the wake of the propeller are identical to similar tables calculated before for the propeller blades. The use of the induction coefficients permits calculations at any control point on the analyzed blade for any component of velocity induced by the selected sector of the propeller wake only if coefficients a(i,j) describing circulation distribution in that sector are known. Furthermore, note that the induction coefficient tables I(p,q,) for the same component of induced velocity are additive, that is, if, in a large part of the propeller wake or in the whole system composed of the propeller and the free surface vortices, the distribution of circulation is the same, one can add appropriate tables I(p,q) before they are multiplied by coefficients a(i,j).

XI CALCULATIONS OF THE PRESSURE DISTRIBUTIONS ON A PROPELLER BLADE IN AN AVERAGED APPROACHING (ONSET) VELOCITY FIELD

Calculations of the pressure field acting on a propeller blade while it is operating in a circumferentially averaged velocity field are performed the same way whether this is an ultimate goal of the calculations or the aim of the calculations is to establish the description of the pressure field for nonuniform flow. In the second case, the solution obtained for the averaged condition provides a first approximation of the performance of the propeller in a nonuniform field. The important aspect of such calculations is the establishment of the distribution of the strength of the free vortices in the stream of the propeller wake. Furthermore, calculated magnitudes of the pressure distribution can also be used to establish overall average performance characteristics of a given propeller in the form of thrust and torque coefficients and efficiency. It should be stressed that the method discussed in this section, in a strict sense, has been derived for a circumferentially averaged velocity field only when the given field of external velocities is actually axially symmetric. Otherwise, the free surface vortices in the nonsteady region of the propeller wake, as defined in Section V, have nonuniform pitch distributions dependent on variable blade loading in the course of propeller rotation. This will cause some discrepancy with respect to the exact solution obtained for the averaged conditions, but this is justified because, in the course of these calculations, we obtain a distribution of the free vortex strengths, significant in itself, that will be used in the calculation for the nonuniform velocity field.

The first step in determining the pressure field on the propeller blade is to establish the magnitudes of coefficients a(i,j) used in multiplying the terms of a series describing the distribution of bound circulation to the propeller blades (24). The boundary condition used here has the form of Equation (26). The use of this boundary condition for all $n_3 \cdot n_4$ control points c(m,n), that have been chosen on the analyzed blade, leads to the establishment of a set of linear equations that can be schematically defined as follows:

$$K(p,q) \cdot U(q) = H(p) \tag{48}$$

where: K(p,q) - matrix of coefficients multiplying the set of unknowns

U(q) - matrix-vector of unknowns, resulting from a transposition of rectangular matrix a(i,j); vector: $U(q) \equiv a(i,j)$ when $q = (i-1) \cdot n_6 + j$

H(p) - matrix-vector of independent terms

We can obtain the matrix of coefficients that form products with unknowns K(p,q) very simply. Because the propeller is operating in a circumferentially averaged velocity field, that is, in a given environment, all the elements that form the vortex model, both those located on the propeller blades and in the stream of the propeller wake, would have the circulation distribution defined with the same coefficient U(q) (or a(i,j)). All that is necessary is to sum all the induction coefficients for the normal component of the induced velocity using the tables already calculated. Tables for this summation are prepared for all the propeller blades and all the sectors of the unsteady and steady regions of the propeller wake. To determine vector H(p) it is necessary, consistent with Equation (26), to sum for each control point normal components of velocities derived from the external field (Equation (30)) as well as normal components of velocities induced by a discrete source distribution (Equation (45)).

The set of linear equations defined by Equation (48) can be a fully determined set (only when p=q) or overdetermined set (when p>q). In the first case, the number of control points C(m,n) selected on the analyzed propeller blade is equal to the number of unknown coefficients U(q) defining the distribution of circulation. The solution obtained by Equation (48) is then exact and unique, and any indications of errors are a result of limitations in the numerical methods used. In the second case, in which the number of control points is larger than the number of unknown coefficient U(q), we obtain the so-called pseudosolution of an overdetermined set of equations. The pseudosolution arises as a result of imposing specified conditions on the vector difference, which is the difference between the left and the right side of Equation (48) after the calculated results have been substituted into that equation. Most frequently, the vector is required to satisfy the minimum average least square deviation.

The conclusion that calculations should be performed in such a way that the full set of equations is made available to obtain the exact solution is not correct in every situation. The full set of linear equations is very sensitive to the accuracy of calculating the elements of matrices K(p,q) and H(p). Frequently, minimal errors in the designation of one factor causes a diametrically opposite change in the derived solution. This may have particular significance in the case of calculations for a propeller operating in a strongly nonuniform velocity field, where a change in any

one component of the boundary condition may affect, in an inadmissable way, and inconsistent with the contributing physical phenomena, the distribution of circulation on the whole propeller blade. The experience gained in the course of this effort, solving several hundred sets of equations defining the distribution of circulation in two-dimensional and three-dimensional flow, indicates that it is far safer to use an overly determinate set of equations.

In order that neither possibility is eliminated a priori, an algorithm to solve Equation (48) is used that permits calculations of the vector U(q) in both cases. This (Equation (22)) is based on the multiplication of matrices K(p,q) and H(p) in succession by q specifically defined orthogonal matrices. In this way the initial matrix is transformed into a top triangular matrix, and one can readily calculate the vector U(q) by the so-called reverse process. The algorithm is somewhat less efficient (in terms of computational time) than the Gauss-Jordan method of solving a fully determined system, but it is the fastest and best way of solving an overdetermined system.

When the set of Equations (48) is solved, one can determine the strength of the bound vortices at each point of the analyzed blade, especially at each control point C(m,n). To accomplish this, it is sufficient to sum a series of terms defined by Equation (26) for the coordinate (φ, ϑ), specifying the location of the control points, establishing, in that way, the values $G(\varphi, \vartheta)$. The establishment of the values U(q) also permits us to define any component of the induced velocity at all control points (when appropriate tables of induction coefficients are used). At this point one can determine the pressure distribution.

To establish the magnitudes of pressure at all control points of the analyzed blade we use Bernoulli's theorem defined in the propeller coordinate system [1]:

$$\frac{P_0}{\rho} + \frac{V_0^2}{2} = \frac{p}{\rho} + \frac{V^2}{2} - \frac{(2\pi \cdot RC \cdot R_{ps})^2}{2} \tag{50}$$

where: V_0 - flow velocity far ahead of the propeller
P_0 - pressure far ahead of the propeller
V - velocity on the propeller blade (including induced velocity)
p - pressure on the propeller blade
ρ - fluid density

If we assume that the speed V from Equation (50) has the following components:

VS+VX - in the direction of the X axis
$2\pi \cdot RC \cdot RPS+VT$ - in the direction of the T axis
VR - in the direction of the R axis

then, Equation (50) can be transformed into the following nondimensional coefficient:

$$C_p = \frac{P_0 - P}{\frac{1}{2}\rho\left[VS^2 + (2\pi \cdot RC \cdot RPS)^2\right]} = \frac{VI^2 + 2 \cdot (VS \cdot VX + 2\pi \cdot RC \cdot R_{ps} \cdot VT)}{VS^2 + (2\pi \cdot RC \cdot R_{ps})^2} \qquad (51)$$

where: VI - fully induced velocity: $VI = (VX^2 + VR^2 + VT^2)^{1/2}$

Naturally, the induced velocities will be different on the pressure side of the propeller blade than on the suction side. The difference in velocities between the pressure and the suction sides of the blade at any point is equal to the magnitude of circulation $G(\vartheta, \varphi)$ at that point. So, to establish the distribution of pressure on both sides of the propeller blade, it is necessary to know at all control points the three components of the total induced velocity as well as the three components of velocity difference between both sides of the propeller blade. To calculate components of the total velocity induced by the network of singularities, we use the tables of induction coefficients. Because the function of the circulation distribution is the same for all parts of the network of singularities, it is necessary to sum the tables of coefficient I(p,q) separately for each component of the induced velocity and then to multiply the tables by vector U(q). After the products are summed for each control point separately, we obtain the values of VX, VR, VT at those points.

In the case of the velocity difference across the blade surfaces, we assume that:

- the circulation of the bound vortices does not produce a radial component of velocity.
- one-half of that circulation value is the increase of velocity on the suction side of the blade and one-half is the decrease in velocity on the pressure side.

We establish the values of particular components of the velocity difference for the control point C(k,1) on the basis of the following equations:

$$VGT = \frac{1}{2} \cdot G(\vartheta,\varphi)\ NX(k,l) \cdot \frac{1}{\left[A^2 + NX(k,l)^2\right]^{1/2}}$$
$$VGX = -VGT \cdot \frac{A}{NX(k,l)} \tag{52}$$

where: $A = NZ(k,l)\ \cos C\Theta(k,l) - NY(k,l) \cdot \sin C\Theta(k,l)$

At this point we can write the complete equation for the pressure coefficient for both sides of the propeller blade:

$$C_{ps,c} = \frac{(VX \pm VGX)^2 + (VT \pm VGT)^2 + VR^2 + 2\left[VS \cdot (VX \pm VGX) + 2\pi \cdot RC \cdot R_{ps} \cdot (VT \pm VGT)\right]}{VS^2 + (2\pi \cdot RC \cdot R_{ps})^2} \tag{53}$$

XII CALCULATIONS OF THE PRESSURE DISTRIBUTION ON A PROPELLER BLADE IN A NONUNIFORM ONSET VELOCITY FIELD

The process of calculating the pressure field on a propeller blade in a nonuniform velocity field was constructed in such a way that the unsteady phenomena associated with an operating propeller are simulated with the greatest possible accuracy. In none of the mathematical equations considered does the time parameter appear explicitly. Instead, an instantaneous position of the propeller is used in a geometrical sense, while assuming uniform rotation of the propeller which is synonymous with making the phenomena dependent on time. The exact explanation of the method used can best be illustrated with a detailed example. A four-bladed propeller operating in a nonuniform velocity field has been chosen. It is assumed that the unsteady region of the propeller wake includes one full revolution of the helical vortex surfaces and that this region is divided into eight sectors. This implies that eight angular positions of the propeller during a full revolution are analyzed. Note that for such assumptions the calculations have been made and the results discussed in Section XV.

Calculations are made first for the circumferentially averaged velocity field. Two sets of calculations are made, one for each of the two full revolutions of the propeller. In both sets of calculations we use the boundary condition in the form defined by Equation (27); that is, all velocities except the ones induced by the singularities of the analyzed blade and the first sector following it are assumed known. We write a set of linear equations resulting from the boundary condition:

$$K(p,q)\ U_i(q) = H_i(p) \tag{54}$$

where: $U_i(q)$ - solution for the i position of the blade

$H_i(p)$ - matrix of free terms for the i position of the blade

Matrix K(p,q) is, in all calculations for the nonuniform velocity field, constructed from a summation of the tables of induction coefficients of the normal component of the velocity induced for the analyzed blade and the first sector of the vortex trail behind that blade. As mentioned previously, velocities induced by the network of sources were calculated for the averaged flow and are treated as fixed. Normal components of the external velocities are calculated each time for the actual position of the control points on the analyzed blade relative to the external velocity field. Eventually, velocities induced by the remaining propeller blades and the singularities of the propeller wake are calculated again for each position using appropriate

PRECEDING PAGE BLANK-NOT FILMED

tables of induction coefficients for a known distribution of circulation intensity in the particular regions. For the steady-state region of the propeller wake, a circulation distribution obtained from calculations of the averaged case is always used. Thus the unsteady phenomena are accounted for in the calculations based on computation of the matrix of the free terms H(p) at each propeller position on the basis of actual values of both the inflow velocity and the velocities induced by the singularities of the unsteady region of the propeller wake and adjacent blades.

The first series of calculations in the unsteady velocity field is not used directly to establish the distribution of pressure on the propeller blade. It is used, however, to compute the distribution of circulation intensity in the particular sectors of the unsteady region of the propeller wake. The sequence of steps is illustrated in Figure 15. In the first series of calculations, it is assumed that the remaining propeller blades (with the exception of the analyzed blade) and the free vortex sheets extending from those blades possess the same distribution of circulation defined by values U(q) calculated for the averaged velocity field. The effects of a propeller operating in a nonuniform velocity field become apparent only in the unsteady region behind the analyzed propeller blade. At first, this part of the unsteady region has the circulation distribution defined in full by U(q). Figure 15 shows how to use successively computed solutions of $U_i(q)$ to establish velocities induced by the respective sectors within the area of the propeller wake. After all eight propeller positions corresponding to one revolution have been analyzed, one proceeds to the next series of calculations.

In the second series of calculations, the effects of the propeller operating in the nonuniform velocity field on all free vortex sheets in the unsteady region of the propeller wave become apparent. To calculate velocities induced by the respective sectors of the free vortex sheets behind blades numbers 2, 3, and 4, one uses the circulation distributions computed in the previous series of calculations, arranged in appropriate sequence. The unsteady region behind the analyzed blade is at first defined with these distributions, and then, sequentially supplemented by the results $U_i(q)$ obtained in this series.

The sequence of steps is shown schematically in Figure 16. At this time, in addition to establishing successive distributions of circulation $U_i(q)$, one also calculates the distribution of pressure on both sides of the analyzed blade for each propeller position in the course of one revolution. To perform that, Equation (53) is used, substituting into it each time a component of the induced velocity and the

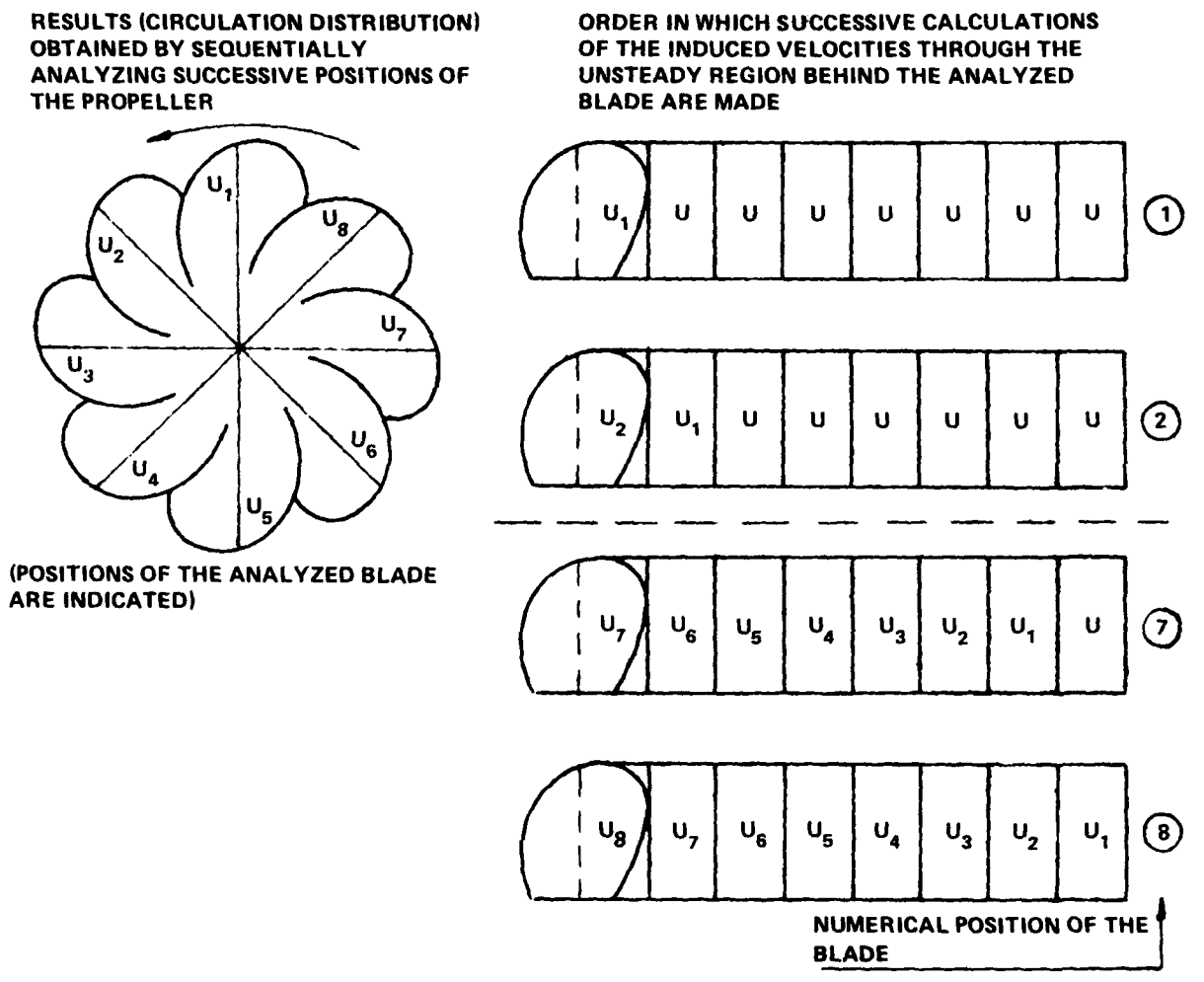

Figure 15 - Schematic of the First Sequence of Calculations for Establishing the Pressure Distribution on a Propeller Blade in a Nonuniform Velocity Field

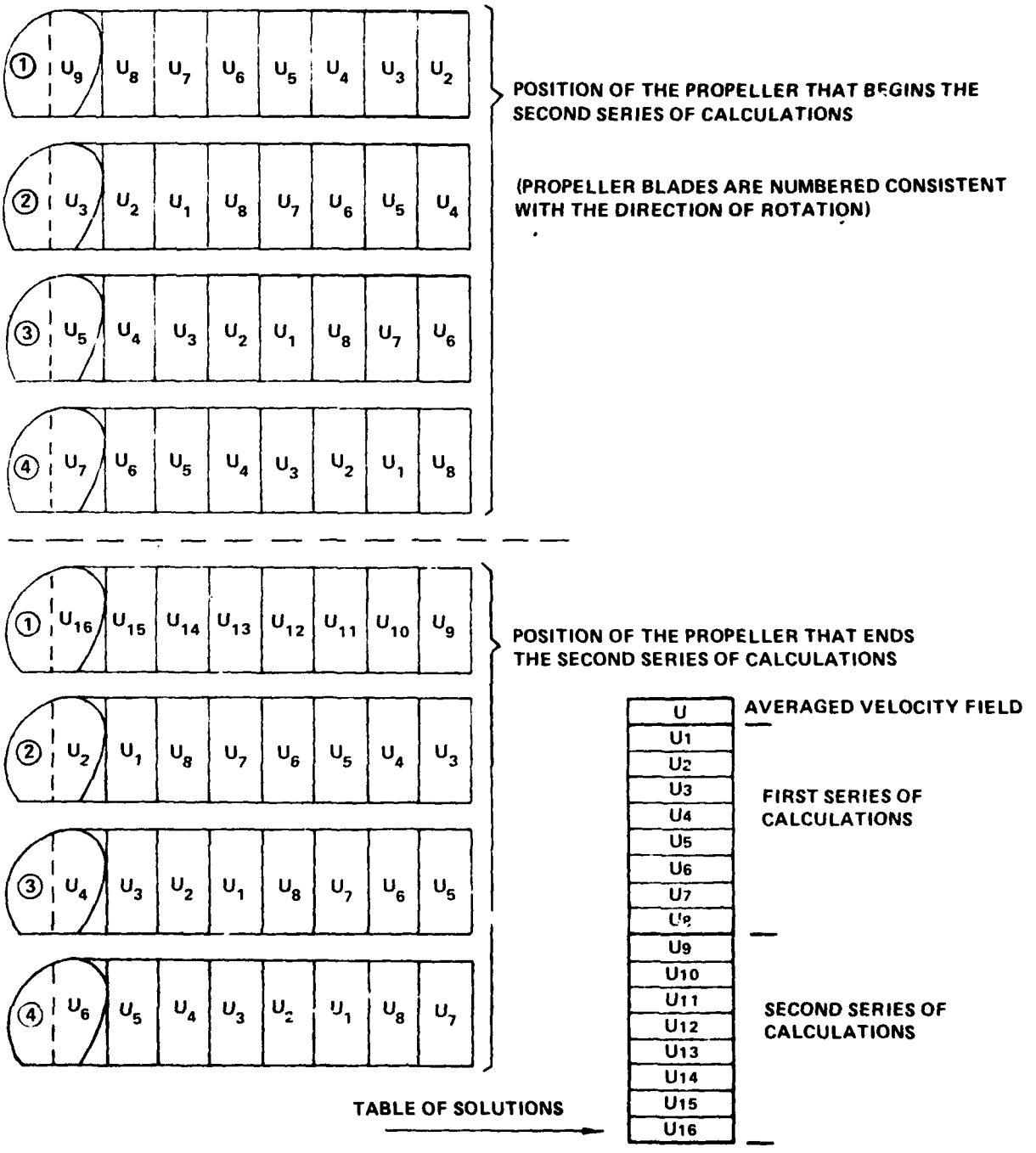

Figure 16 - Schematic of the Second Series of Calculations for Establishing the Pressure Distribution on a Propeller Blade in a Nonuniform Velocity Field

velocity difference established for the actual position of the blade. The completion of the second series of calculations concludes the method.

XIII COMPUTER PROGRAM AND CALCULATIONS

On the basis of the descriptions of the method used to calculate the pressure distribution on a propeller blade, presented in Sections II through XII, a digital computer program was developed. The flow chart of the program is shown in Figure 17. The program was written in FORTRAN IV suitable for the digital computer ICL-4-70. At present, this computer is the fastest and best equipped in peripherals in northern Poland.

As can be seen from the block diagram the overall program is composed of a main program and six subroutines. The elements of the program accomplish the following functions:

a) Main Program
   - input of the preliminary set of data
   - establishment of memory areas for dynamic assignment in the course of calculations
   - coordination of the employment of subroutines

b) Subroutine SUB 1
   - calculation of the Fourier series terms from the given components of the onset velocity field
   - calculation of the vector components of the singularities located on analyzed blade and the coordinates of the vector centers
   - designation of the control point coordinates
   - designation of the vector components normal to the surface of the propeller blade at the control points
   - calculation of the values of the integral of the trigonometric functions within the limits established by the actual distribution of the singularity network on the propeller blade

c) Subroutine SUB 2
   - calculation and storing on a memory disk of tables of induction coefficients for all propeller blades
   - calculations of velocity components at the control points induced by the network of sources and sinks

d) Subroutine SUB 3
   - calculation and storing on a memory disk of tables of induction coefficients for all steady regions and all sectors of the unsteady region of the propeller wake

PRECEDING PAGE BLANK-NOT FILMED

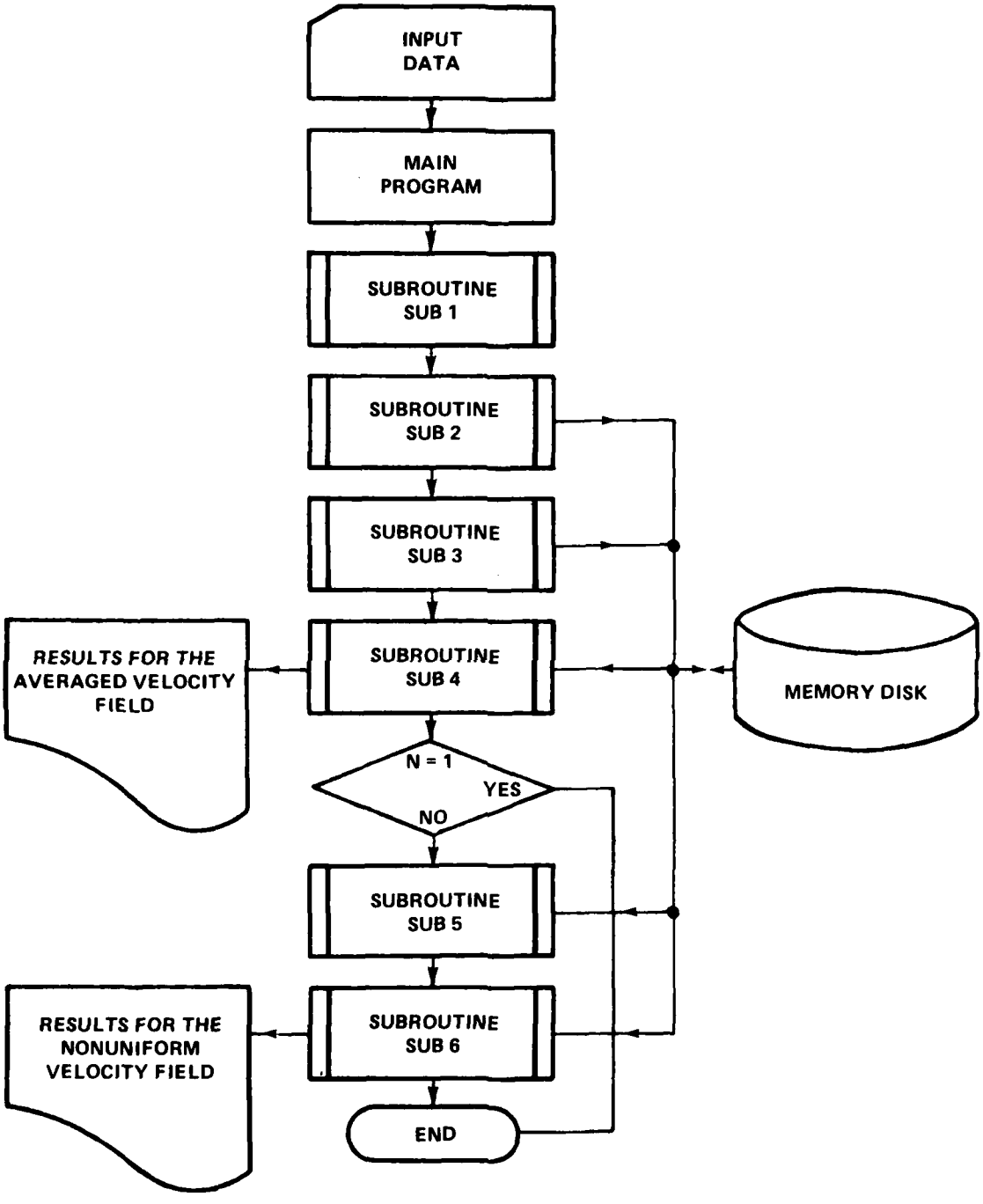

Figure 17 - Flow Chart for the Digital Computer Program

e) Subroutine SUB 4 (performs all the steps connected with the calculations of the pressure distribution for the circumferentially averaged velocity field)
   - calculations of components of the circumferentially averaged onset velocity field at the control points
   - calculation of the independent terms of the matrix in the set of linear equations
   - calculations of the coefficients that multiply the unknown in the set of equations
   - solving the set of equations
   - calculation of the magnitude of bound vortex circulation at control points
   - calculation of the induced velocity components at the control points
   - calculation of the pressure distribution on both sides of the analyzed blade
   - printout of results

f) Subroutine SUB 5 (performs all the steps connected with solving the first series of calculations in the nonuniform velocity field)
   - calculation of the velocity components induced by propeller blades 2, 3, ... Z and the unsteady region of the free vortex sheets located behind these blades as well as the steady region of the propeller wake
   - calculation of the matrix of coefficients that multiply the unknowns in the set of equations
   - calculation of the velocity components induced by sectors 2, 3, ... N of the unsteady region behind the analyzed blade
   - calculation of the onset velocity field components for the actual position of the analyzed blade
   - calculation of the independent terms of the matrix in the set of equations
   - solving the set of equations

   (steps 3 through 6 are repeated in sequence for all analyzed positions of the blade during one propeller revolution)

g) Subroutine SUB 6 (performs all the steps connected with solving the second series of calculations in the nonuniform velocity field)
   - calculations of the matrix of coefficients multiplying the unknowns in the set of linear equations
   - calculation of velocities induced by the steady region of the propeller wake
   - calculation of the velocities induced by the unsteady region of the propeller wake and blades 2, 3, ... Z

- calculation of the independent terms of the set of equations
- solving the set of equations
- calculation of the magnitude of bound vortex circulations at the control points
- calculation of the induced velocities at the control points
- calculation of the pressure distribution on both sides of the analyzed blade

(steps 3 through 8 are repeated in sequence for all analyzed positions of the blade during one propeller revolution)

For the most expedient use of the computer memory, a subblock structure in the program was used. Only the main program and one subroutine that is actually used are stored in the computer memory at the same time. The remaining subroutines are stored in the memory disk. Such an approach does not cause a measurable increase in computer time because each subroutine is used only once in a given set of calculations. The program uses a total of 140 kB (kilobytes) of operational memory. The total memory of the ICL-4-70 computer is 514 kB. In addition to the computer memory, the program also uses disk memory for the pool of numerical data, which contains the tables of induction coefficients. The size of the disk memory used depends on the density of the discrete network, that is, the number of propeller blades, control points, and sectors of the unsteady region of the propeller wake. If we take the typical case:

Number of blades	4
Number of vortex segments on the analyzed blade	585
Number of vortex segments on the remaining blades per blade	204
Number of control points	48
Number of sectors in the unsteady region	8
Number of analyzed blade positions	8
Number of terms in the function of the circulation distribution	16

the size of the disk memory would be 465 kB which is relatively small. The time it takes to perform these calculations is also dependent upon the density of the discrete network. For the example given, it takes 9 minutes to obtain the results for an averaged onset velocity field (that is, through the calculations of subroutine SUB 4). To complete the whole program (that is, to calculate the pressure distribution for the 8 propeller blade positions), it takes 33 minutes. It can be assumed that the requirement to analyze each additional propeller position would increase that time by 3 minutes. Considering the degree of complexity of such calculations, this is a rather short time. The use of the induction coefficient concept contributed the most to shortening the calculations, and it proved to be effective and efficient. It is

equally important to eliminate from the program any iteration processes so that there is no risk of inability to get sufficient convergence. The whole computer program was developed in a way that ensures the greatest amount of flexibility, that is, permits the easy addition of new subroutines as well as an exchange of the present ones for modernized versions. For example, such a major modification of the theoretical method as insertion of a completely different type of distribution of circulation function would require a minimal change in only one of the subroutines.

XIV AN EXAMPLE OF CALCULATIONS MADE FOR A UNIFORM VELOCITY FIELD

Before each theoretical method may be practically applied, it must pass a verification period for results. The best verification method is a comparison of results obtained by theoretical means and appropriately conducted experiments. The verification stage is particularly important for theoretical methods pertaining to the hydromechanics of ship propulsors because these theoretical models are in continual need of improvement. During verification certain empirical correction coefficients that significantly increase the practical value of these methods are introduced. The situation is relatively straightforward when one considers methods of ship propeller design or calculations of their overall hydrodynamic performance characteristics. In this field an enormous number of experimental efforts have been completed dealing with ship propellers of different geometrical configurations; furthermore, testing a propeller of any geometry does not present a problem. It is far more difficult to measure the distribution of pressure on a blade of an operating ship propeller model. At this time such measurements are not possible in Poland. The principal difficulty is having a sufficiently large cavitation tunnel (propeller tunnel) and a model basin that could accommodate a propeller model on the order of 0.5 m and a propeller dynamometer of sufficient size to power such a propeller. Additional problems are having a sufficiently small measuring probe that could be placed inside the propeller blade model (it should be remembered that the blade section at the radius of 0.9 for a 0.5 m propeller model has a maximum thickness of barely 0.005 m) and having a pressure transmitting and an electrical signal processing system. We will be able to make such measurements in Poland after a large propeller tunnel is built and activated at the Center of Ship Technology. For now, the only available means of verifying the described theoretical method is with results obtained outside Poland. Such measurements are scarce because very few research establishments outside of Poland publicize such experiments, and it is even rarer to see such results published.

As the first stage in the verification of this theoretical method with respect to a propeller operating in a uniform velocity flow, measurements of the pressure distribution on a model propeller blade, conducted by N.S.F.I. at Trondheim (Norway) and published in Reference [7], were used. The model in these experiments was a three-bladed propeller of diameter 0.5653 m, hub diameter 0.16 m, and expanded area ratio coefficient of 0.512. Table 1 gives the geometrical particulars of this propeller.

PRECEDING PAGE BLANK-NOT FI

TABLE 1

Nondimensional Radius	Chord Length	Propeller Pitch	Maximum Section Thickness	Maximum Camber
–	[m]	[m]	[m]	[m]
0.30	0.1955	0.3840	0.02639	0.003589
0.40	0.2115	0.3691	0.02213	0.004150
0.50	0.2245	0.3608	0.01976	0.004288
0.60	0.2330	0.3565	0.01654	0.003949
0.70	0.2350	0.3520	0.01270	0.003900
0.80	0.2270	0.3520	0.01022	0.003614
0.90	0.1890	0.3507	0.00600	0.002730
0.95	0.1490	0.3483	0.00447	0.001982

The propeller blades are constructed based on a composite profile having a NACA 16 section thickness distribution and a NACA a = 0.8 camber line. To measure the pressure distribution, 27 pressure taps were built into the blade along three chords at radii of 0.4, 0.7, and 0.9 as well as along a radius of the propeller at a distance of 25% of the chord from the leading edge of the propeller blade. It was possible to position sensors in a region of the blade tip (above 0.9 radius) despite the fact that miniature probes of 0.8 mm thickness were available. The electrical signals from the transducers were transmitted from the propeller shaft through slip rings and then amplified and recorded on a multichannel oscillograph. The measurements were made in the N.S.F.I. model basin. Experiments were conducted at five different advance coefficients: 0.1068, 0.251, 0.375, 0.437, and 0.593. The middle value coefficient was at the design point of the tested propeller model. The experimental results were reported in the form of nondimensional pressure coefficients:

$$C_p = \frac{p - p_s}{\frac{1}{2}\rho\left[V^2 + (2\pi \cdot RC \cdot R_{ps})^2\right]} \tag{55}$$

where: p - total pressure at the point of measurement

p_s - static pressure at that point

V - propeller advance velocity

RC - radius defining the point of measurement

R_{ps} - propeller rpm

The measuring instrumentation was calibrated before and after the experiments. In the course of the calibration the standard deviations of the measured quantities, that is, rotational and propeller advance speed, sensor output, and height of the wave caused by the operating propeller in the basin, were made. These measurements established standard deviations in the distribution of pressures that were shown graphically in the form of vertical segments in the final presentation of results.

Theoretical computer calculations as described in the preceding section were made using the known geometry of the propeller. Calculations were made for all five advance coefficients. On the propeller blade 48 control points were selected and distributed at six radii 0.4, 0.5, 0.6, 0.7, 0.8, and 0.9. At each radius, the control points were positioned at 0.15, 0.25, 0.35, 0.45, 0.55, 0.65, 0.75, and 0.85 of the chord, measured from the leading edge. On the analyzed blade of the propeller there were 19 bands with 15 segments of bound vortices, supplemented with 20 bands with 15 segments of shedding vortices (together, 585 singularities of the line vortex type and 285 singularities of the source sink type). The remaining blades had a significantly less dense network of singularities (204 segments of line vortices and 96 of source sink each). A 16 term function was used to define the distribution of circulation (four to define the change in circulation in the radial direction and four in the chordwise direction). The calculated results are shown in Figures 18 through 22 with experimental data from Reference [7] included. Analyzing the results we conclude that good agreement was achieved between the calculated and the experimental data for all advance coefficients. Note that in almost all cases, the calculated results give a slightly greater difference in pressure between both sides of the propeller blade than the appropriate experiments. One would expect the lifting forces at the respective blade sections to be somewhat greater than the measured ones. This can be explained by the fact that the theoretical method does not include the effects of fluid

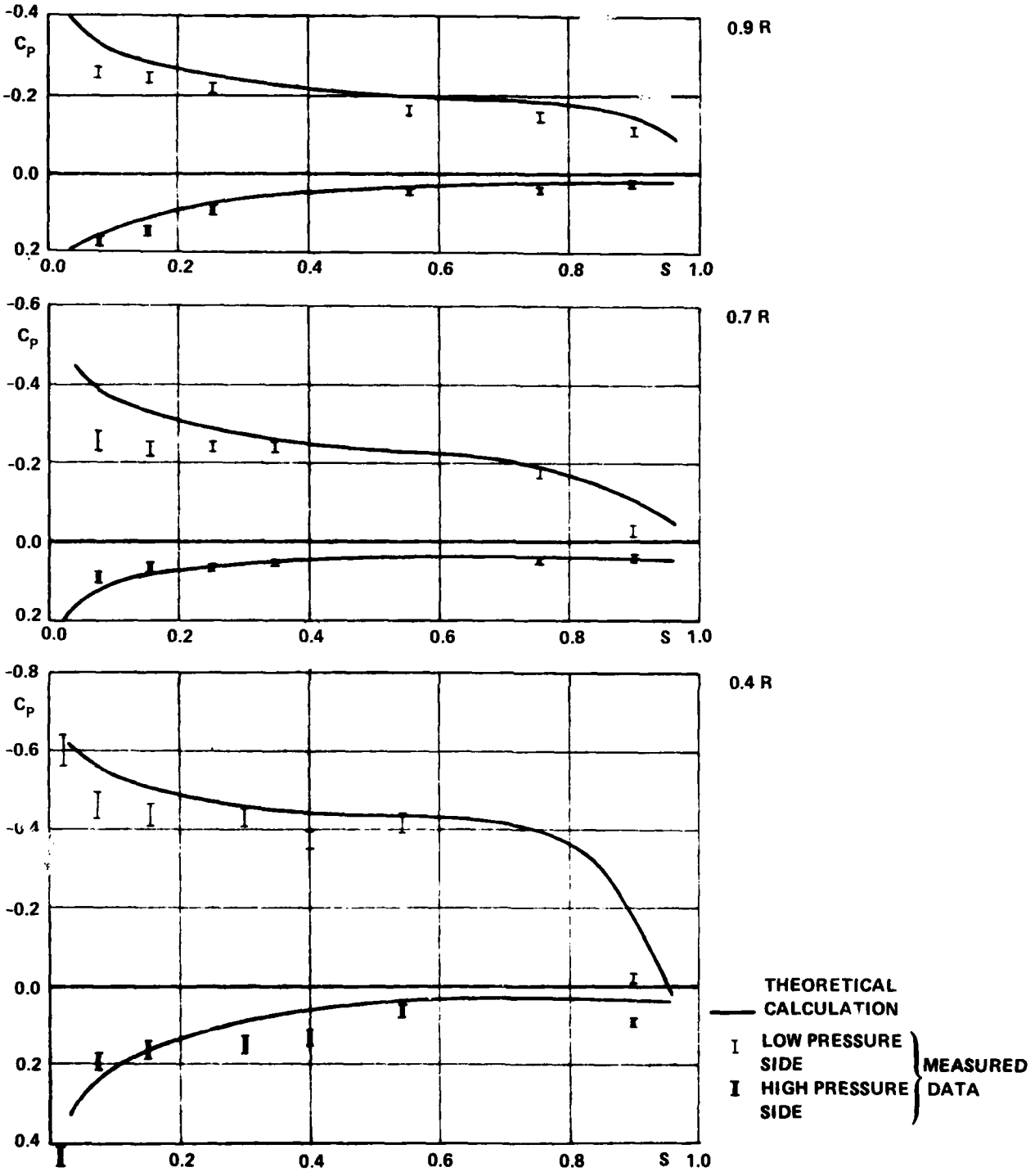

Figure 18 - Results of the Calculated and Experimental Data for a Uniform Velocity Field at J = 0.1068

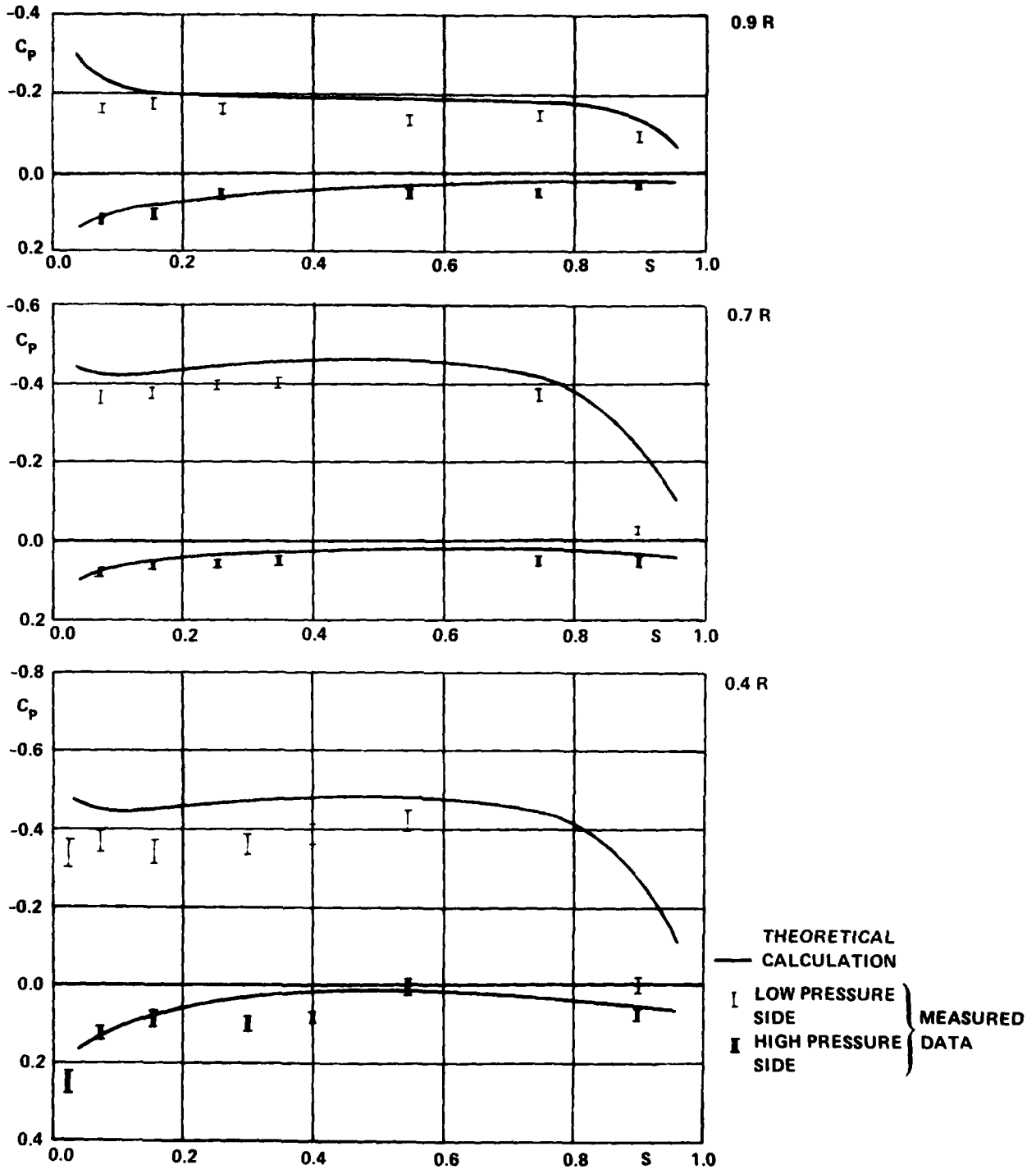

Figure 19 - Results of the Calculated and Experimental Data for a Uniform Velocity Field at J = 0.251

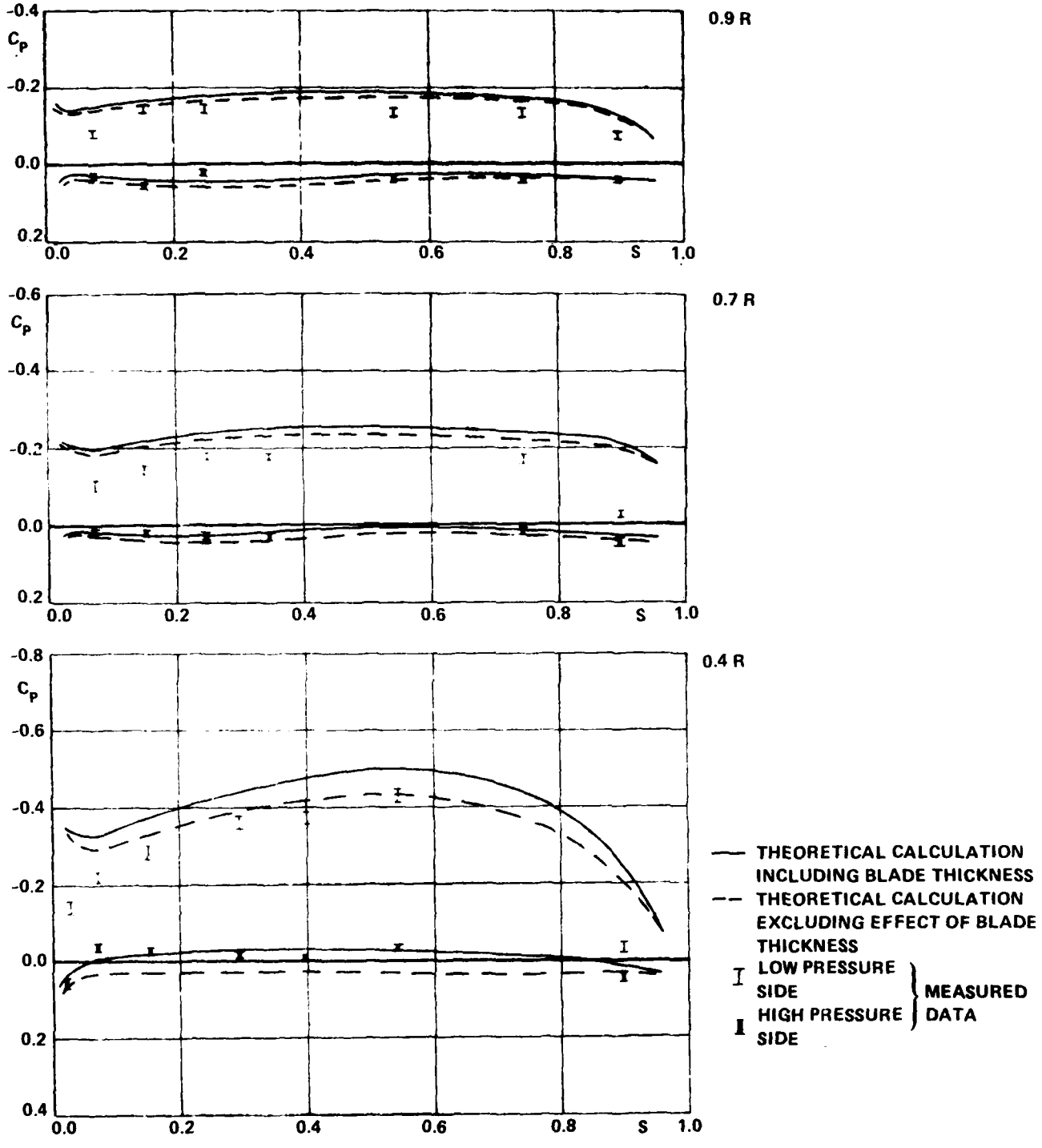

Figure 20 - Results of the Calculated and Experimental Data for a Uniform Velocity Field at J = 0.375

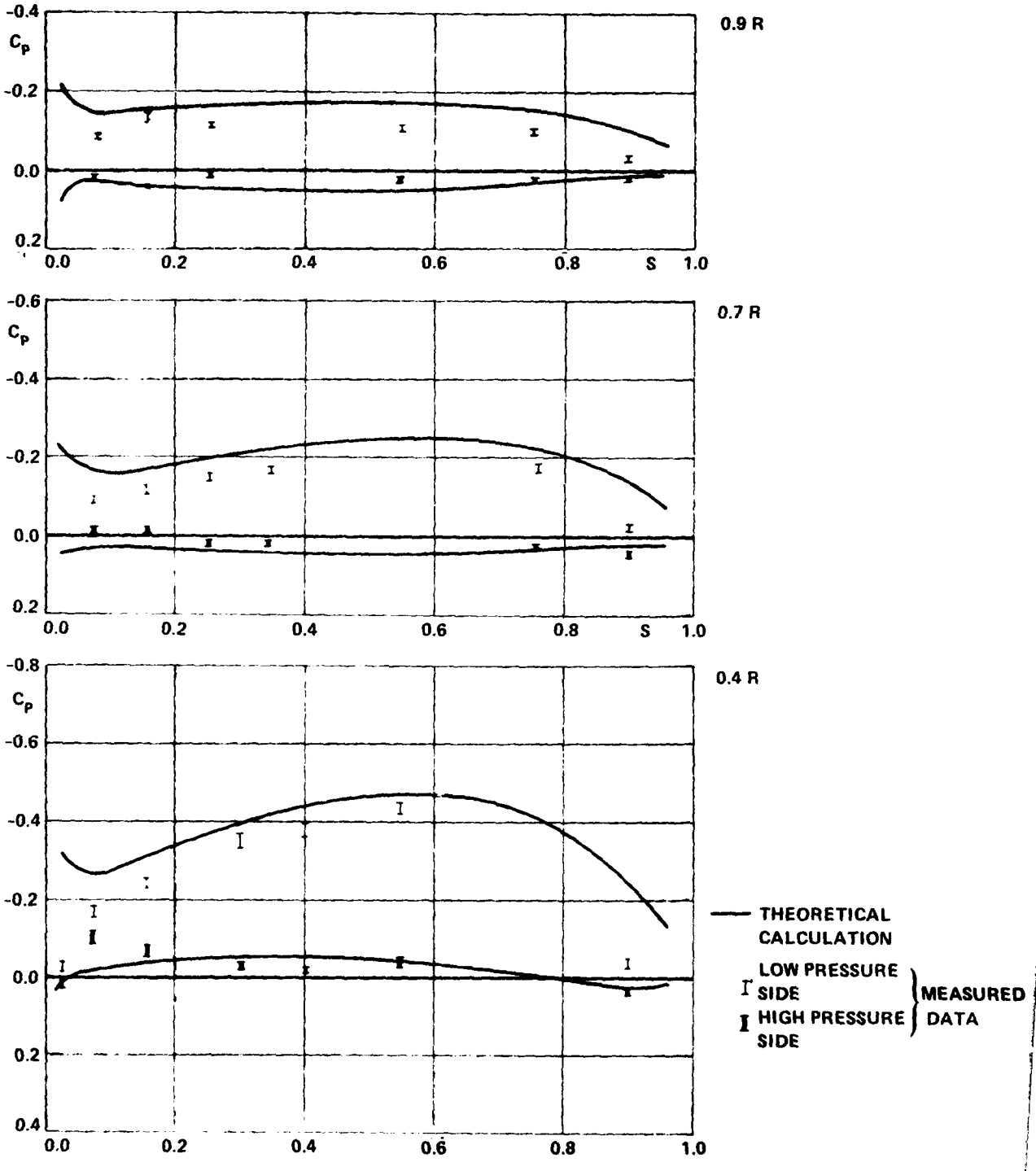

Figure 21 - Results of the Calculated and Experimental Data for a Uniform Velocity Field at J = 0.437

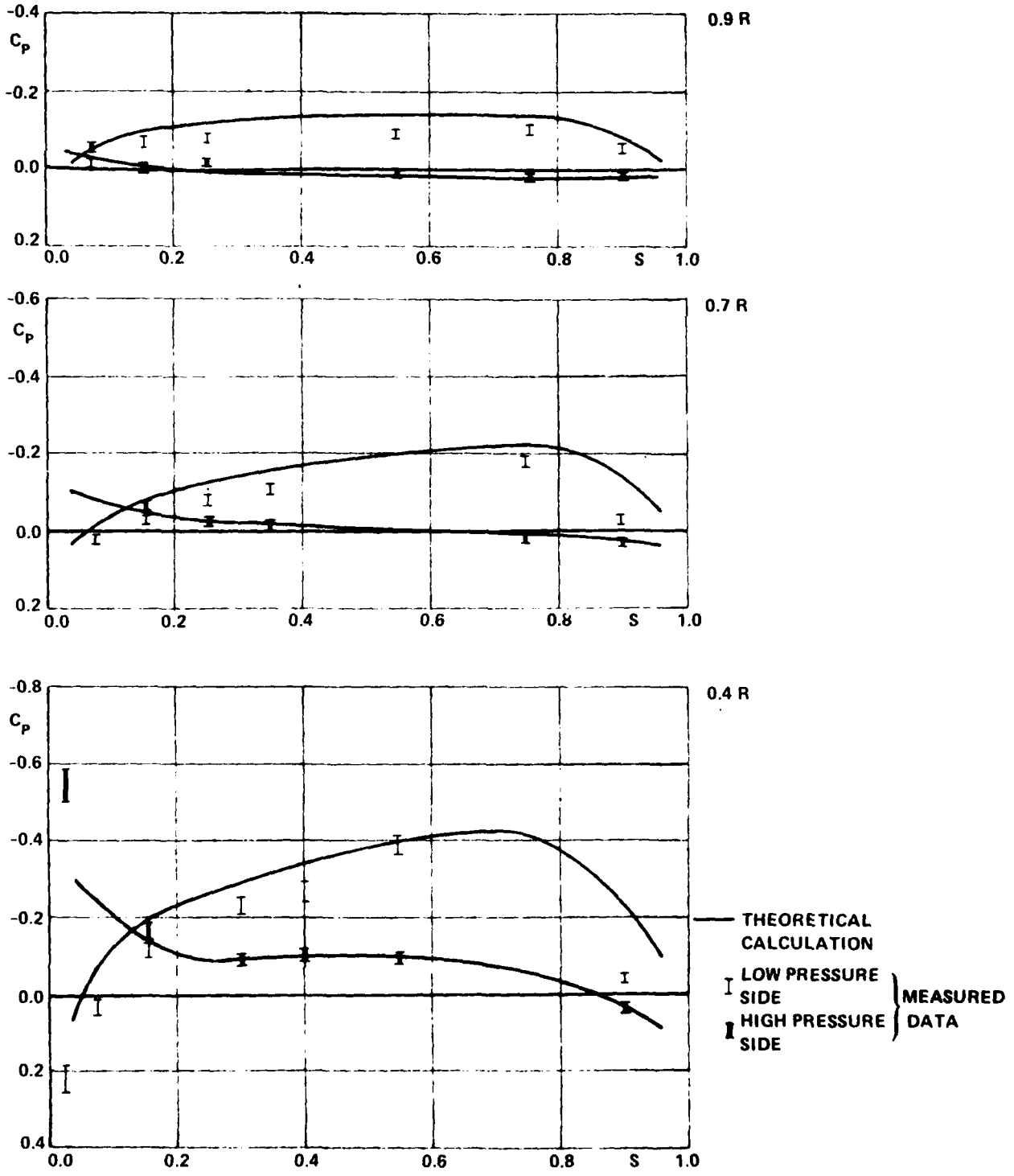

Figure 22 - Results of the Calculated and Experimental Data for a Uniform Velocity Field at J = 0.593

viscosity on the pressure distribution over the propeller blade. From the literature [31], it appears that the effect of fluid viscosity is minimal on the pressure side of the blade; on the suction side, however, the effects of viscosity can reduce the calculated pressure distribution for an ideal fluid by about 12-15%. The character of the differences, as can be observed in Figures 18 through 22, seems to be of the same nature and could be caused by the viscous problems. From the analysis of the results one may also observe that certain differences between calculated and measured data exist (even after the effects of viscosity have been included) for the region of the leading and the trailing edges of some of the section profiles. This is particularly noticeable for the advance coefficients farthest from the design point, that is, when the propeller blades are operating at a large angle of attack. Most probably the reason for this occurrence is the use of circulation distribution functions with a singularity on the leading edge of the blade and the impossibility of positioning control points sufficiently close to the edges of the section profiles. This causes inaccurate calculation of the values of terms in the function containing singularities (Equation (24)). The prospects of using this method for analyzing cavitation characteristics necessitates a detailed examination of the reasons for this difference in theoretical calculations in the region where a cavity initiates. It appears that an improvement could be obtained by a geometrical arrangement of the singularity network on the analyzed blade such that the border control points would be located closer to the leading edge, for example 0.05, of the chord. The accuracy of the measured results in that region of the blade should also be confirmed. This would be possible after further experimental measurements were acquired.

In the course of theoretical calculations, the effect of propeller blade thickness has also been determined. To obtain these results, calculations were repeated at the design point advance coefficient, introducing at this time a zero thickness of the blades. The results of these calculations are shown in Figure 20. Comparing the results of both sets of calculations, it can be seen that the finite thickness of the blade has little influence on the difference in pressure between both sides of the propeller blade; however, it does "shift" substantially the calculated pressure distribution in the direction of negative values. As expected, the influence of thickness is more pronounced where the blade is thicker. It clearly appears that the calculations of pressure distribution according to methods that do not take into account the finite propeller blade thickness cannot be used for the purpose of cavitation analysis because they give substantially reduced values of negative pressure on

suction side. Such results can, however, be used to adequately appraise the overall forces acting on the propeller blade.

It took 7 minutes to make the calculations presented in this section for each value of advance coefficient. At 1977 prices, this is equivalent to 750 zl or $23.00 (at 33 zl per $) to make the calculations for one advance coefficient. Note that such calculations are several times cheaper than equivalent experiments, not to mention the time to prepare and conduct the experiments, which would be about one month (including building a propeller). The agreement of the calculated results with the experimental data is sufficient and it is possible to fully replace the experiments with a computer calculation when the propeller is operating in a uniform velocity field. Satisfactory results were obtained for a wide variation of advance coefficients. In summary, we conclude that the method meets expectations in the area of calculations performed for the uniform external velocity field. This conclusion does not exclude the need to conduct further verification, particularly for propellers of a nontypical geometry. This will be accomplished as appropriate new experimental data are acquired.

XV AN EXAMPLE OF CALCULATIONS MADE FOR A NONUNIFORM VELOCITY FIELD

The principal utility of the method described herein is the ability to calculate the pressure distribution on a propeller blade operating in a nonuniform velocity field. The results of such calculations should be subject to careful verification. Unfortunately, this is not a simple matter, because until now a set of measurements of the pressure distribution on a propeller blade operating in a nonuniform velocity field has not been published anywhere in the world. Experimental investigations of this type have another problem in addition to the problems mentioned in the previous section: The values of pressure at the different points of measurement on the propeller blade undergo very rapid time changes. A model of about 0.5 m diameter uses a rotational speed of about 800 revolutions per minute. Considering that, for a typical velocity distribution field in a nonuniform stream in the course of one revolution, the propeller blade passes twice through the region of lower and twice through the region of higher velocity flow, then about 50 significant changes in pressure may be expected in the course of one second. The correct way to measure such a pressure requires the use of a low inertia transducer. Typical induction transducers are not adequate for this purpose. In measuring rapid changes in pressure, there may also be some hydrodynamic problems, for example, in the narrow tubes carrying the pressure signal to the transducers within the blade.

Consequently, the only available means of verification is the use of a relatively large body of information obtained visually, studying cavitation on propellers operating in a nonuniform velocity field. The leading research centers outside Poland have, as a rule, several hundred propeller models thoroughly tested in a nonuniform velocity field. A significant part of these tests have been published. In Poland such experiments are at the stage of practical verification of the methodology of research (this pertains particularly to the selection of the optimum method of simulating the velocity field in the test section of the cavitation tunnel (propeller tunnel)). The use of visual cavitation data to check the calculations of the pressure distribution on the propeller blade has two weak points: first, inadequate knowledge of the relationship between the observed pattern of cavitation and the pressure distribution that produced that pattern, and second, even the best interpreted data contributes only to the qualitative basis and not to the quantitative evaluations of the calculated pressure distribution.

As an example for these calculations the left side propeller of a fast cargo ship was chosen with the results published in Reference [16]. This four-bladed propeller

has a diameter of 4.2 m, a hub diameter of 1.26 m, and an expanded area ratio equal to 0.64. The propeller was designed to transmit power of 14750 hp at 209 revolutions per minute and a ship speed of 28 knots. Detailed geometrical characteristics of the propeller are listed in Table 2. In the design of the propeller, composite profiles used the Walchner 3 type thickness distribution and a camber line NACA a - 1.0. The cavitation experiments were conducted on this propeller at Wageningen using a 1/16 scale model. The velocity field was simulated in the propeller tunnel with a large section of the ship hull model. The components of the velocity field measured in the propeller tunnel in the area of the operating propeller are shown in Tables 3, 4, and 5. These values are presented in terms of nondimensional coefficients proportional to ship speed.

The configuration of the control points and singularities for this propeller calculation is the same as the one in the previous section. It was assumed that the unsteady region of the propeller wake includes only one full revolution of the

TABLE 2

Nondimensional Radius	Chord Length	Propeller Pitch	Maximum Section Thickness	Maximum Camber
–	[m]	[m]	[m]	[m]
0.30	0.975	5.250	0.198	0.0
0.40	1.362	5.254	0.132	0.024
0.50	1.706	5.246	0.099	0.029
0.60	1.920	5.204	0.074	0.029
0.70	1.963	5.111	0.055	0.028
0.80	1.804	4.960	0.040	0.024
0.90	1.383	4.750	0.026	0.018
0.95	1.011	4.628	0.019	0.014
1.00	0.0	4.490	0.012	0.0

propeller vortex sheets, which seems to be sufficient due to the large angles of pitch of these surfaces. The unsteady region was divided into eight sectors, and calculations of the pressure distribution were made at the same number of positions of the analyzed blade (every 45°). It took 33 minutes for these calculations, at a cost of 3564 zl or $108 (at 33 zl per $). The results of these calculations are shown graphically in the form of a nondimensional pressure coefficient C_p on both sides of the blade for sections at radii: 0.5, 0.7, and 0.9 in Figures 23 through 27. In the first figure, the results of the calculations for the circumferentially averaged velocity field are shown. In the subsequent figures the results for the

TABLE 3

AXIAL COMPONENT OF THE NONUNIFORM VELOCITY FIELD

ϕ	R = 0.30	R = 0.50	R = 0.70	R = 0.90
0	0.970	0.991	0.997	1.021
20	0.996	0.997	1.008	1.002
40	0.995	1.000	1.000	1.002
60	0.979	0.983	0.987	0.983
80	0.969	0.969	0.986	0.981
100	0.966	0.966	0.918	0.982
120	0.959	0.962	0.984	0.955
140	0.956	0.960	0.962	0.940
160	0.992	0.979	0.967	0.874
180	0.895	0.961	0.953	0.869
200	0.778	0.887	0.849	0.735
220	0.893	0.948	0.898	0.849
240	0.906	0.989	1.003	0.947
260	0.963	1.009	1.028	1.008
280	0.961	0.992	1.014	0.998
300	0.970	0.986	0.999	0.976
320	0.970	0.985	0.939	0.986
340	0.969	0.987	0.964	0.997

NOTE: $\phi = 0$ is equivalent to a position vertically down. The increase in the coordinate ϕ corresponds to a left rotation.

TABLE 4

TANGENTIAL COMPONENT OF THE NONUNIFORM VELOCITY FIELD

ϕ	R = 0.30	R = 0.50	R = 0.70	R = 0.90
0	-0.073	-0.062	-0.055	-0.069
20	-0.031	-0.029	-0.020	-0.116
40	0.007	0.010	0.012	0.010
60	0.051	0.043	0.046	0.042
80	0.081	0.067	0.067	0.066
100	0.094	0.079	0.080	0.079
120	0.103	0.076	0.078	0.074
140	0.115	0.053	0.060	0.065
160	0.032	-0.051	0.081	0.045
180	0.024	-0.005	0.008	0.005
200	-0.029	-0.051	-0.065	-0.064
220	-0.123	-0.087	-0.114	-0.164
240	-0.187	-0.157	-0.152	-0.157
260	-0.183	-0.170	-0.163	-0.162
280	-0.187	-0.172	-0.161	-0.156
300	-0.175	-0.156	-0.147	-0.138
320	-0.150	-0.133	-0.121	-0.110
340	-0.096	-0.101	-0.089	-0.082

TABLE 5

RADIAL COMPONENT OF THE NONUNIFORM VELOCITY FIELD

ϕ	R = 0.30	R = 0.50	R = 0.70	R = 0.90
0	–0.203	–0.156	–0.130	–0.119
20	–0.200	–0.152	–0.128	–0.116
40	–0.193	–0.142	–0.118	–0.108
60	–0.179	–0.125	–0.100	–0.085
80	–0.158	–0.101	–0.074	–0.058
100	–0.139	–0.075	–0.044	–0.029
120	–0.124	–0.046	–0.006	–0.007
140	–0.138	–0.019	0.026	0.024
160	–0.120	0.043	0.050	0.061
180	–0.089	0.024	0.064	0.065
200	–0.089	0.005	0.045	0.054
220	–0.104	0.026	0.079	0.073
240	–0.096	0.042	0.069	0.046
260	–0.084	–0.007	0.016	0.014
280	–0.119	–0.060	–0.032	–0.037
300	–0.152	–0.099	–0.070	–0.082
320	–0.177	–0.128	–0.102	–0.110
340	–0.188	–0.135	–0.113	–0.114

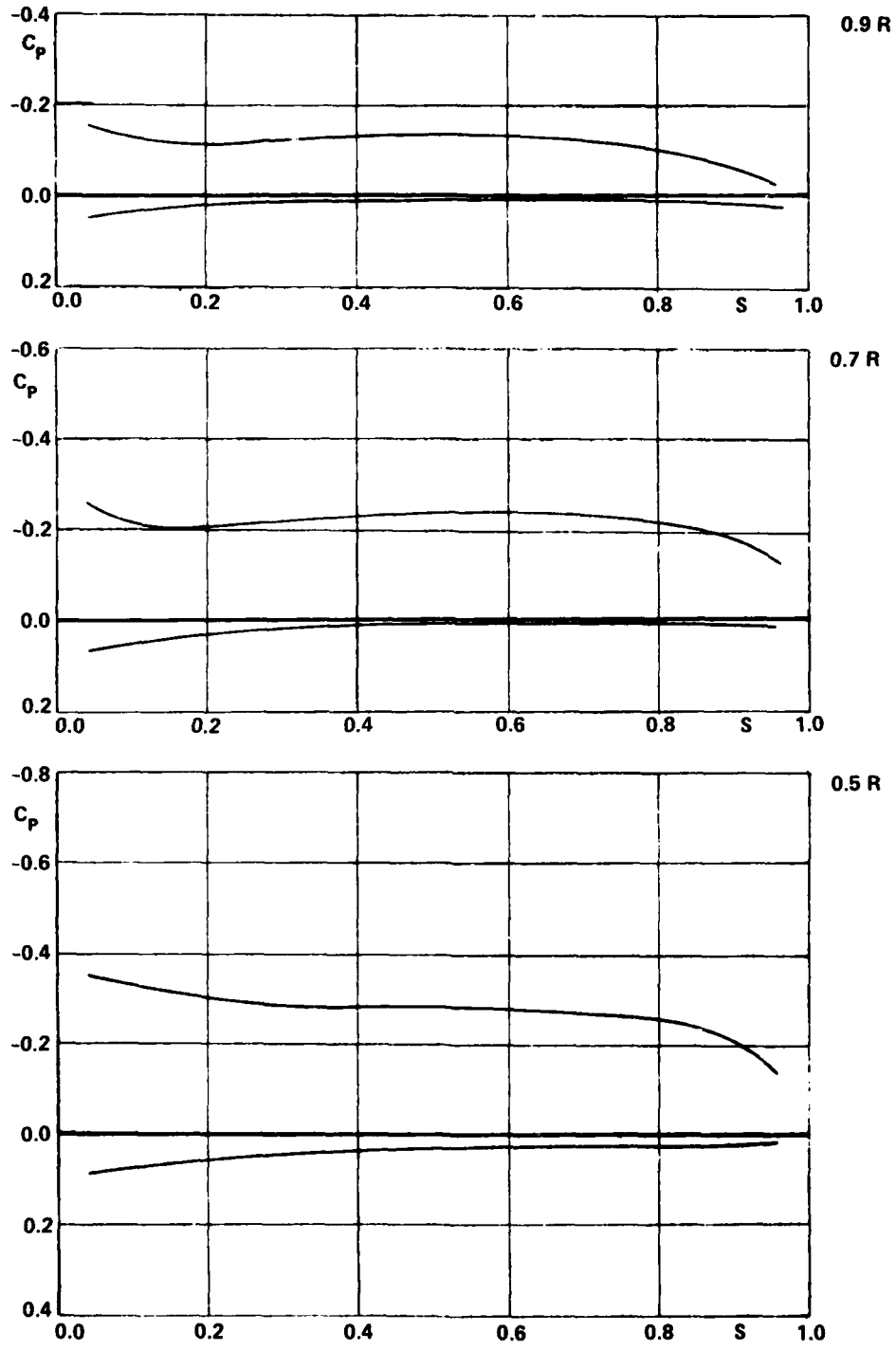

Figure 23 - Pressure Distribution Calculated for the Averaged Nonuniform Velocity Field

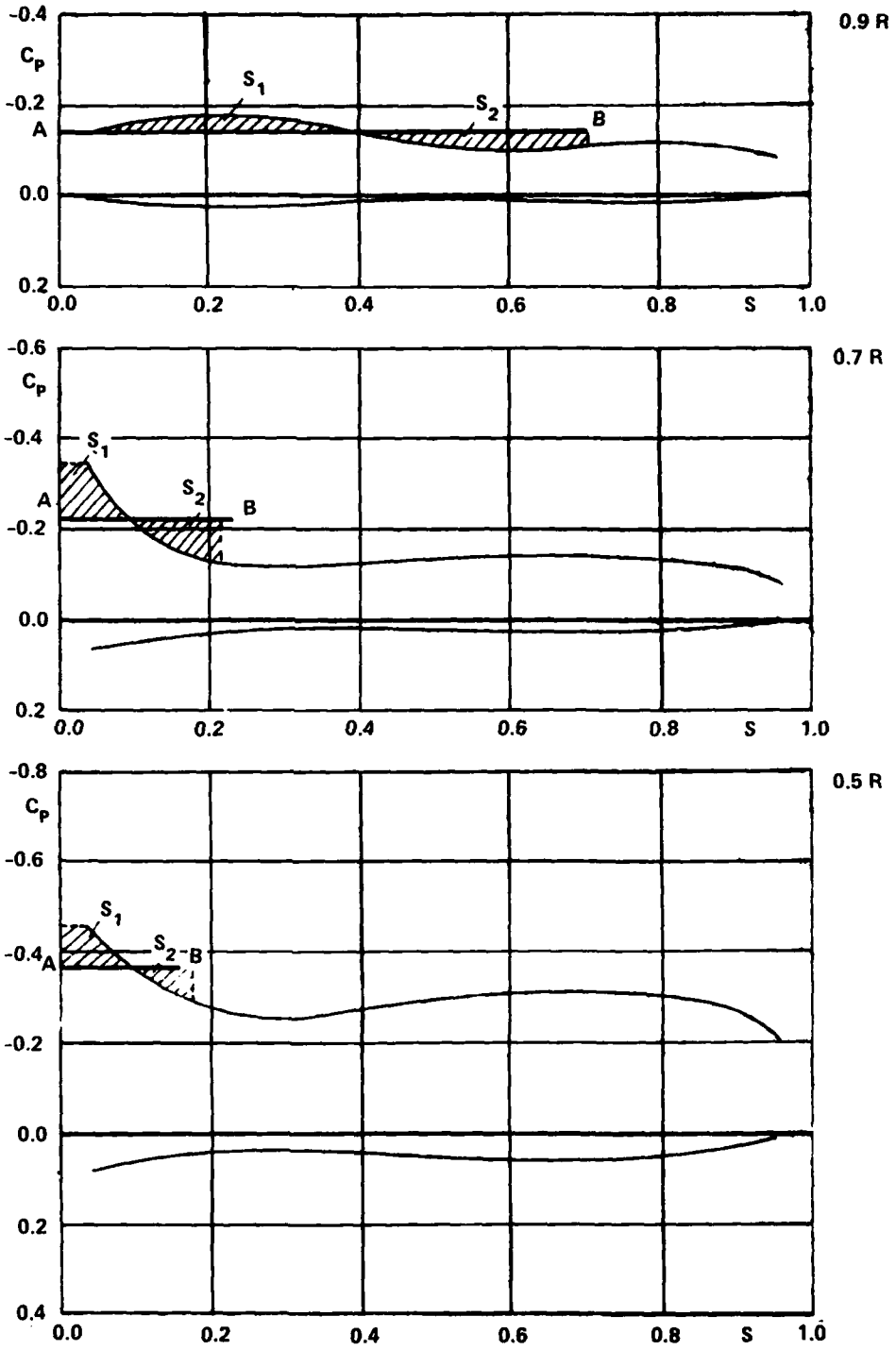

Figure 24 - Calculated Pressure Distribution in a Nonuniform Velocity Field for the 0 Degree Blade Position

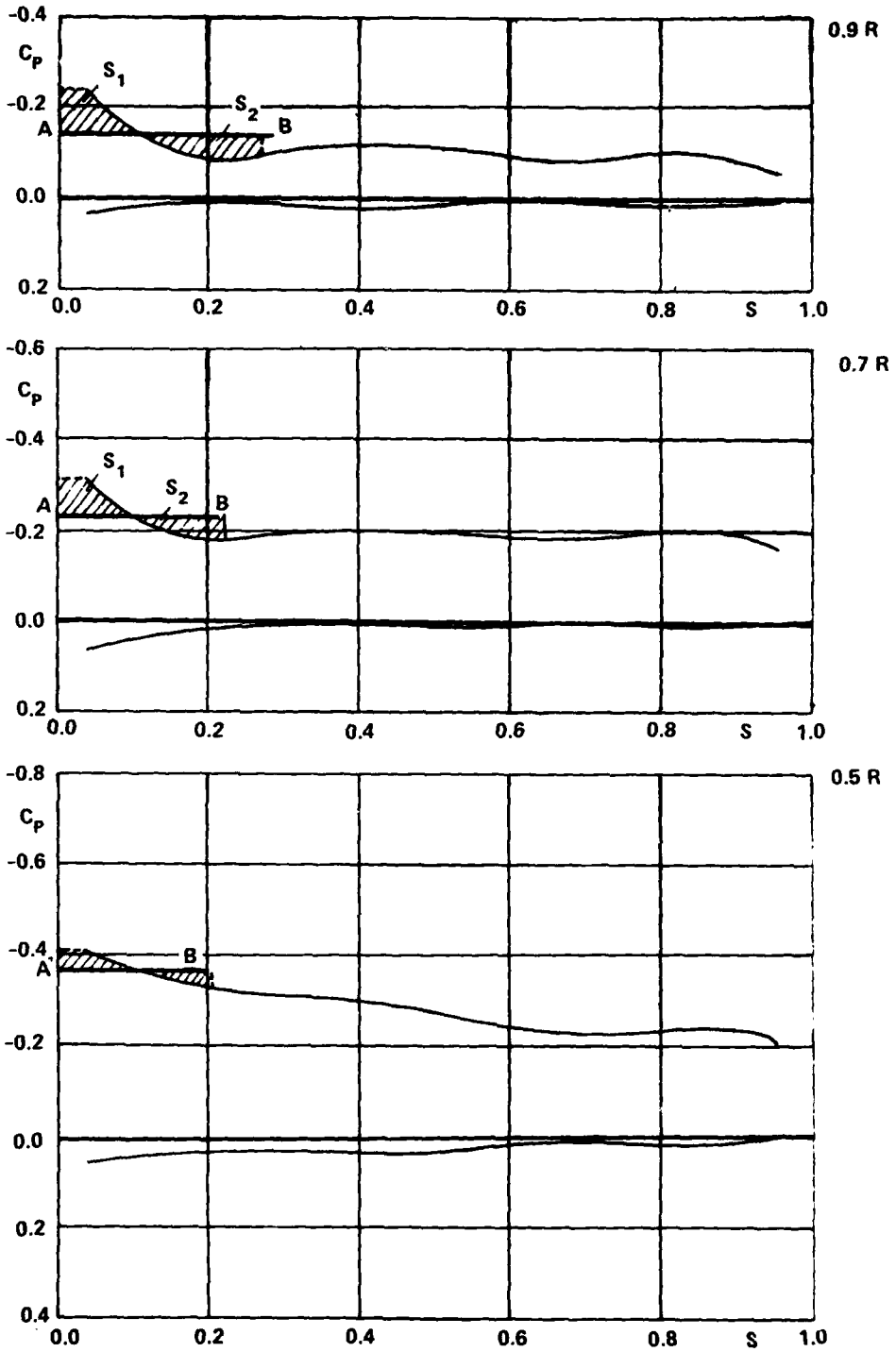

Figure 25 - Calculated Pressure Distribution in a Nonuniform Velocity Field for the 90 Degrees Blade Position

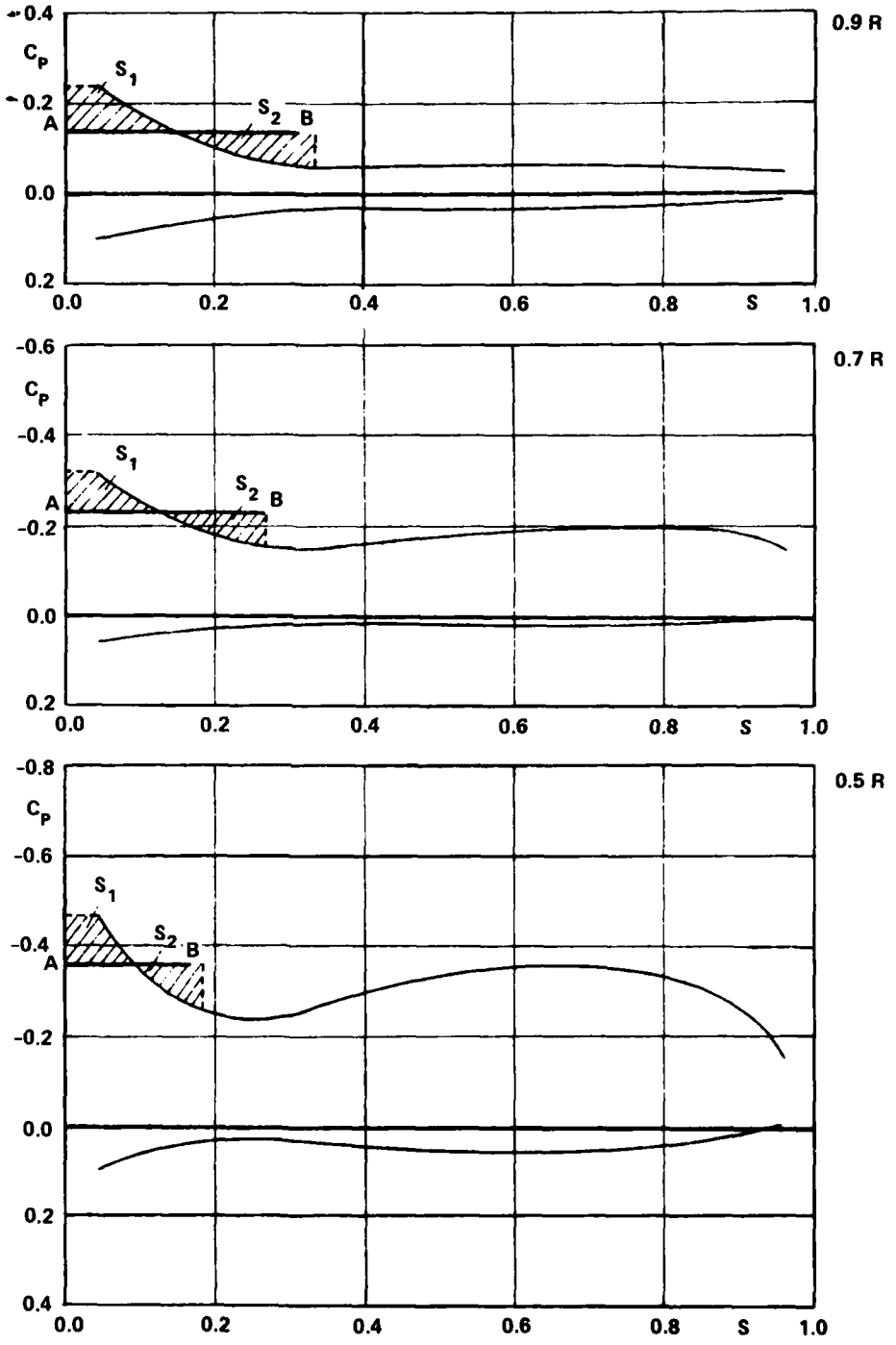

Figure 26 - Calculated Pressure Distribution in a Nonuniform Velocity Field for the 180 Degrees Blade Position

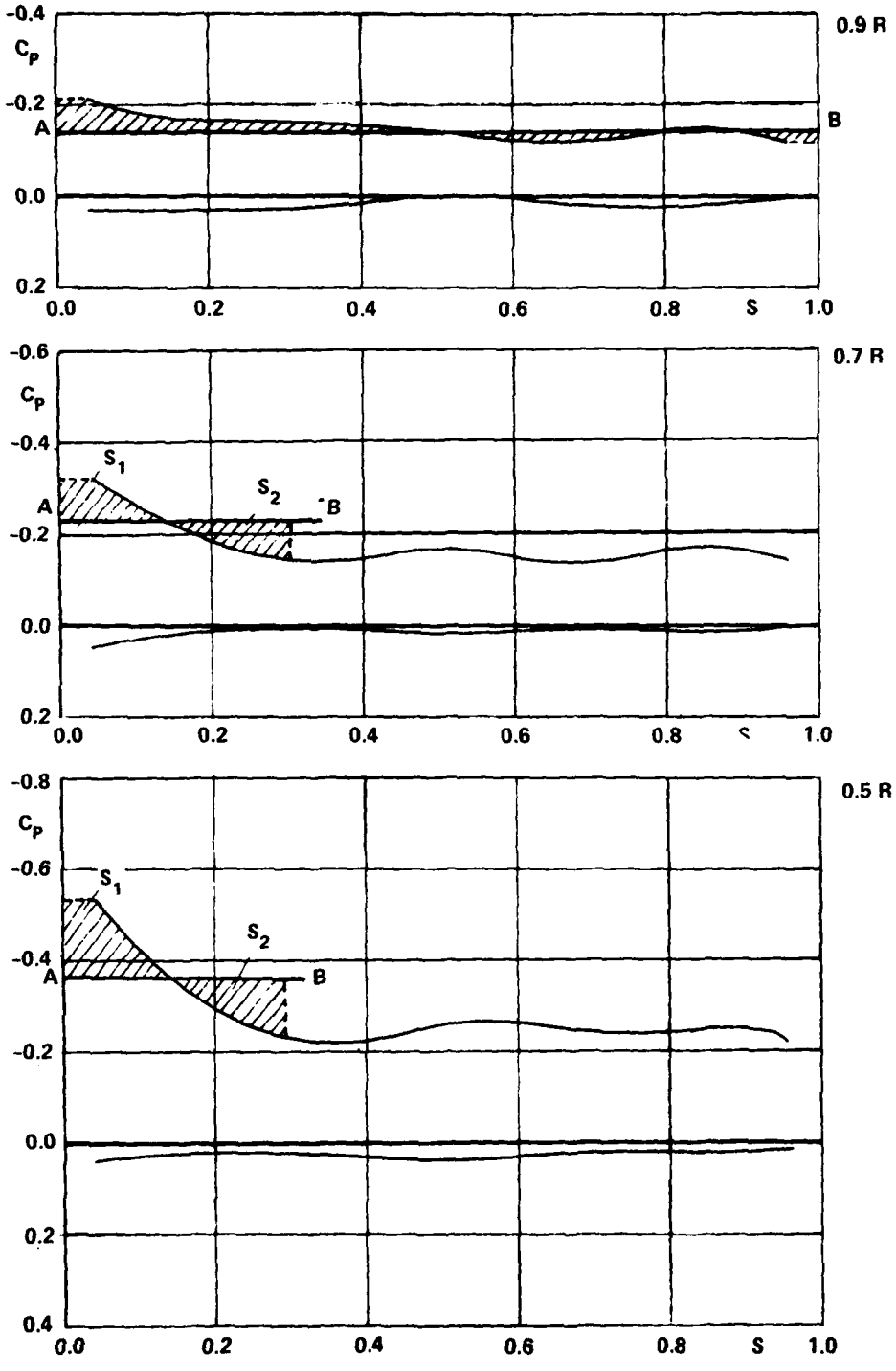

Figure 27 - Calculated Pressure Distribution in a Nonuniform Velocity Field for the 270 Degrees Blade Position

four principal positions of the analyzed blade are shown: 0° (vertically down), 90°, 180°, and 270°.

In all the graphs, segments AB of constant pressure are included. These pressures were established on the basis of the cavitation number that prevailed during the observation (that is, they indicate the critical value of pressure below which the water vaporizes). Their length corresponds to the part of the blade section profile at a given radius that was covered by a cavity at the indicated propeller position. Segments AB indicate the total scope of information contributed by cavitation experiments on the propeller model. There is no doubt that the presence of cavitation significantly changes the pressure distribution over a propeller blade in comparison to the pressures that would have occurred at those places in a flow without cavitation. To evaluate this phenomenon, we use a simplified hypothesis that says, if cavitation does not yet cause a decrease in the propeller thrust, then part of the pressure distribution "cut" because of the cavity presence in the region of the leading edge has to be equalized by an identical increase in pressure in the region located somewhat in the direction of the trailing edge (that is, in the location where the pressure was previously higher than the critical value). Despite its seeming simplicity, this hypothesis has shown very good agreement with reality, both in theoretical predictions of the area of the propeller blade affected by the cavitation and in comparison with an experimental study of profile sections in a two-dimensional flow [16]. In Figures 24 through 27 regions S_1 are shown indicating the "cut" areas and, equal to them, areas S_2 having equivalent and compensating pressures. The length over which the improvised constructed distribution of pressure attains a critical value should correspond to the part of the profile covered by the cavity (that is, segment AB).

An analysis of all the figures shows that adequate agreement has been achieved between the observed length of cavity and the values theoretically calculated for all propeller positions. Noted differences, as small as they are, indicate a certain regularity. In the propeller positions where the cavity occupies a relatively narrow strip situated near the leading edge, the theoretically predicted lengths of the cavity are larger than the observed ones. Inversely, in cases where the cavity immediately occupies a large blade area (for example, at radius 0.9 and position 270°), the theoretical calculations give shorter lengths. The cause of this occurrence may be a deficiency in the calculations of the pressure distribution indicated in the previous section in the region of the leading edge, or the simplistic theoretical method of designating the cavity length. Recall that the theoretically calculated

pressure distribution does not include the effects of viscosity. From the analysis of the results presented, it also appears that the theoretically calculated pressure distribution does not reach a critical value anywhere outside the observed cavitation. All the above evaluations are at best a qualitative, not quantitative nature. More precisely, no error was ascertained in the computer program for the case of a propeller operating in the nonuniform velocity field, but no assurance has been achieved that the results are completely accurate. There are potentially significant differences in the results in the region not affected by cavitation. Since the basic goal of the theoretical method described is to supply data to define the area of the propeller affected by cavitation, in that task the method fulfills the expectations. Further improvements should be directed first to the transformation of the calculated pressure distribution for an ideal fluid into a cavity on the propeller blade. Besides, it appears justifiable to state that calculations for several dozen different propellers operating in a nonuniform velocity field and comparison of these results with observations of cavitation tests and measurements of the overall oscillatory forces in the propeller shaft (thrust and torque), would present very extensive and comprehensive verification of this theoretical method even without the necessity to pursue direct measurements of pressure.

From the structural composition of the theoretical model discussed in the previous chapter, it appears that denser division of the unsteady region of the propeller wake into more sectors may influence the accuracy of the calculated results. A larger number of sectors increases the fidelity of the theoretical model of the propeller wake as compared to the actual one where the free vortex lines have a continuously changing character. In order to check the significance of the propeller wake structure, calculations were repeated for the same propeller, dividing the unsteady region into 16 sectors. It took 56 minutes to complete the calculations, at a cost of 6048 zl or $183, at 33 zl per $. These results indicated minimal differences from the calculated results using 8 sectors. The differences are so small that they could not be seen graphically in the scale of Figures 23 through 27. This is in agreement with earlier expectations because, first, velocities induced by singularities of the propeller wake are only a part of the total velocities induced, and second, in the example given, the variation in the external velocity field was relatively small. One should, however, consider making such calculations using a larger number of sectors, because otherwise one might miss a propeller position particularly

AD-A111 949 DAVID W TAYLOR NAVAL SHIP RESEARCH AND DEVELOPMENT CE--ETC F/G 13/10
A METHOD TO DETERMINE PRESSURE DISTRIBUTION ON A SHIP PROPELLER--ETC(U)
JAN 82 J SZANTYR

UNCLASSIFIED DTNSRDC/TRANS-354 NL

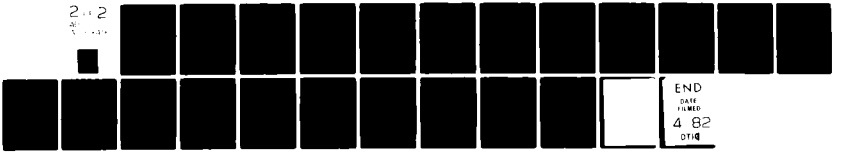

END
DATE FILMED
4 82
DTIC

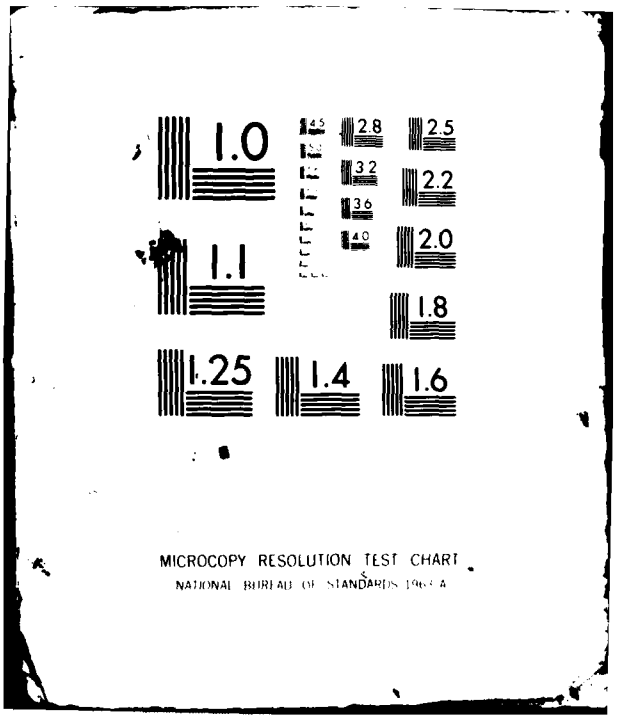
1.0
1.1
1.25
1.4
1.6
2.8
3.2
3.6
4.0
2.5
2.2
2.0
1.8
MICROCOPY RESOLUTION TEST CHART
NATIONAL BUREAU OF STANDARDS 1963-A

susceptible to cavitation. Even when a large number of sectors is used, the cost of calculations is many times smaller than the cost of an equivalent experimental test where the same amount of information is available.

XVI THE PROBLEM OF CONVERGENCE OF THE CALCULATED RESULTS

Theoretical methods that employ a discrete network of singularities to calculate induced velocities have a distinct advantage compared to methods that employ special integral equations. The principal advantage is a very simple method of calculating the induced velocities without any problem with mathematical singularities. There is, however, another serious problem that could be identified as a convergence of the solution defined, in this case as follows: If, for a propeller of unknown geometry, one obtains by the analytical method the same results independent of the assumed form of the discrete network of singularities, then one may say that the method gives converged solutions to the problem. The literature outside Poland gives numerous examples that indicate an amazingly strong dependence of the solution on the parameters of the discrete network of singularities used ([10] and [28]). One gets the impression that some authors have not recognized in depth the causes of this undesirable phenomenon, even though it is crucial to the usefulness of this theoretical method. The user of this method must be convinced of its effectiveness solving differently matched (within defined limits) parameters of a discrete network of singularities. Otherwise, correctly calculated solutions could be a matter of lucky coincidence. Appreciating the significance of this issue, the convergence problem of the solution was studied in detail before all the efforts on the lifting surface method were completed.

There are three groups of parameters that could be within the concept of the "framework of a discrete network of singularities": the number and distribution of control points, the number and distribution of vortex lines, and the number of terms of the function describing the distribution of the bound vortex circulation. To analyze the impact of these three groups of parameters on the pressure distribution, a special computer program was developed that could calculate the pressure distribution on a blade section operating in a two-dimensional flow. The theoretical model used was a simplified version of the model developed in this report for a two-dimensional flow based on the same main features such as the discrete vortices modeling the bound circulation, the method of induced velocity calculations, equations describing the distribution of circulation, etc. In the two-dimensional flow, the network of free vortices was not used. The choice of section profile in the two-dimensional flow employed in the numerical experiments was dictated by several premises. One of them was the simplicity of the computation program that permitted accurate control and analysis of the causes contributing to any deviation in results.

PRECEDING PAGE BLANK-NOT FILMED

The second one was the ability to make direct beyond-question comparisons with a wealth of experimental data or data theoretically calculated by other methods recognized as accurate [16]. Over one hundred sets of calculations were made, analyzing carefully selected NACA profiles: NACA 65, NACA a = 0, NACA a = 0.5, NACA a = 0.8, and NACA a = 1.0. Most of the calculations were made for infinitely thin profiles; some were made for section profiles with thicknesses corresponding to NACA 16 and NACA 66. Each profile was studied under different positive and negative angles of attack. For some of the section profiles, nonuniform inflow was simulated introducing a variable flow vector along the chord. For each profile, calculations were made for a wide range of discrete singularity network parameters. The number of discrete bound vortices was varied from 13 to 40, with different combinations of local distribution. The number of control points varied from 6 to 18. Finally, the number of terms in the function defining the distribution of circulation was varied from 4 to 18, never exceeding, however, the actual number of control points. All these results were compared with the NACA data obtained on the basis of conformal mapping by Theodorsena. In the course of the calculations a number of numerical methods were tested pertaining to the method of interpolation, solving sets of linear equations, calculations of Fourier coefficient, etc., selecting the most effective ones for use in the lifting surface method presented. The results can be synthesized as follows:

a) The density of the discrete vortex network used, in itself, does not influence the results. This seemingly surprising theorem was proved in the following way: The induced velocities calculated at a given point of the profile with a known distribution of circulation, independent of the number of discrete vortices used, are identically in agreement with the velocity calculated solving appropriate integral equations. This theorem is satisfied for circulation distributions that can be defined with linear functions and functions of the second order. For functions of higher order, small errors appear. In practice, however, such functions, are generally not used. In Figure 28 the pressure distribution calculated by the program mentioned is shown for an infinitely thin NACA a = 0.8 profile and three different densities of the vortex network. One can readily see the minimal effects of the network density on the calculated results.

b) To obtain correct values of induced velocities by the discrete vortex network technique, the control point must always be in the middle between neighboring vortex lines.

c) To obtain the correct circulation distribution, which also implies correct

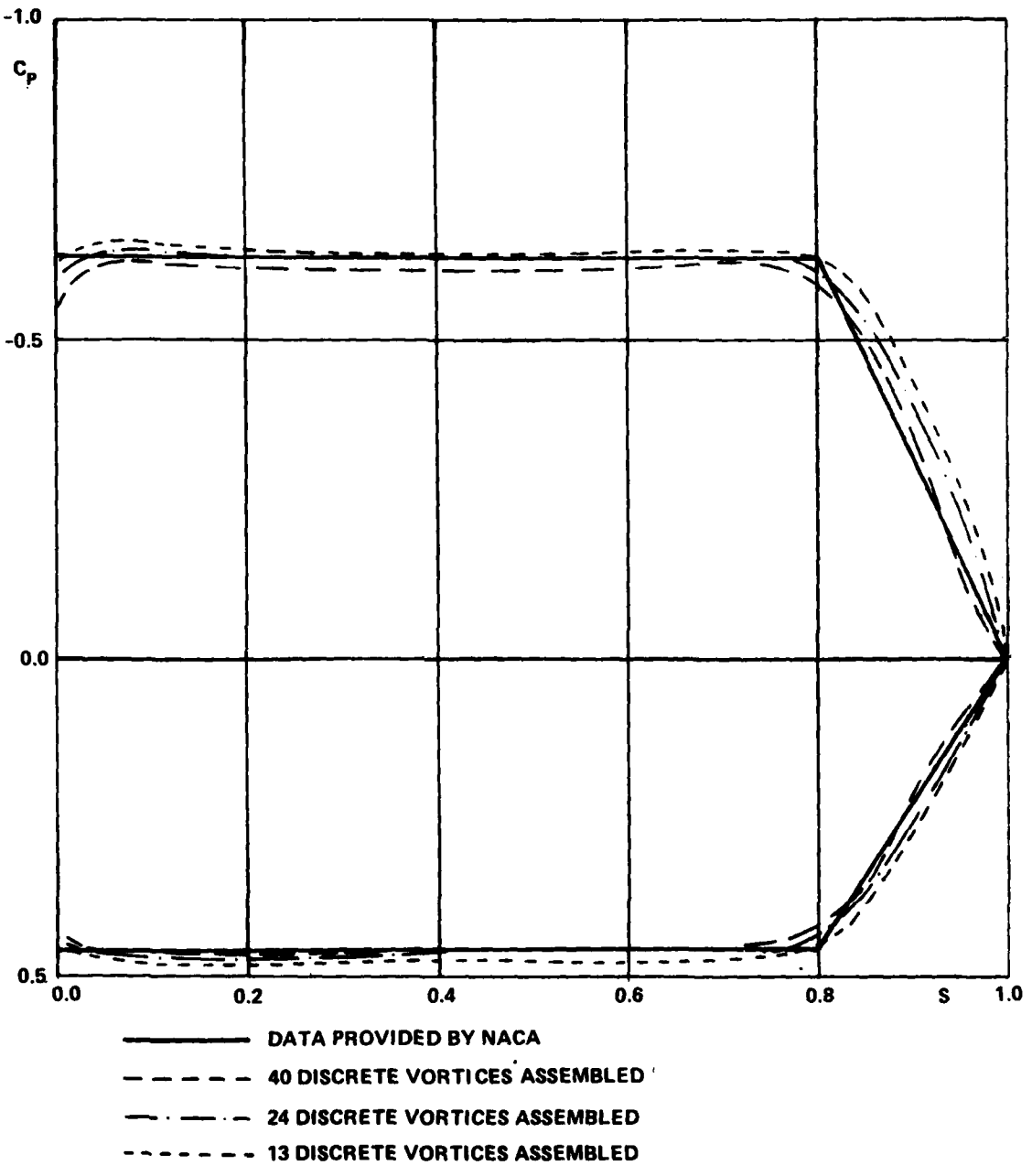

Figure 28 - Pressure Distribution Calculated for an Infinitely Thin NACA a = 0.8. Section Profile in a Two-Dimensional Flow for Different Numbers of Vortices

pressure distribution, the control points located near the edges of the section profile should be separated by at least three discrete vortex lines from the profile's edge. Comments b) and c) indicate a mutual dependence of the network of the vortex singularities and distribution of control points. Frequently, the desire to distribute the control points appropriately and the necessity to satisfy conditions b) and c) force a specific configuration of the discrete vortex lines on the section profile or the blade. Thus it is not possible to reduce the number of discrete vortex lines below certain limits (for a section profile in two-dimensional flow this is normally 13 vortices). Because of this the computer program includes the flexibility that one may use a denser vortex network near the control points (analyzed blade) and a less dense network on the remaining blades. This allows optimal use of the full flexibility of the theoretical model.

d) The essential significance for the calculated results depends upon the best possible definition of the mean camber line geometry. When the data are taken from an atlas of section profiles, it is necessary to interpolate for the established vortex coordinates and control points. It was found that the best results were obtained with interpolation done with an incomplete Fourier series containing only the sine functions. Despite the fact that differences with respect to other methods of interpolation would appear sometimes in the third significant figure, the "so-defined" section profile was almost insensitive to whatever changes in the discrete structure were used in the calculations.

e) The number of control points employed has an influence on the calculated results. The correctness of this statement is limited by a saturation ceiling, that is, increasing the number of control points above a certain number does not improve the results. The significance of the control points stems from the fact that at these very points the mutual interaction is seen between the geometry of the section profile and the field of the velocity flow. Figure 29 shows the calculated pressure distribution for the same section profile as used previously using 6, 8, and 18 control points. As is apparent from the figure, as well as from other calculations, 8 to 9 control points are sufficient to adequately calculate the pressure distribution, and increasing that number unreasonably prolongs the calculating time.

f) Besides the number of control points it is important to appropriately define the directions of the normals to the mean camber line of the section profile at those

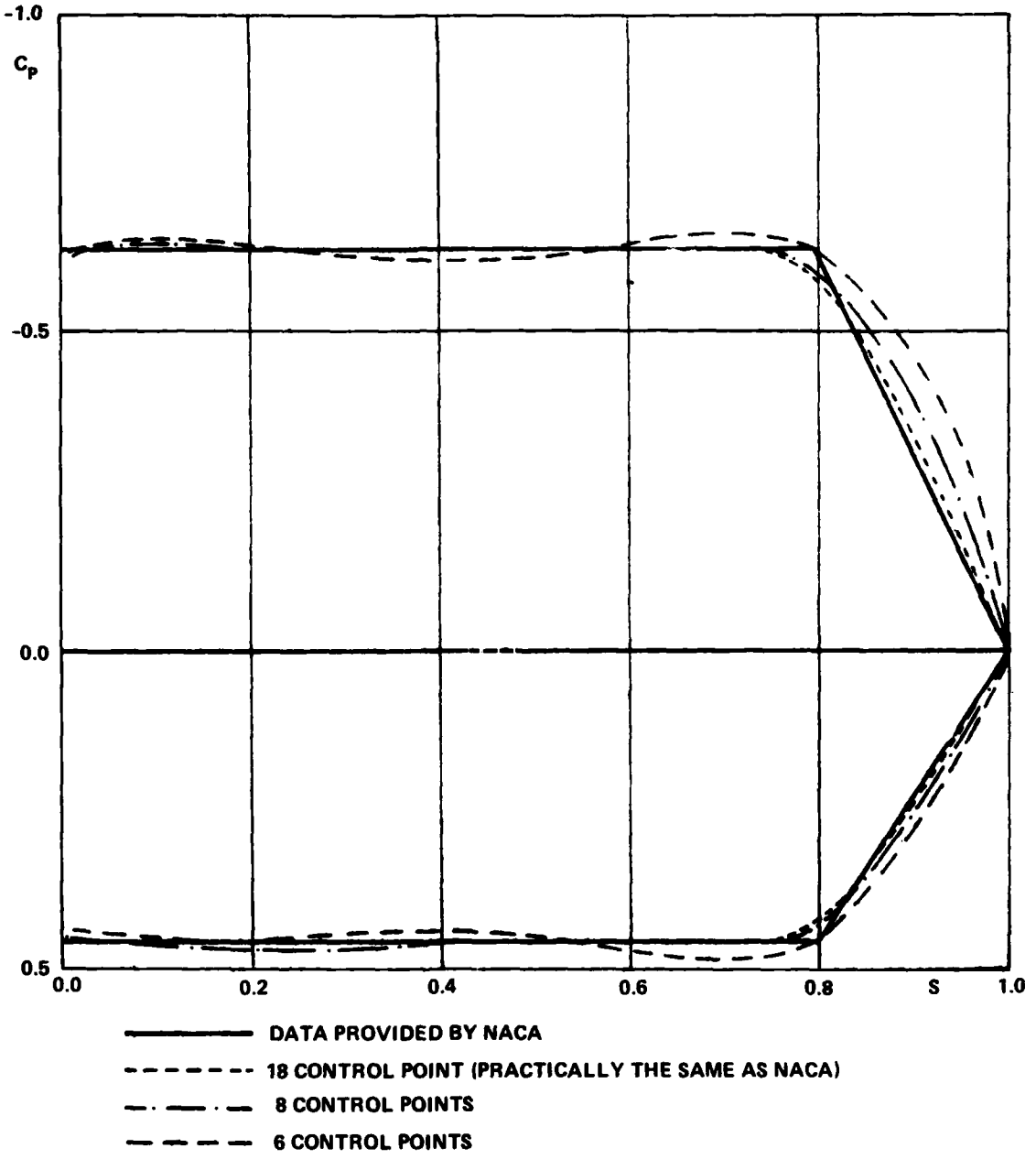

Figure 29 - Pressure Distribution for an Infinitely Thin Profile NACA a = 0.8 in a Two-Dimensional Flow Calculated for a Different Number of Control Points

points. Different methods to determine the local normal were tried. The best results were obtained by the method based on the calculations derived from the functions interpolating the geometry of the mean camber line. For this reason the described method of interpolation was very useful.

g) For a uniform flow one can obtain correct results when the number of terms in the function defining the pressure distribution is equal to the number of control points as well as when it is smaller. One should not, however, limit the number of terms in the function below a certain limit (4 to 5 terms) because one may experience difficulty defining more complicated pressure distributions (for example, NACA a = 0.5). For some profiles (for example, NACA 65) only a two term function gives accurate results. The use of a number of terms smaller than the number of control points protects the effort, rather well, from the effects of changes in the configuration of the control points. Figure 30 illustrates the results of pressure distribution calculations for the NACA a = 0.8 profile using 4 and 8 terms in the circulation distribution function. Both calculations were made using eight control points. One can clearly see the effect of overly restricting the number of terms in the function.

h) A small number of calculations made for the two-dimensional nonuniform velocity flow field have proven that it is proper to use a smaller number of terms in the function than the number of control points. Occasionally, totally improbable results were obtained using an equal number of both parameters. The cause of this is a characteristic peculiarity of the set of linear equations. The use of a small number of terms leads to results that were easily justified by the character of the velocity field (sinusoidal changes were made in the inflow angle with a different number of cycles along the chord length). During these calculations it was concluded that the NACA method of establishing the pressure was not usable for a nonuniform velocity field.

All experiences obtained in the course of the experiments, with the program calculating the pressure distribution over a section profile in a two-dimensional flow, were employed in the construction of the computational method based on the lifting surface model. However, this, did not guarantee that the method describing the combined effects of the three-dimensional flow would ensure the convergence of the solution. It was necessary, using the program described in Section XIII, to perform calculations that would ascertain the correctness of the method. It was not possible, in a short time, to perform an equally extensive analysis as was done for the

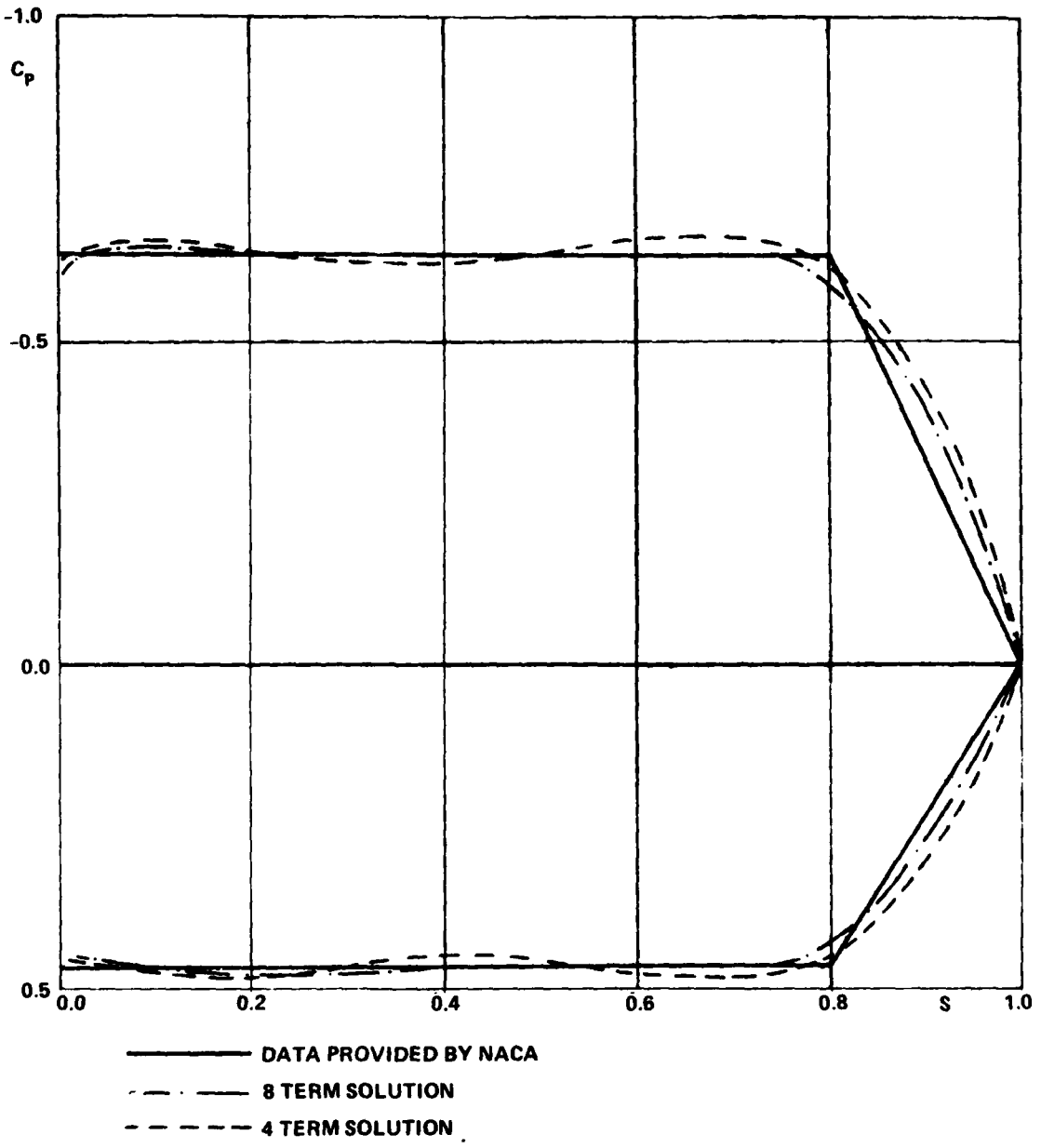

Figure 30 - Pressure Distribution Calculated for an Infinitely Thin NACA a = 0.8 Profile in a Two-Dimensional Flow for a Different Number of Terms in the Circulation Distribution Function

two-dimensional flow, partly because of the costs of performing such calculations and partly because of the difficulty of controlling, in detail, such a complicated program (at the beginning of the program each complete set of calculations produced over 4000 numerical values for checking). Furthermore, it was considered justifiable that a detailed analysis of the properties of the theoretical model in a two-dimensional flow would make it less important to check the model equally extensively in a three-dimensional flow. Three additional calculations were then made only for a propeller operation in a uniform velocity field at the design conditions (compare Section XIV), using a set of 36, 42, and 48 control points, while the remaining parameters of the discrete network were unchanged. The control points were always appropriately distributed on the same six profiles at radii 0.4, 0.5, 0.6, 0.7, 0.8, and 0.9, with 6, 7, and 8 points. In the first case the points were located at 0.15, 0.25, 0.45, 0.55, 0.75, and 0.85 of the chord length from the leading edge; in the second case, at 0.2, 0.3, 0.4, 0.5, 0.6, 0.7, and 0.8; and in the third, at 0.15, 0.25, 0.35, 0.45, 0.55, 0.65, 0.75, and 0.85. All calculated results of the pressure distribution on the propeller blade were found to be in mutual agreement, so that to indicate differences in the scale of Figures 18 through 22 was impossible to discern.

A comparison of these results with the convergence of solutions of computational methods published by authors outside Poland [10], and [28] leads to the conclusion that the method presented is, in this area, clearly superior. In the Japanese method, transition from 77 to 49 control points distorts the calculated pressure in a way that impairs the possibility of the practical use of that method. The American method, on the other hand, indicates an overly significant dependence upon the density of the vortex network, that is, most likely a convergence problem of the vortex network in the region of the propeller blade tip (which uses a configuration that is not necessarily the best). In summary, the calculated solution of the present computational method converges adequately.

XVII SUMMARY AND CONCLUSIONS

In the previous sections of this report a theoretical method for calculating the pressure distribution on a propeller blade operating in a nonuniform velocity field was presented. A detailed discussion of the formulation of the theoretical model, the structure of the computer model, and a comparison of the calculated results with available experimental data were included. Finally, in this summary, two groups of questions are introduced: one, what new and useful method has this brought to the field, and two, how can this method best be used to provide direction for future efforts.

The most important innovation in the domain of the structure of a ship propeller vortex model is the use of a free vortex in the propeller wake. As previously mentioned the particular application cannot be considered final. However, it simulates relatively well the physical realities of the dependence of free vortices upon the unsteady phenomena taking place on the propeller blade. It also includes, on the basis of back pressure, the influence of the "history" of the previous performance of the propeller on the phenomena that do take place on the propeller at this time. For the first time in the free vortex sheets vortex lines are directed radically. As a consequence of the assumed structure of the free vortex sheets, it also contributes to the concept of induction factor tables to calculate the induced velocities. Although the induction coefficients can be considered more as part of the numerical process than of the theoretical model, their use contributes to a relatively fast and effective execution of calculations. The next concept, also original, is the employment of a three-step approximation cycle in the description of the propeller performance in a nonuniform velocity field. The first step is the analysis of propeller performance in a circumferentially averaged velocity field, the second, partially accounting for the unsteady phenomena about one propeller blade only, and finally in the third step, a complete analysis of propeller performance in a nonuniform velocity field. A new element of less significant value is the allowance for local values of the external velocities at all control points for every propeller blade position. The form of the discrete network of singularities modeling the propeller blade is also different from the ones presently used. It appears that it is more useful to simulate continuous realistic blade load distribution. Furthermore, a number of small improvements of a numerical nature have been introduced in the computer program, making it more effective compared to similar theoretical methods available outside Poland. The method has proven accurate with respect to the analytical

results for a uniform velocity field as well as for a nonuniform velocity field. Convergence (stability) of t e solutions proved to be better than equivalent methods published outside Poland. The principal objective of the first order of importance was the use of the method for calculating the pressure distribution on a propeller blade to predict the onset of cavitation on a propeller operating in a nonuniform velocity field. Therefore, it was essential to supplement the existing method in elements linking the pressure distribution calculated in an ideal fluid flow with the area and character of cavitation as it occurs in a real flow. We find two possible avenues of approach. One of them, using, to a large extent, theoretical means, would be based on the inclusion of viscous phenomena, specifying the character of the boundary layer parameters and relating it to the range and kind of cavitation in a way similar to the one described in Reference [16]. The second method of approach, of a more empirical nature, would assume that a relationship can be obtained between the pressure distribution in an ideal flow and the cavitation phenomena by a statistical analysis of calculations and experimental observations of a large series of propeller models. It is difficult to say which method will prove to be more effective. Work should continue in both areas, with a closely related and ever important broad verification of calculated results in a nonuniform velocity field.

The next important application of the developed method will be its use to define oscillating loads on the propeller operating in a nonuniform velocity field and then transmitted through the propeller shaft to other parts of the ship. Because the cavitation phenomena have such a direct effect on the magnitude of the oscillating forces induced on a propeller blade, it is essential to develop an analytical method that defines a pressure distribution sensitive to changes in the cavity volume. Then, with simple methods of integration of the pressure distribution, one may establish all the necessary components of the oscillating forces on the propeller. It will also be possible to use this method to calculate average total propeller characteristics in terms of thrust, torque, and efficiency as a function of advance coefficient.

A further application of the method is its adaptation to predict blade spindle torque in controllable pitch propellers. Here the method will be applied to calculate the values of moments of the hydrodynamic forces about the controllable pitch propeller blade axis for a wide range of advance coefficients and the adjustable pitch angle. In this case, again, the cavitation phenomena play an essential role, impossible to consider in previous theoretical methods based on a lifting line model. The question of predicting correct control forces is one of the basic problems in the

design of controllable pitch propellers, and solving it will permit a substantial increase in the available power that can be transmitted by a propeller of this type.

It is also planned to use this theoretical method to calculate a new set of corrections for the lifting surface effect. Properly established corrections would permit a very effective propeller design with simple theoretical models based on a lifting line. It is anticipated that a complete set of corrections for the purpose of propeller design will be calculated. Such a set of corrections would be compared with those presently used, calculated in the United States about ten years ago; if better results are obtained they could be used in the present methods of propeller design. Furthermore, it is planned to use the new method to calculate other types of corrections for the effect of lifting surface, particularly to calculate propeller hydrodynamic characteristics away from the design point. If the results of these calculations are successful, a simple and effective method to calculate these characteristics using a simple theoretical lifting line model would be achieved.

After the method described here is verified and supplemented by the indicated additions, it will become a very useful tool in the design of ship propellers. It will be possible to realize all the objectives that were discussed at the beginning of this report; to optimize propeller designs, particularly from the point of view of adapting them to operate in a nonuniform velocity field; and to eliminate, partially, costly and time-consuming cavitation tests. The diversity of problems for which the method may find application indicates its importance in the contemporary hydrodynamic problems of ship propellers. The actual state of advancement provides hope for the realization of the goals discussed.

XVIII REFERENCES

[1] Basin, A.M., Miniowicz, I.J. - Teoria i razczet grebnych wintow (Ship Propeller and Calculations). Sudpromgiz 1963.

[2] Cummings, D.E. - Numerical Prediction of Propeller Characteristics. Journal of Ship Research 1/1973.

[3] Drewko, J., Kaczorowski, J. - Analiza okresowo zmiennych obciazen indukowanych na srubie napedowej pracujacej w niejednorodnym polu predkosci na podstawie teorii powierzchni nosnej (Analysis of Periodically Varying Induced Loads on a Ship Propeller Operating in a Nonuniform Velocity Field on the Basis of Lifting Surface Theory). Materialy III Sympozjum Hydromechaniki Okretowej (Proceedings of the 3rd Ship Hydrodynamic Symposium), Gdansk 1975.

[4] Gent, W. - Unsteady Lifting Surface Theory for Ship Screws. Journal of Ship Research 4/1975.

[5] Gent, W., van Oossanen, P. - Influence of Wake on Propeller Loading and Cavitation. International Shipbuilding Progress No. 228, 1973.

[6] Glover, E. - A Design Method for Heavily Loaded Propellers. The Naval Architect 1973.

[7] Hoiby, O.W. - Three Dimensional Effects on Propeller Theory. Norwegian Ship Model Experimental Tank Publ. No. 105, 1970.

[8] Johnson, C.A. - Correlation of Predictions and Full Scale Observations of Propeller Cavitation.

[9] Kerwin, J.E. - A Design Theory for Subcavitating Propellers. Transactions S.N.A.M.E., Vol. 72, 1964.

[]0] Kerwin, J.E. - Computer Techniques for Propeller Blade Section Design. International Shipbuilding Progress No. 227, 1973.

[11] Koronowicz, T. - Okreslenie osiowej zmiennosci predkosci indukowanych w strumieniu srubowym (The Determination of the Axial Variation of the Induced Velocities in the Propeller Wake). Biuletyn (Report) I.M.P. P.A.N. 83/745/1974.

[]2] Kuiper, G. - Some Remarks on Lifting Surface Theory. International Shipbuilding Progress No. 193, 1971.

[13] Lerbs, H.W. - Moderately Loaded Propellers. Transactions S.N.A.M.E., Vol. 60, 1952.

PRECEDING PAGE BLANK-NOT FILMED

[14] Morgan, W.B. - Propeller Lifting Surface Corrections.
Transactions S.N.A.M.E., Vol. 76, 1968.

[15] Noordzij, L. - Pressure Field Induced by a Cavitating Propeller.
International Shipbuilding Progress No. 260, 1976.

[16] Oossanen, P. von - Method for Assessment of the Cavitation Performance of Marine Propellers.
International Shipbuilding Progress No. 245, 1975.

[17] Oossanen, P. von - Calculation of Performance and Cavitation Characteristics of Propellers Including Nonuniform Flow and Viscosity.
N.S.M.B. Publication No. 457.

[18] Patience, G. - Minimizing Cavitation Erosion: A Pressure Distribution Approach to the Design of Marine Propellers.
Transactions N.E.C.I.E.S., 1974.

[19] Pien, P.C. - The Calculation of Marine Propellers Based on Lifting Surface Theory.
Journal of Ship Research 2/1961.

[20] Pien, P.C., Strom-Tejsen, J. - General Theory for Marine Propellers.
VII Symposium on Naval Hydrodynamics, Rome 1968.

[21] Prosnak, W.J. - *Mechanika Plynow* (Fluid Mechanics).
Warszawa 1970.

[22] Ralston, A. - Analiza numeryczna (Numerical Analysis).
Warszawa 1971.

[23] Robinson, A., Laurman, M.A. - Wing Theory
Cambridge University Press 1956.

[24] Schwanecke, H. - Comparative Calculations on Unsteady Propeller Blade Forces.
14 I.T.T.C. Report of the Propeller Committee.

[25] Sparenberg, J.A. - Application of Lifting Surface Theory to Ship Screws.
International Shipbuilding Progress No. 67, 1960.

[26] Strscheletzky, M. - A Method for Determining the Velocities which are Induced by the Free Vortices of the Propeller.
Hydrodynamics for Designing Ship Propellers, Karlsruhe, 1950.

[27] Sugai, K. - Hydrodynamics of Screw Propeller Based on a New Lifting Surface Theory.
J.S.N.A. Japan, Vol. 229, 1966 and Vol. 123, 1968.

[28] Sugai, K. - A Method for Calculation of the Hydrodynamic Characteristics of Marine Propellers.
J.S.N.A. Japan, Vol. 129, 1970.

[29] Tanibayashi, H. - Practical Approach to Unsteady Problems of Propellers.
International Shipbuilding Progress No. 226, 1973.

[30] Tsakonas, S., Jacobs, W.R., Ali, M.R. - An Exact Linear Lifting Surface Theory for a Marine Propeller in a Nonuniform Flow Field.
Journal of Ship Research, 4/1973.

[31] Thwaites, B. - Incompressible Aerodynamics.
Oxford, 1960.

XIX NOMENCLATURE

a(i,j)	- coefficients of a function defining distribution of bound circulation over the blade
$\overline{B}$	- vector of a discrete bound vortex over the blade
BX, BY, BZ	- coordinates of vector $\overline{B}$
BSX, BSY, BSZ	- coordinates of midpoints of vector $\overline{B}$
CX, CY, CZ, CQ	- coordinates of control point C
C_p	- nondimensional pressure coefficient
C_{ps}	- nondimensional pressure coefficient on the suction (low pressure) side of the blade
C_{pc}	- nondimensional pressure coefficient on the (high) pressure side of the blade
d	- coefficient defining the angle of pitch of the free vortex surfaces
E(k)	- propeller rake ordinates
FCX(k,i)	- coefficients of the Fourier series for the cosine functions
FSX(k,i)	- coefficients of the Fourier series for the sine functions
$G(\vartheta,\varphi)$	- functions of the distribution of the bound circulation
H(p)	- independent terms of the set of linear equations
K(p,q)	- coefficient multiplying the unknowns in the set of linear equations
$\overline{L}$	- distance vector between the singularity and the control point
LX, LY, LZ	- components of vector $\overline{L}$
m(ι)	- offset of the meanline divided by the maximum camber
M(k)	- maximum camber of the mean profile
n_1	- number of points W in the direction of blade radius
n_2	- number of points W in the direction of the section chord
n_3	- number of control points in the direction of the blade radius

PRECEDING PAGE BLANK-NOT FILMED

n_4 - number of control points in the direction of the section profile

n_5 - number of coefficients a(i,j) in the direction of blade radius

n_6 - number of coefficients a(i,j) in the direction of section profile

NX, NY, NZ - coordinates of vectors normal to the blade surface at the control points

N - number of sectors in the unsteady region of the propeller wake

$\overline{P}$ - radial segment of the vortex line in the propeller wake

P(k) - propeller pitch angle

P_o - fluid pressure infinitely far from the propeller

P - fluid pressure on the propeller blade

Q - sink or source strength

R_P - propeller hub diameter

R_T - propeller tip diameter

R(k) - actual radius of the propeller blade

RC(k) - radius defining location of the control point

R_{ps} - propeller revolutions per second

S(k) - propeller skewback ordinates

$\overline{T}$ - vector of the vortex trailing segment (on the propeller blade in the wake of the propeller)

TX, TY, TZ - coordinates of vector $\overline{T}$

U(q) - solution of the set of linear equations, equivalent to coefficient a(i,j) after change of index

V_o - velocity of fluid infinitely far from the propeller

V - velocity of fluid on the propeller blade

$\overline{VI}$ - total induced velocity at a given point on the propeller blade

VX, VY, VZ, VR, VT, VN - coordinates of vector $\overline{V}$

VE - normal component of the external velocity field at a given control point

VW - normal component of velocity induced by the singularities forming propeller blade model

VZ - normal component of velocity induced by the unsteady region of the propeller wake

VC - normal component of velocity induced by the steady region of the propeller wake

VQ - normal component of velocity induced by sources modeling finite blade thickness

VS - ship speed

VGX, VGT - components of velocity difference between the suction and pressure sides of the blade

W - points establishing the structure of discrete network of singularities on the propeller blade

WX, WY, WZ - components of points W

X_p - component of the distance from the control point to the vortex line element in the propeller wake

Z - number of propeller blades

α_p - angular distance from the control point to the vortex line element in the propeller wake

$\beta(k)$ - pitch angle of the free vortex sheet

γ - strength of the vortex element circulation

γ_B - strength of the circulation of the bound vortex element

γ_T - strength of the circulation of the trailing vortex element

γ_P - strength of the circulation propeller wake radial vortex element

$\delta(k)$ - angle of incoming flow

ρ - density of water

ϑ - angular coordinate along the section chord

φ - angular coordinate along the blade radius

Note: The nomenclature does not include symbols used in Section II, in which the same notation is used as in the original published work; such notation is defined following the equations.

APPENDIX I: ALGORITHM DEFINING FORCES AND MOMENTS ACTING ON A PROPELLER BLADE

One of the possible uses of the pressure distribution on a ship propeller blade operating in a circumferentially nonuniform velocity field, calculated according to the algorithm described in previous sections, is to establish the forces and moments acting on a propeller blade. One should remember, however, that the algorithm used in calculating the pressure distribution does not include changes in that pressure as a result of viscous effects and does not include forces due to viscous drag. The calculated forces and moments acting on a propeller blade may differ significantly from the magnitudes measured experimentally or established by other methods that include viscous effects. When the method presented here is adapted to include the fluid viscous effects, the following equations may be used without changes.

Figure 31 shows an orthogonal coordinate system OXYZ fixed to the propeller. A propeller blade is shown schematically with an arbitrary distribution of pressure along the blade section and radius. The figure also shows the three vector components of the hydrodynamic forces F_x, F_y, F_z and the three vector components of the hydrodynamic moments M_x, M_y, M_z, which are the objects of these calculations. The calculation of any component of force or moment, as, for example, F_z, can be performed according to the following equation:

$$F_z = \int_{r=r_p}^{R} \int_{s=0}^{L(r)} \Delta p(r,s) \cdot n_z(r,s) \cdot dr \cdot ds \tag{56}$$

where: $\Delta p(r,s)$ - pressure difference between the high and low pressure sides of the propeller blade

n_z - component of a unit vector normal to blade surface in the axial direction

R - radius of the blade tip

$L(r)$ - chord length of a blade profile at a radius

r_p - propeller hub radius

r - variable along the blade radius

s - variable along the chord of a blade profile

PRECEDING PAGE BLANK-NOT FILMED

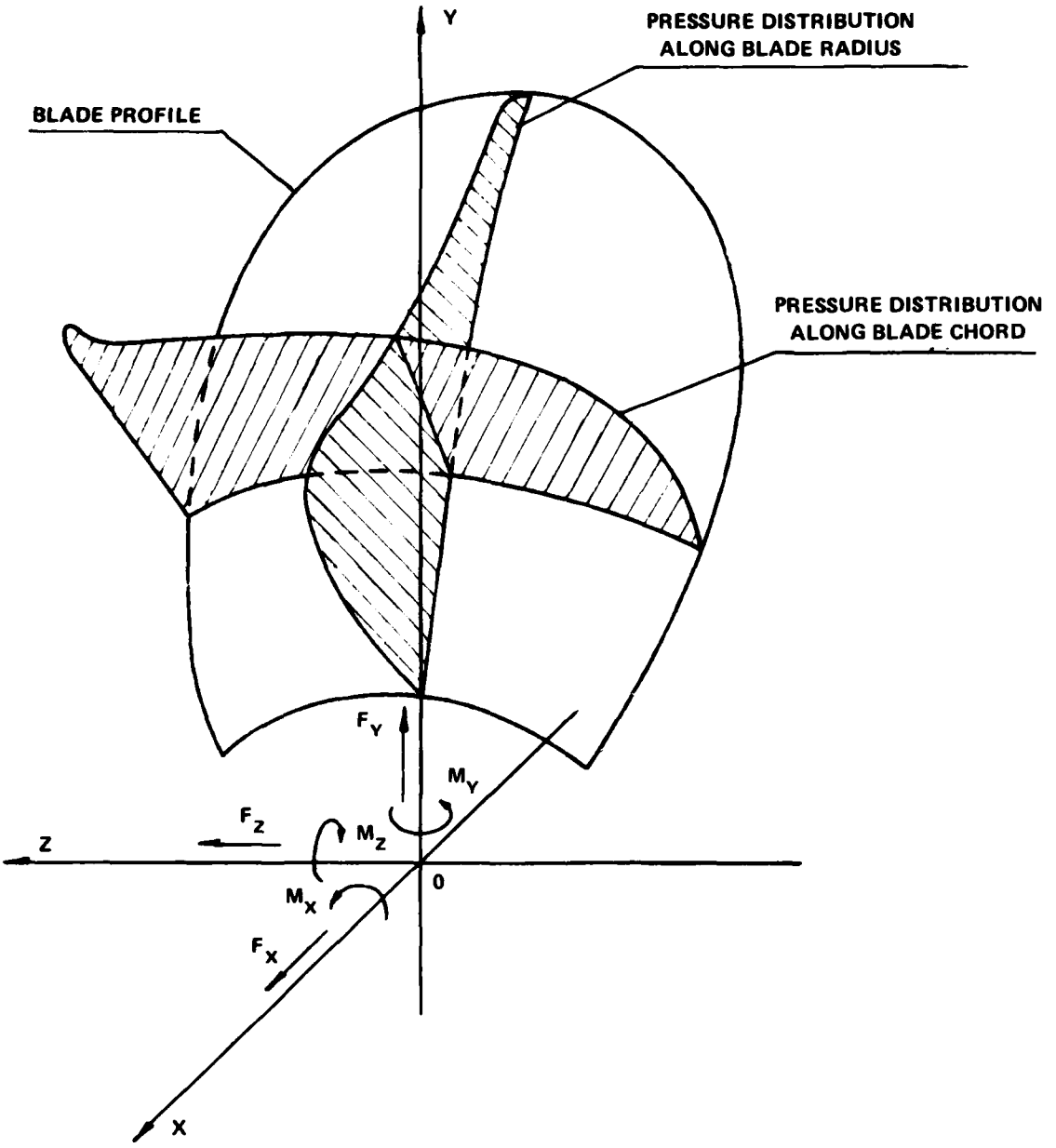

Figure 31 - Force and Moment Components of the Hydrodynamic Forces Acting on a Propeller Blade

Next, calculations of a component of the hydrodynamic moment can be performed according to equation:

$$M_z = \int_{r=r_p}^{\ell L(r)} \int_{s=0} \Delta p(r,s) \cdot \left[n_y(r,s)\, a_x(r,s) + n_x(r,s) \cdot a_y(r,s) \right] dr\, ds \qquad (57)$$

where: a_x, a_y - appropriate moment arms of force components relative to the axis of the coordinate system, defined according to the following equations:

$$a_x(r,s) = r \cdot \cos\left\{ \left[\frac{L(r)}{2} - sk(r) + s \right] \frac{\cos\varphi(r)}{r} \right\}$$

$$a_y(r,s) = r \cdot \sin\left\{ \left[\frac{L(r)}{2} - sk(r) + s \right] \cdot \frac{\cos\varphi(r)}{r} \right\} \qquad (58)$$

$$a_z(r,s) = \left[\frac{L(r)}{2} - sk(r) + s \right] \cdot \sin\varphi(r) + rk(r)$$

where: $\varphi(r)$ - blade pitch distribution

sk(r) - function defining blade skewback

rk(r) - function defining blade rake

Functions analogous to Equations (56) and (57) may be written for all the force and moment components, substituting only appropriate components of the unit vectors normal to the blade surface and moment arms.

In practical cases the pressure difference between both sides of the blade, Δp is defined at a given set of points on the blade surface. Therefore, integration over the blade surface is performed according to an appropriate numerical method, such as, for example, the Simpson rule. This leads to the following expressions:

$$F_x = \frac{d_R}{3} \sum_{i=1}^{m} C_{Ri} \; \frac{d_s}{3} \sum_{j=1}^{n} C_{sj} \cdot \Delta p_{ij} \cdot n_{xij}$$

$$F_y = \frac{d_R}{3} \sum_{i=1}^{m} C_{Ri} \frac{d_s}{3} \sum_{j=1}^{n} C_{sj} \Delta p_{ij} \cdot n_{yij} \qquad (59)$$

$$F_z = \frac{d_R}{3} \cdot \sum_{i=1}^{m} C_{Ri} \frac{d_s}{3} \sum_{j=1}^{n} C_{sj} \cdot \Delta p_{ij} \cdot n_{zij}$$

and, appropriately, to moment components:

$$M_x = \frac{d_R}{3} \sum_{i=1}^{m} C_{Ri} \frac{d_s}{3} \sum_{j=1}^{n} C_{sj} \cdot \Delta p_{ij} \left[n_{yij} \cdot a_{zij} + n_{zij} \; a_{yij} \right]$$

$$M_y = \frac{d_R}{3} \sum_{i=1}^{m} C_{Ri} \frac{d_s}{3} \sum_{j=1}^{n} C_{sj} \cdot \Delta p_{ij} \left[n_{xij} \cdot a_{zij} + n_{zij} \cdot a_{xij} \right] \qquad (60)$$

$$M_z = \frac{d_R}{3} \sum_{i=1}^{m} C_{Ri} \frac{d_s}{3} \sum_{j=1}^{n} C_{sj} \cdot \Delta p_{ij} \left[n_{xij} \cdot a_{yij} + n_{yij} \cdot a_{xij} \right]$$

In the above equations the following notation used was:

d_R - integration interval in the direction of the radius

d_s - integration interval in the direction of the blade chord

C_R, C_S - Simpson rule coefficients for appropriate integration intervals.

Equations (59) and (60) can be used directly in the computer program. In the calculations for a propeller operating in a circumferentially nonuniform velocity field, the pressure distribution, and, therefore, all components of forces and moments, are functions of a momentary position of the blade and, therefore, functions of time. Therefore, when one calculates appropriate components of a load on the whole propeller, simple multiplication of the results obtained by Equations (59) and (60) is not correct. One should add the magnitudes of forces calculated by these equations separately for all the blades in a given position of the propeller.

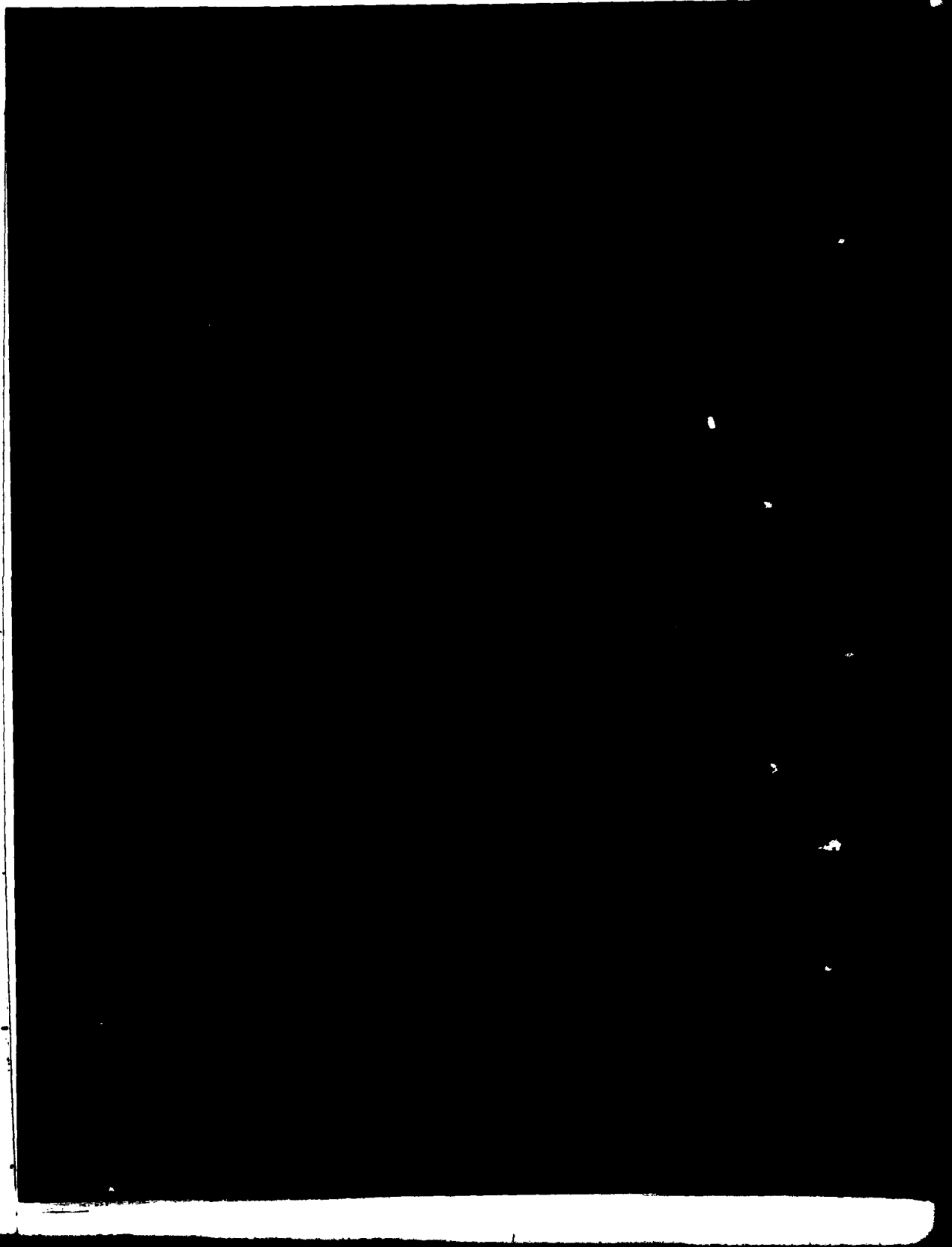

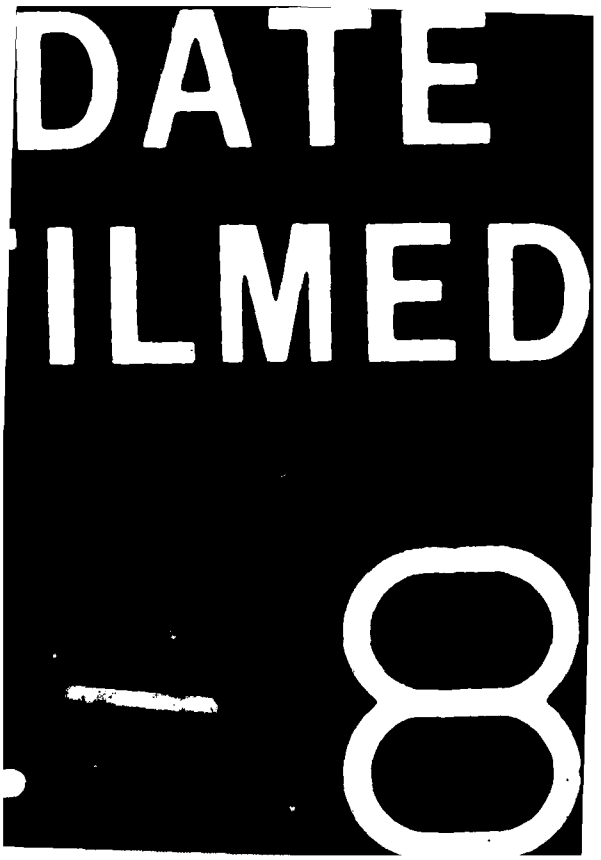
DATE
ILMED
8